# DEMONSTRATION OF PHARMACOMETRIC APPLICATIONS TO ANTI-INFECTIVE CHEMOTHERAPY

A DISSERTATION

SUBMITTED TO THE FACULTY OF THE GRADUATE SCHOOL

OF THE UNIVERSITY OF MINNESOTA

BY

AHMED HAMED AHMED SALEM

IN PARTIAL FULFILLMENT OF THE REQUIREMENTS

FOR THE DEGREE OF

DOCTOR OF PHILOSOPHY

Dr. Richard C. Brundage, Adviser

Dr. Ayman M. Noreddin, Co-adviser

June 2010

# Acknowledgements

It is a pleasure to thank those who made this thesis possible. First and foremost, I would like to thank Allah; our Lord, the All-Knowing, the Almighty, the most Merciful and the most Compassionate. All praise and thanks are due to Him; I praise Him, seek His pardon, turn to Him, and seek refuge with Him from the evils of myself and from the evil consequences of my deeds.

I would like to offer my deepest gratitude to my advisor, Professor Richard Brundage, for his support, help and advices throughout the program. Professor Brundage introduced me to the exciting field of pharmacometrics and I believe this was a turning point in my life. I have become very passionate about gaining knowledge and experience in this field and learning more about its applications to pharmacotherapy and clinical drug development. I believe this is the field where I want to spend the rest of my life working on.

This thesis would not have been possible without the guidance of Dr. Ayman Noreddin. I am indebted to him in many ways and I cannot thank him enough for his mentorship. On the personal level, Dr. Noreddin was very approachable and was always very concerned about my personal development.

I would like also to thank Dr. Lynn Eberly; the chair of my final oral examination committee, for the time she dedicated to review my thesis. I would like also to thank Dr.

Heather Vezina and Dr. Marnie Peterson for serving on my committee. Their time and comments are much appreciated.

I am grateful to Dr. Scott Chapman, my preceptor in the clinical rotation at North Memorial Medical Center. My experience during the rotation was very rewarding and it was great to work with patients and be able to make a direct impact on the health care they receive.

It is also an honor for me to thank Professor Randy Seifert, the Senior Associate Dean, and Professor Lester Drewes for their continuous support and encouragement. I cannot count how many times I sought their help and they were always very willing to offer what they can to make sure I have the best education experience.

I would like also to show my gratitude to the Office of Clinical research (currently the Clinical and Translational Science Institute) at University of Minnesota for granting me the clinical and translation research fellowship in 2008. In addition, I would like to thank Dr. Julie Stone and Dr. Luzelena Caro for supervising me during my clinical PK/PD internship at Merck and Co. in 2009. This internship was a great opportunity for me to get experience in clinical drug development.

Working as a graduate teaching assistant for pharmacotherapy, pharmacokinetics and applied pharmacokinetics courses was a great learning opportunity for me. I would like to thank all the course instructors for their confidence in my capabilities. I appreciate the friendship of all the students I interacted with and I am grateful to Class 2011 and

Class 2012 for granting me the Teaching Assistant of the Semester Award in 2008 and 2009.

I am grateful to Dr. Melanie Wall for her help in arranging for my PhD minor in Biostatistics in her capacity as the director of graduate studies in the Biostatistics program. Moreover, her Biostatistical Modeling and Methods course was in many ways the best Biostatistics course I ever had. Her applied teaching approach contributed positively to our learning experience.

I would like to offer my great appreciation to the ECP department for giving me the opportunity to receive a world-class education in clinical pharmacology. I am also indebted to Dr. Nael Mostafa for his friendship in the last 4 years. His advices and mentorship were invaluable.

Last but certainly not least, I would like to thank my parents, Dr. Hamed Salem and Professor Aisha Salama for everything they have done for me. I appreciate their sacrifice and continuous encouragement. I am indebted forever to them as well as to my brothers and sisters for their unconditional love and support. I am blessed to have such a great family and I pray to Allah to bless them all and reward them for all what they have done.

# Dedication

To My Wonderful Parents

*"I Love you to pieces, to you I dedicate this thesis"*

# Table of Contents

# List of Tables

# List of Figures

# Introduction

## 1.1 PHARMACOMETRICS

Pharmacometrics can be defined as the branch of science concerned with mathematical models of biology, pharmacology, disease, and physiology used to describe and quantify interactions between xenobiotics and patients, including beneficial effects and side effects resultant from such interfaces [1]. The term pharmacometrics was coined in the literature in 1982 [2] and has continued to evolve since then in concordance with the advances in computational speed, stochastic modeling and simulation methods and identification of novel biomarkers. Pharmacometrics deals with pharmacokinetic models that describe the drug concentration-time data, pharmacodynamic models that relate the drug exposure to pharmacologic, toxicologic responses, surrogate markers and/or clinical outcomes. It also involves disease progression models that characterize the disease behavior in presence and absence of a drug. In addition, pharmacometrics allows quantification of the uncertainty and variability in these mathematical relationships.

Since its emergence, pharmacometrics has played a major role in guiding drug development programs in the pharmaceutical industry [3,4]. This application was encouraged by the FDA via its use of pharmacometrics methodologies in submissions review and via issuance of guidances on population pharmacokinetics and exposure-response relationships [5,6]. Moreover, pharmacometrics lies at the heart of the critical path initiative that FDA issued recently [7] since it helps to identify tools that can demonstrate medical utility and assess safety and hence expedite drug development. Likewise, pharmacometrics has high potential in guiding rational pharmacotherapy via optimizing dosage regimen of existing drugs to maximize their efficacy while minimizing the adverse events.

## 1.2 POPULATION PHARMACOKINETIC MODELING

This section aims to provide the population pharmacokinetic basis of pharmacometrics. Pharmacokinetics describes the absorption, distribution, metabolism and elimination of xenobiotics in serum and at other sites of action. Due to variation in these biological processes, not all people exhibit the same pharmacokinetic profile upon administration of the same dose. This variability in pharmacokinetics is an important contributor to the variability in the drug response observed with different patients and the importance of its characterization cannot be overstated. Population Pharmacokinetics is the study of the sources and correlates of variability in drug concentrations among individuals who are the target patient population receiving clinically relevant doses of a drug of interest [8].

Variability in pharmacokinetics could be studied using several approaches; the two main approaches will be discussed in this section:

### 1.2.1 Standard Two-Stage Approach

In the first stage of this approach, the pharmacokinetic model is fit to the concentration-time data (usually rich data) of each subject separately and the individual pharmacokinetic parameters are estimated. Using these estimates, the mean and the variance of pharmacokinetics parameters could then be obtained in the second stage and stepwise regression could be performed to identify the important covariates that are responsible for the variability of the pharmacokinetic parameters. Although the estimate of the mean pharmacokinetic parameters using this approach is usually adequate, the variability of these parameters is often overestimated [9-12]. Another limitation of this

approach is the need to have rich data for each subject that is sufficient to allow the algorithm to obtain the individual pharmacokinetic parameters.

### 1.2.2 Nonlinear Mixed Effects Modeling

This approach was first introduced by Sheiner and Beal in the late 1970s [13]. In this type of modeling, the unit of the analysis is the population study sample that is used in one stage to directly estimate the population mean parameters and the variability within the population. The individual parameter estimates are then obtained using empirical Bayesian approach using the population parameters as priors and the individual observations. The word mixed means that it involves both fixed effects, which are the pharmacokinetic parameters and their associated covariates, as well as random effects. It is often also called hierarchical modeling since it incorporates variability in two hierarchies or levels. The first level includes the intra-individual variability which could be mathematically represented as follows:

$$C_{ij} = f_1(p_i,\ t_{ij},\ d_i) + \varepsilon_{ij}$$

Where $C_{ij}$ is the $j^{th}$ observed concentration in the $i^{th}$ individual, $f_1$ is the pharmacokinetic model predicting the concentration, $p_i$ is the vector of pharmacokinetic parameters in the $i^{th}$ individual and is calculated according to the equation below, $t_{ij}$ is the time of the $j^{th}$ observed concentration in the $i^{th}$ individual, $d_i$ is the dosing history in the $i^{th}$ individual, $\varepsilon_{ij}$ is the residual error which is assumed to be independent and normally distributed with a mean of zero and a variance of $\sigma^2$ which represents the intra-individual variability.

The second level is the inter-individual variability in the pharmacokinetic parameters and could be shown as follows:

$$p_i = f_2(\theta, Cov_i) + \eta_i$$

Where $f_2$ is the function that describes the relationship between the individual pharmacokinetic parameters ($p_i$) and the individual covariates levels ($Cov_i$). $\theta$ is the typical population value of the pharmacokinetic parameter pi, $\eta_i$ is the random difference between the $p_i$ and $\theta$ which is assumed to be independent and normally distributed with a mean of zero and a variance of $\sigma_b^2$.

Unlike the standard two-stage approach, the mixed effects modeling approach is able to handle sparse data. This is particularly advantageous in drug development when sparse PK data are collected in Phase2/3 clinical trials and it enables quantification of the pharmacokinetic variability as well as its sources. This feature is also of great value in studying the pharmacokinetics in special populations such as neonates [14,15]and patients with AIDS [16] , where the number of samples is limited due to medical or ethical concerns. Finally, the ability to model sparse data allows the nonlinear mixed effects modeling approach to play a vital role in direct patient care via its use in therapeutic drug monitoring to individualize dosage regimens.

### 1.2.3 Implementation of Nonlinear Mixed Effects Modeling

Nonlinear mixed effects modeling of pharmacokinetic data is most commonly performed by the NONMEM software (ICON Development Solutions, Ellicott City, Maryland) using the maximum likelihood estimation approach. Due to the nonlinear dependence of the observations on the variability terms in the model described earlier, the

likelihood cannot be evaluated analytically and approximations have to be done. In NONMEM, this is typically implemented using the first-order conditional estimation (FOCE) and the laplacian methods which linearize the nonlinear function using first order and second order Taylor series expansion, respectively, around the conditional estimates of the random effects [17,18].

Steps of nonlinear mixed effects modeling are summarized in Figure 1-1. The first step is usually referred to as the exploratory data analysis where the raw data are examined graphically and statistically to reveal patterns and relationships and check underlying assumptions about the distributions [19,20]. This step is interwoven with the next step where the basic structural PK model is identified by studying the dose dependence of the pharmacokinetic parameters, the number of the compartments in the model, and absorption profile [21]. In addition, the random effects model structure is determined.

When the structural pharmacokinetic and error models have been identified, the pharmacometrician seeks to identify the covariates that can explain the inter-individual variability in the pharmacokinetic parameters. Covariates commonly screened for their influence on pharmacokinetic processes include body weight, gender, race, age, Cytochrome P450 (CYP450) genotype and renal and hepatic insufficiency [22]. Potential covariates could be identified by examining the correlation between the empirical Bayesian estimates of the individual pharmacokinetic parameters and the covariate vectors.

Development of the covariate model is often done using stepwise regression with the forward inclusion/backward elimination approach [23]. The NONMEM objective function value (OFV= -2 log likelihood) is assumed to be $\chi^2$ distributed and hence the

likelihood ratio test (LRT) could be used to compare nested covariate models. Significance level of 0.05 could be used as an inclusion criterion for covariates while a more conservative significance level of 0.01 or lower is typically used for the backward elimination step. For discrimination of non-nested models, the Akaiki information criterion, which is equal to the OFV plus 2* the number of parameters, is used [24].

Finally, population pharmacokinetic models need to be evaluated. Goodness of fit of the models are assessed using diagnostic plots such as plots of the observed vs. predicted concentrations, conditional weighted residuals (CWRES) vs. time, CWRES vs. predicted concentrations and CWRES vs. covariates [19,25]. The confidence intervals of the parameters estimates are also checked to ensure reliability of the parameters and hence the model. These intervals could be obtained using the NONMEM standards errors estimates, bootstrapping or the likelihood profiling methods [6,21,26]. Moreover, models intended to be used for prediction purposes have to be validated, i.e. assessed for their predictive performance [6,27]. This could be attempted using resampling techniques such as bootstrapping [27,28] or simulation-based techniques such as posterior predictive check and visual predictive check [29,30].

## 1.3 PHARMACOMETRICS IN INFECTIOUS DISEASES

Infectious diseases is one of the therapeutic areas where pharmacometric principles and methodologies are utilized the most. This could be attributed to the ease of quantification of antimicrobial activities in in vitro and in vivo models and the availability of pharmacokinetic/pharmacodynamic (PK/PD) indices that can serve as surrogate markers for therapeutic outcome. Pharmacometrics allows integration of the pharmacodynamic knowledge from in vitro and in vivo studies in order to predict the therapeutic efficacy and optimize dosage regimens of anti-infective agents.

This section will present a brief introduction to the pharmacodynamics of antimicrobial agents, their PK/PD indices and the application of the pharmacometrics in infectious diseases.

### 1.3.1 Antimicrobial Pharmacodynamics

Pharmacodynamics (PDs) is the term used to reflect the relationship between measurements of drug exposure in serum, tissues, and body fluids and the pharmacological and toxicological effects of drugs [31]. Characterization of such a relationship is essential to ensure that the maximal benefit from the drug is gained while minimizing its associated risks. While for most drugs, the site of action is part of the human body such as a receptor or an enzyme, for anti-infectives, the site of action is a pathogen or an invading organism such as a bacterium, fungus or a virus. Since almost all pathogens could be isolated to be studied in vitro, a direct measurement of the potency of the anti-infective agent is usually feasible. This allows characterization of the variability

in interaction between the anti-infective and its site of action, an advantage that is not currently attainable with drugs from other pharmacologic classes [32].

### 1.3.2 Measures of the Anti-Infective Activity

The in vitro susceptibility of a pathogen to a drug is most commonly measured by the minimum inhibitory concentration (MIC) and the minimum bactericidal concentration (MBC). The MIC is the lowest concentration of the agent that results in no visible growth while MBC is the minimum concentration that kills 99.9% of the original number of pathogens. Since MIC assesses only growth inhibition assuming that the host immune system will eradicate the infection, the MBC is a more relevant measure of susceptibility for infections in immunocompromised patients and infections where the immune system is less efficacious such as meningitis, endocarditis and osteomyelitis [33]. For fungi, a similar parameter is used that is the minimum fungicidal concentration (MFC) while for viruses the effective concentration that reduces growth by half ($EC_{50}$) is often used but little has been done regarding its clinical relevance [32].

Despite the importance of MIC, MBC and MFC as measures of the anti-infective potency and its ease of determination and popularity in microbiological laboratories, they show poor correlation with therapeutic efficacy [34]. For example, if a drug has a lower MIC than another one, this does not necessarily mean that it will be more effective. This limitation is due to the fact that this parameter does not account for the drug pharmacokinetics. It only reflects the net effect observed after exposure to a fixed concentration of the drug for a certain period of time and provides no information about the impact of varying concentrations on the rate and extent of anti-infective activity. It

lacks also information about the anti-infective effect that may persist after the exposure. Such an effect could be attributed to the postantibiotic effect (PAE), the postantibiotic sub-MIC effect (PAE-SME), and/or the postantibiotic leukocyte enhancement (PALE) [35-37]. PAE could be defined as the delay in bacterial regrowth which occurs as a result of transient anti-infective exposure after the removal of the drug. PAE-SME is the increase in the PAE duration due to sub-MIC levels of the drug while PALE is used to describe the increase of the vulnerability of the pathogen for phagocytosis or intracellular killing during the postantibiotic phase [36,38].

Therefore, parameters which incorporate both pharmacokinetics and pharmacodynamics of the anti-infective have been identified in order to serve as surrogate markers to the activity of the anti-infective agents [39-41]. These parameters are usually referred to as the pharmacokinetic/pharmacodynamic (PK/PD) indices. Although several PK/PD indices have been proposed, only three of them have been commonly been used to reference the pharmacokinetics of an anti-infective to its MIC versus a given pathogen. These indices are the ratio of the area under the concentration-time curve to the MIC of the agent against the pathogen (AUC/MIC), the ratio of peak serum concentration of the anti-infective agent in relation to the MIC of the agent against the pathogen (Cmax/MIC), and the time of exposure of a pathogen to concentrations of the drug that exceeds the MIC against the pathogen (T>MIC) (Figure 1-2) [42-44].

### 1.3.3 Patterns of Anti-infective Activity

There are two main characteristics that are used to classify the pharmacodynamic patterns of anti-infectives. The first one is whether the killing effect on the pathogen is

dependent on the drug concentration or the duration of exposure [42,43,45]. The second characteristic is whether the drug has a persistent inhibitory effect after the exposure [38,46]. According to these two characteristics, anti-infectives are believed to follow three distinct pharmacodynamic patterns [31]. The first pattern is characterized by time dependent killing and minimal to no persistent effects. Examples of antimicrobial agents that exhibit this pattern include flucytosine and beta-lactams such as penicllins, carbapenems and cephalosporins. For these agents, the goal of therapy would be to maximize the duration that the drug level exceeds a certain inhibitory level such as the MIC of the drug to the pathogen of interest, usually through small frequent doses or continuous infusion. T> MIC is considered the PK/PD index that shows the best correlation with the therapeutic outcome of this class.

The second pattern exhibits time dependent killing and moderate to prolonged persistent effects. Glycopeptides (e.g. vancomycin and dalbavancin), tetracyclines (e.g. tigecycline), oxazolidinones (e.g. linezolid) are examples where this pattern is observed. In contrary to the previous pattern, the dosing frequency of this class of drugs is not an important determinant of their anti-infective activities, rather, it is the amount of drug administered that needs to be optimized to ensure that killing takes place for at least part of the time and there is no regrowth observed at other times. The AUC/MIC is the outcome linked PK/PD index for this group of antimicrobials.

The third pattern of anti-infective activity is characterized by concentration dependent killing and moderate to prolonged persistent effects. This pattern is observed with fluoroquinolones (e.g. moxifloxacin), aminoglycosides, daptomycin, amphotericin, metronidazole as well as others. Higher concentrations of these agents will result in

greater extent and increased rate of killing and hence the goal of therapy would be to maximize the concentrations. Less frequent dosing is often feasible with this class because of the persistent effects after the elimination of the drug. For this group of agents, both Cmax/MIC and AUC/MIC could be used to predict the efficacy.

### 1.3.4 Identification of the Outcome-Linked PK/PD Index and its Target Level

Large clinical trials typically evaluate one dosage regimen of the anti-infective agent, making it hard to determine the PK/PD index that shows the best correlation with the antimicrobial activity of the drug under investigation. Therefore, in vitro and animal infection models have been the cornerstone of antimicrobial pharmacodynamics research. The outcome-linked PK/PD index is usually the same and its magnitude that is predictive of efficacy is usually similar across agents from the same class [42,43,47-49]. However, when comparing the magnitudes across different antibiotics, it is critical to account for the differences in the protein binding between these drugs since only free drug is microbiologically active [47,50,51]. This target magnitude is often the same for different pathogens, but exceptions may arise due to differences in the PAE effect exhibited against different pathogens [49].

One main challenge to the identification of the primary PK/PD index is the collinearity between the three PK/PD indices. For example, a higher dose of an antimicrobial would result in higher Cmax/MIC and AUC/MIC as well as longer T> MIC and hence it would be difficult to disentangle which PK/PD index correlates best with the activity observed. This limitation is overcome via the use of dose-fractionation studies [52-55]. In these studies, the same total daily dose of the drug is administered over different

time intervals and hence, each dosage regimen will have a different Cmax/MIC, T> MIC but the same $AUC_{0-24}$/MIC.

In vitro models used to study antimicrobial pharmacodynamics could be divided into two groups based on whether the pathogen is exposed to constant or fluctuating concentrations of the anti-infective agent. Although models with static concentrations are useful to study the concentration dependence of the agent, these models do not simulate the in vivo situation where the drug concentration changes according to its pharmacokinetics. Dynamic models, on the other hand, can be used to mimic the antimicrobial pharmacokinetics in order to identify the dominant PK/PD index. For this purpose, experiments are conducted with varying doses and frequencies as mentioned above and the PK/PD index that shows best correlation with the antimicrobial activity is chosen as the primary index for the drug under investigation. End points for antimicrobial activity that are used in these studies include the time to kill 90% or higher of the initial inoculum , log change in the count after the exposure to the drug for a certain period of time (Δ log), and areas of the kill curve that depends on both the time and changes in the count. These areas include the area under the bacterial kill curve from time zero to t (AUBC), the area above this curve (AAC), the area between the control growth curve and the bacterial kill curve from the time zero to t (ABBC) or to the time point when the regrowth curve reaches the maximum value observed by the control ($I_E$; intensity of the effect) [56].

Dose fractionation studies have also been used extensively in in vivo models to determine the outcome-linked PK/PD index [47,57-59]. The drug is usually administered into infected normal or neutropenic mice and the colony forming units (CFU) remaining in

the body after 24 hours of therapy or the survival of the mice after several days of therapy is plotted against the PK/PD indices to find the best predictor of activity. Accumulated clinical PK/PD data have demonstrated that the target levels of the PK/PD index that were necessary for clinical effectiveness were similar to those identified in animal models [60].

### 1.3.5 Applications of Pharmacometrics in Anti-Infectives Research

Knowledge of PK/PD indices of anti-infective agents has allowed optimization of their clinical and microbiologic efficacy. This has been mainly performed through the use of Monte Carlo simulation approach. This approach was introduced in anti-infective research by Dr. George Drusano at a meeting of the FDA Anti-Infective Drug Products Advisory Committee [61] and has been heavily used since then in anti-infective research. Monte Carlo simulation is a stochastic simulation which means that it treats the parameters as random variables that follow certain distributions with finite means and variances [62]. This tool allows researchers to account for the variability of the anti-infective exposure as well as the variability of the susceptibility of the pathogen to this agent. The variability in the drug exposure has been recently characterized via the use of population pharmacokinetic modeling approach which was discussed in section 1.2. Variability in the susceptibility of the organism is usually obtained from the MIC data collected in national surveillance studies. Incorporation of the variability of pharmacokinetics and pharmacodynamics in the Monte Carlo simulation analysis allows characterization of the distribution of the levels of the PK/PD index in a simulated patient

population and the estimation of the probability of attaining the outcome-linked PK/PD target.

The PK/PD approach coupled with Monte Carlo simulation has wide applications in the anti-infective therapy. It has shown great value in comparing the efficacies of different drugs or different doses of the same drug against different pathogens. Such information has been widely used to develop formularies and establish treatment guidelines such as the guidelines for acute bacterial rhinosinusitis, community-acquired and nosocomial pneumonia and otitis media [63,64]. Monte Carlo simulation also provides a useful tool to define the susceptibility breakpoints for the anti-infective agents using integrated PK/PD information rather than defining these breakpoints only on the basis of the distribution of MIC values in the collected isolates [65]. Finally, Monte Carlo simulation has been also applied in drug development to optimize the dosage regimens of the anti-infectives under investigations in Phase 2 and 3 studies [61,66]. This use of PK/PD knowledge is advocated by FDA and is often confirmed and/or refined after PK/PD analysis of data from late stage development studies [67].

## 1.4 SCOPE AND OBJECTIVES OF THE DISSERTATION

The scope of this dissertation is the application of PK/PD modeling in assessment of anti-infective agents. The specific objectives of the projects were:

1- Development of a population pharmacokinetic model for Efavirenz that describes the maturation of its metabolic clearance in children and adolescents.

2- Use of Monte Carlo simulation for pharmacodynamic profiling of ceftobiprole, dalbavancin, daptomycin, tigecycline, linezolid and vancomycin in the Treatment of Methicillin Resistant Staphylococcus aureus (MRSA) in the ICU Settings.

3- Use of response surface analysis to quantify the effect of vancomycin/rifampin combination against MRSA biofilm.

4- Pharmacodynamic assessment of moxifloxacin vs. vancomycin against MRSA and methicillin resistant Staphylococcus. epidermidis (MRSE) and evaluation of the efficacy-linked PK/PD indices.

**Figure 1-1: Flowchart of Population Pharmacokinetic Models Development**

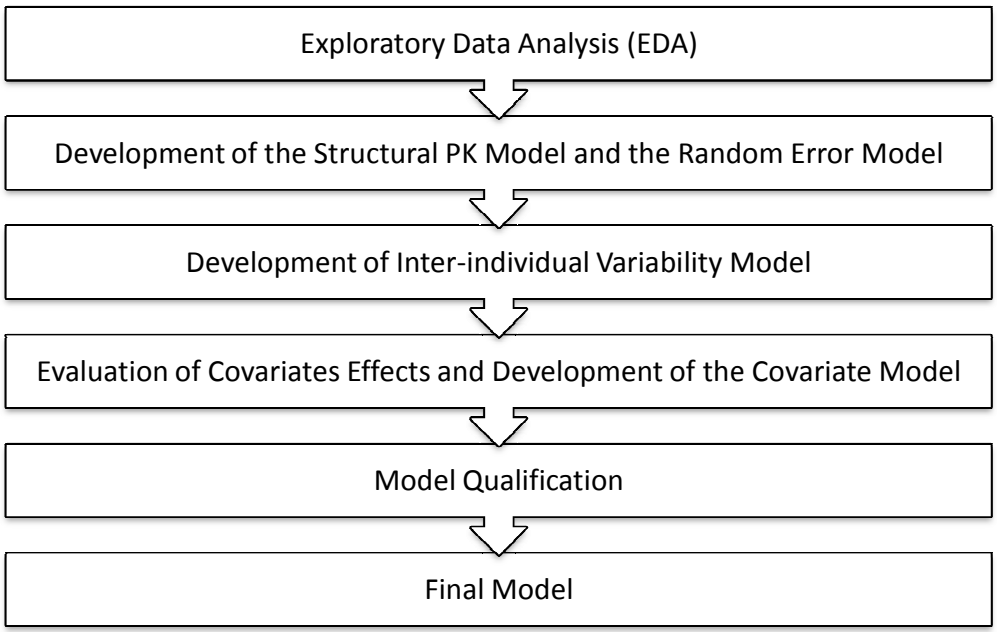

**Figure 1-2: Pharmacokinetic/Pharmacodynamic Indices of Anti-Infective Agents**

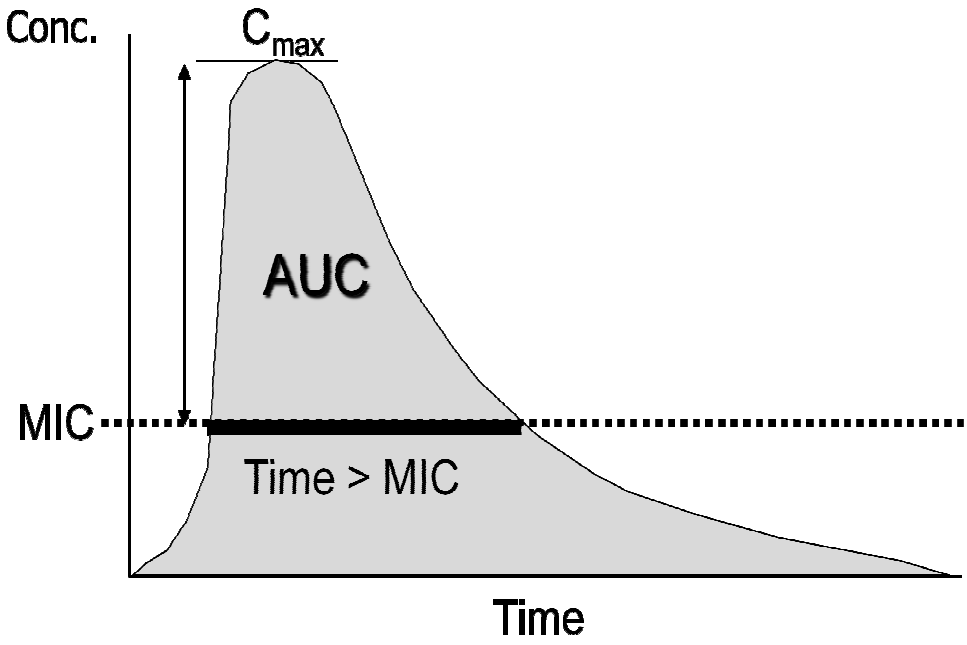

# Population Pharmacokinetic Analysis of Efavirenz in Pediatric Human Immunodeficiency Virus (HIV) Patients

# 2.1 INTRODUCTION

Efavirenz is a potent non-nucleoside reverse transcriptase inhibitor (NNRTI) that is indicated in combination with other antiretroviral agents for treatment of human immunodeficiency virus type 1 (HIV-1) infection [1]. Efavirenz is highly bound to plasma proteins, predominantly albumin [2]. It is mainly metabolized by the Cytochrome P450 enzymes to hydroxylated derivatives that are subsequently glucouronidated and renally excreted [2].

High inter- and intra-individual variability in efavirenz pharmacokinetics (PK) has been observed in both adults and children [3-5]. This variability is of particular concern due to the narrow therapeutic index of efavirenz [6,7]. Studies have shown that elevated efavirenz concentrations are associated with an increased risk of central nervous system (CNS) toxicity [8] and elevated liver enzymes [9]. In addition, differences in efavirenz concentrations were found between responders and non-responders [4] and children with higher intra-individual variability have been reported to have higher likelihood of viral rebounds and a shorter time to their first viral rebound [3].

Sources of efavirenz PK variability have been extensively studied in adults [4,5,10-12]. Covariates found to account for this variability include the polymorphic nature of Cytochrome P450 2B6 (CYP2B6) and other isoforms that are responsible for efavirenz metabolism [13-16]. In addition, some studies have shown efavirenz PK to vary across genders and ethnicities [10-12,17]. Nevertheless, little information is available about the correlation between efavirenz PK parameters and pediatric population covariates and the influence of developmental changes that take place during infancy and childhood on

CYP2B6 expression and efavirenz pharmacokinetics [18]. Moreover, some clinical studies have reported high prevalence of subtherapeutic efavirenz levels among children suggesting need to develop alternative dosing guidelines for this important population [19-21]. The aims of the current study were to quantify inter-individual and intra-individual variability of efavirenz pharmacokinetics in pediatric HIV-1 patients, to identify factors that describe this variability including growth and maturation and to develop a population pharmacokinetic model that incorporate these covariates in order to guide efavirenz dosing in children.

## 2.2 METHODS

### 2.2.1 Patient Population and Study Design

The population pharmacokinetic analysis included efavirenz plasma concentration data from HIV-1 infected children who participated in the Pediatric AIDS Clinical Trials Group 382 (PACTG382) study [22]. This was an open label Phase I/II study that was conducted on children who were less than 16 years old and had a plasma HIV-1 RNA level of more than 400 copies per milliliter using the reverse-transcription polymerase chain reaction (Amplicor™) Monitor assay. The trial included two cohorts; cohort I enrolled patients who were 3-16 years old, and cohort II where the age of the patients was between 2 months and 8 years at the time of enrollment. The trial was approved by the institutional review boards of all the eighteen participating sites. Informed written consent was obtained from the parents or guardians of the patients.

Efavirenz was administered orally as one of three formulations, capsule, suspension or solution. It was initially dosed allometrically according to the following formula: Dose (in milligrams/day) = (weight of child in kilograms $\div 70)^{0.7}$ x (600 for the capsule formulation or 720 for the oral suspension or solution). Doses were rounded to the nearest 25 milligrams increment. Blood samples were obtained for quantification of the efavirenz concentration before a dose and 2, 5, 8, and 12 hours after a dose at weeks 2, 6, 10 if necessitated by a dosage change, 56 and 112. Additional samples after 6 and 24 hours were obtained for cohort I patients. A 24 hours steady-state area under the concentration time curve ($AUC_{24}$) was computed at weeks 2 and 6 and used to guide efavirenz dosing. If the AUC for efavirenz was not within the prespecified target range of 190 to 380 µM.hr, the efavirenz dose was adjusted proportionately, up to a 200-mg

maximum dosing increase. Patients were monitored for up to 4 years and clinical evaluations that included efavirenz trough concentrations and determination of plasma HIV-1 RNA levels were conducted monthly.

### 2.2.2 **Population Pharmacokinetic Analysis**

All subjects who had at least one efavirenz plasma concentration were included in the analysis. Pharmacokinetic model fittings were performed using the nonlinear mixed effects modeling methodology as implemented in the NONMEM software (Version VII, level 1.2) [23] . The first-order conditional estimation with INTERACTION was used throughout the model development. Diagnostic graphical analysis was performed using R (Version 2.10.1).

*Development of the Population Pharmacokinetic Base Model*

Based on exploratory data analysis and our previous experience with efavirenz [3,19], we used a one-compartment model with first order absorption and elimination (ADVAN 2 subroutine in NONMEM). The model was parameterized in terms of absorption rate constant, oral clearance (CL/F), apparent volume of distribution (V/F). Four residual error models were explored; namely, exponential error model, proportional error model, additive error model and combined proportional plus additive error model. Individual CL/F and V/F were assumed to be log normally distributed and their variability was estimated using an exponential error model as follows:

$$\theta_i = \theta \times \exp(\eta_i)$$

Where $\theta$ is the typical population PK parameter estimate, $\theta_i$ is the individual PK parameter and $\eta_i$ is the random variable representing the difference between the $\theta_i$ and $\theta$

which is assumed to be independent and normally distributed around 0 with a variance that represents the variability of the PK parameter. Since patients were sampled on several occasions over several years, partitioning the variability of the PK parameters into inter-individual (IIV) and inter-occasion variability (IOV) was tested.

*Development of the Covariate Model*

Covariates screened for their possible effect on pharmacokinetic parameters included body weight, body surface area, age, race, gender, formulation, CYP2B6-G516T polymorphism, Multidrug-resistance transporter gene (MDR1) C3435T polymorphism and liver function tests (Bilirubin, BUN, AST, ALT). Covariate modeling was done using the forward-inclusion, backward-elimination approach and was guided by evaluation of the empiric bayesian PK parameters estimates vs. covariates plots as well as changes in the estimates of PK parameters variability and residual variability. Mixture modeling as implemented in NONMEM was used to identify any significant patterns in patients whose CYP2B6-G516T genotype or MDR1-C3435T genotype was missing (about 25% of the patients).

Body weight was chosen as the primary covariate in the population analysis [24]. Both total body weight and fat free mass were used as a measure of body size and the results were compared [25]. Fat free mass was computed from total body weight (WT) and height (HT)using the following equations [26]:

$$FFM\ (male) = \frac{42.92 \times WT}{30.93 + WT/HT^2}$$

$$FFM\ (female) = \frac{37.99 \times WT}{35.98 + WT/HT^2}$$

CL/F and V/F were allometrically scaled to a weight of 70kg to allow the use of the model for prediction of adult pharmacokinetics and to facilitate comparison of the parameter estimates with those obtained in other studies [24]. The exponent in the allometric model was fixed to 0.75 and 1, for CL/F and V/F, respectively to allow separation of the effect of growth and body size from the effect of age and maturation in the children [27].

The maturation of CL/F in the patients was tested using a sigmoid E-max model to allow a gradual increase in clearance during early life years and a mature clearance to be achieved at a later age as following [27,28]:

$$CL/F = CL_{pop} * \left(\frac{WT}{70}\right)^{0.75} * \frac{AGE^{H_{CL}}}{AGE^{H_{CL}} + TM_{50,CL}^{H_{CL}}}$$

Where $CL_{pop}$ is the population estimate for the oral clearance standardized to a 70-kg person using allometric model ; WT is the weight of the subject in kilograms, AGE is the postnatal age of the subject in months, $TM_{50,CL}$ is the age in months at which clearance is 50% that of the mature value and $H_{CL}$ is the Hill coefficient for the maturation of the oral clearance.

Maturation of volume of distribution was explored using a similar sigmoid Emax model as well as using the following exponential asymptotic model [27,29,30]:

$$V/F = V_{pop} * \left(\frac{WT}{70}\right) * \left[1 + \beta * EXP\left(-AGE\ x\ \frac{Ln(2)}{T_{\frac{1}{2}}}\right)\right]$$

Where $V_{pop}$ is the population estimate for the apparent volume of distribution standardized to a 70-kg person using allometric model, β is a parameter estimating the

fractional volume upon birth and $T_{\frac{1}{2}}$ describes the maturation half-life of the age-related changes in the apparent volume of distribution.

Differences in bioavailability among the three efavirenz formulations were tested using relative bioavailability fraction. Oral capsule was used as the reference formulation in this comparison. We used an exponential error model to explore the need for an inter-individual variability term to describe the variability of the relative bioavailability. Change in relative bioavailability with age was assessed using the sigmoid Emax model:

$$F_{Liq/Cap} = F_{pop} * \frac{AGE^{H_F}}{AGE^{H_F} + TM_{50,F}^{HH_F}}$$

Where $F_{pop}$ is the estimate for relative bioavailability achieved at maturity; $TM_{50,F}$ is the age in months at which the relative bioavailability is 50% that of the mature value and $H_F$ is the Hill coefficient for the maturation of the relative bioavailability.

The models throughout the population analysis were evaluated by the examination of the convergence of the estimation and covariance routines and the visual assessment of the diagnostic plots; including, but not limited to; the agreement in scatterplots of the population and individual predicted versus measured observations and the lack of trends or patterns in scatterplots of conditional weighted residuals versus predicted observations and versus time.

Precision of the final model parameters estimates was assessed using the asymptotic standard errors obtained by the covariance routine in NONMEM as well as by the bootstrap confidence intervals. In bootstrapping, patients were randomly sampled with replacement from the dataset that was used in model development to obtain 500 datasets that have the same number of patients as the original dataset. The final model

was then fitted to each of these datasets and the parameter estimates were compared to the estimates from the original dataset.

*Model Qualification*

The final model was qualified by prediction-corrected visual predictive check (PC-VPC) where the final parameter estimates were used to simulate 1000 replicates of the observed dataset. Both observations and the simulated data were normalized for the typical model prediction in each bin in order to account for variation in sampling times and predictive covariates introduced by binning of the observations [31]. The median, 5$^{th}$ and 95th percentile concentrations of the simulated datasets were then plotted against the original observations. Bootstrapping and PC-VPC simulations were performed using Perl Speaks NONMEM (PsN, version 3.1) [32].

## 2.3 **RESULTS**

A total of 3172 plasma concentrations from 96 subjects were analyzed. The baseline characteristics of the subjects are shown in Table 2-1. A one compartment disposition model with first order absorption and elimination adequately described the data. Combined proportional and additive error model best accounted for the residual unexplained variability of the observed concentrations. IOV of the oral clearance was found to be significant and was incorporated into the model. IOV of the apparent volume of distribution, on the other hand, was minimal and hence was not added to the model.

Covariate analysis is summarized in Table 2-2. Use of fat free mass as a body size covariate was equivalent to the use of total body weight and did not explain more of the variability in CL/F or V/F and hence total body weight was incorporated into the model for simplification. CL/F increased with age reaching 90% of its mature value by the age of 9 months (Figure 2-1). The mature CL/F was estimated to be 11.2 $L.hr^{-1}.70kg^{-1}$ (90% confidence interval: 10.2-13.5). Children with the CYP2B6-516-T/T genotype were found to have an oral clearance that is 51% lower than that of the other children. No decrease in oral clearance was observed in children with CYP2B6-516-G/T genotype and mixture modeling did not suggest the presence of the T/T genotype in children whose genotype information was missing.

The model suggested lower bioavailability for the oral liquid formulations compared to the capsule formulation with no difference in bioavailability between the suspension and the solution. The relative bioavailability was found to increase with age to reach a mature value of 0.79. Change in relative bioavailability due to age was initially described by a sigmoid Emax model. However, the Hill factor was not significantly

different from 1 and hence the maturation model was reduced to an Emax model and the Hill factor was fixed to 1.

After accounting for the previous covariates, no influence on CL/F or V/F was attributable to gender, race, liver function markers, or MDR-1 polymorphism. In addition, no age related changes in volume of distribution was found. Covariates explained 11% and 16% of the variability in CL/F and V/F, respectively. The final model included body weight effect on CL/F and V/F, a sigmoid Emax maturation function and CYP2B6-516-T/T genotype effect on CL/F as well as a formulation effect on the drug bioavailability and an Emax model to describe the age related changes in relative bioavailability. Estimates from the final model parameters and the precision associated with their estimation are shown in Table 2-3. The final equation for CL/F was as follows:

$$Oral\ Clearance\ (L/hr) = 11.2 * \left(\frac{WT\ in\ kg}{70}\right)^{0.75} * \frac{(AGE\ in\ months)^{3.4}}{(AGE\ in\ months)^{3.4} + 4.6^{3.4}} * 0.49^{Flag}$$

Where Flag is equal to 1 if the patient has a CYP2B6-516-T/T genotype or is equal to 0 if not. The final equation for the relative bioavailability of oral liquids compared to the oral capsule was as follows:

$$F_{Liq/Cap} = 0.79 * \frac{AGE\ in\ months}{AGE\ in\ months + 10.6}$$

The goodness of fit to the pharmacokinetic data is demonstrated in Figure 2-2 and Figure 2-3. Population predicted concentrations are predicted using population parameter estimates and covariate information while individual predicted concentrations are based on post hoc empiric Bayes estimates of the PK parameters. The conditional weighted

residuals plots showed symmetrical distribution and no time or concentration related trends (Figure 2-4 and Figure 2-5).

The median, $5^{th}$ and $95^{th}$ percentiles of the parameter estimates from the fit of the final model to the bootstrap samples are shown in Table 2-3. The asymptotic estimates obtained from the original dataset showed close agreement with the median and were all included within the $5^{th}$ to the $95^{th}$ percentile of the bootstrapping values indicating model stability. The results from the PC-VPC are shown in Figure 2-6. About 90.7% of the original data fit within the $5^{th}$ and $95^{th}$ percentiles of the simulated datasets.

## 2.4 DISCUSSION

Pediatric patients can exhibit differences in absorption and distribution, altered activity of metabolizing enzymes and immature renal function that result in pharmacokinetic profiles that are not predictable from pharmacokinetics in adults. These differences are due to physiological changes that are associated with two distinct processes; growth and development [25]. Influence of these two processes could be examined by investigating the effect of body size and age, respectively, on drug pharmacokinetics. Due to the lack of information on the development or the maturation of efavirenz pharmacokinetic parameters in pediatrics, current dosing guidelines are solely based on body weight [33]. This is insufficient [34-36] and contributes to the vulnerability of pediatric patients to drug toxicities, suboptimal therapy and emergence of resistance [33].

In this study, we present a population pharmacokinetic model that describes the effect of growth and maturation on efavirenz pharmacokinetics in pediatrics. We have used the allometric size model to characterize the influence of body size on efavirenz clearance and volume of distribution due to its strong mechanistic and biological basis [37,38]. Since adipose tissue has minimal contribution to clearance and has distribution characteristics, different fractions of fat mass were proposed as predictors of the effect of body size on pharmacokinetic parameters [25]. In our study, we compared the use of fat free mass to the total body weight. Adjustment for the fat free mass has been previously shown to improve the description of the link between size and clearance [39]and golmerular filtration rate [40]. In the current study, however, fat free mass was found to explain similar

magnitude of the variability in CL/F and V/F as the total body weight and consequently total body weight was used throughout the model development. This observation could be explained by the minimal fat tissue in HIV-infected children in general [33].

The exponents of the allometric size models were fixed at 0.75 and 1 for clearance and volume, respectively. Fixing these parameters allowed overcoming the strong collinearity between age and weight in pediatrics and enabled the separation of their influences on efavirenz pharmacokinetics [27]. Maturation of the oral clearance was described using a sigmoid Emax model. This model was successfully applied previously to examine the maturation of vancomycin clearance in premature neonates [28]. Compared to other models that have been also used to describe maturation[29,30,41,42], sigmoid Emax model has the distinct advantage of reaching asymptotic mature value in adults and not predicting biologically unreasonable values [25]. In our study, the model predicted an increase in CL/F by age to reach 90% of its mature value by the age of 9 months. Interestingly, the estimates of the maturation model parameters; $TM_{50,CL}$ and $H_{CL}$, are very similar to their reported estimates in the maturation models of GFR[40] and drugs that are metabolized by Phase II metabolism such as acetaminophen[25] and morphine[43]. This finding may indicate similar maturation profile for drugs irrespective of their elimination route.

Effect of age on efavirenz oral clearance in children was recently investigated using a population pharmacokinetic analysis [44]. The study demonstrated a decrease in the oral clearance by age in the patients whose age ranged from 2.77 to 14.70 years. Maturation of hepatic metabolizing enzymes are known to be completed by the age of 2 years and children are considered mature from a pharmacokinetic perspective and differ

from adults only in size [45]. Therefore, the decline in clearance reported in the study is unlikely to be due to age. This time trend could be explained by the use of nonphysiologically based linear model to account for the weight effect on clearance. The increase in efavirenz oral clearance with age that is demonstrated in our study is consistent with a recent study that reported an increase in the expression of CYP2B6, the primary catalyst of efavirenz metabolism, with age [18]. In addition, the model predicted an adult or a mature value of 11.2 $L.hr^{-1}.70kg^{-1}$ (90% confidence interval: 9.9-12.5) for oral clearance which is in close agreement with estimates from population pharmacokinetic studies conducted in adults which ranged between 9.4 and 10.8 L. $hr^{-1}$ [5,11,12]. This further supports the validity of the allometric size model and sigmoid Emax maturation model and their potential in predicting adult pharmacokinetic parameters from pediatric data [27].

In accordance with our previous findings that reported a 57% reduction in the median oral clearance in patients with CYP2B6-516-T/T genotype [46], the population pharmacokinetic model estimated a 51% decrease in the oral clearance in patients with CYP2B6-516-T/T genotype. Association between CYP2B6-G516T polymorphism and increased efavirenz exposure has been reported in several studies [13-16]. It has also been linked to an increased risk of CNS toxicities such as dizziness, insomnia and depression [16]. Lang et al [47] has reported a 28.6% prevalence of the CYP2B6-516-T/T genotype but this frequency increases to 50% in African populations [48,49]. Our results support a genotype specific dosing for efavirenz where patients with the CYP2B6-516-T/T genotype can receive 30-50% of the standard dose [13,50]. This pharmacogenetics guided dosing has been implemented in a Japanese cohort study and resulted in improvement of CNS side effects while maintaining the therapeutic efficacy [51].

We were unable to describe a change in apparent of volume of distribution with age. This could be explained by the fact that maturation of volume of distribution is usually completed within few weeks after birth [45]. Since our study cohort did not include any neonates, characterization of this physiological process was not feasible. On the other hand, we were able to describe an increase in the relative bioavailability of the oral liquid formulations compared to the capsule with age using an Emax model. The model estimated a mature value of 0.79 for the relative bioavailability which is consistent with studies in adults that resulted in the 20% dose increase recommended by the manufacturer when oral liquid formulations are used [52]. However, the model suggests that at age 1 and 3 years, the relative bioavailability is only 0.42 and 0.61, respectively and 90% of the mature value is reached at age of 8 years. Likewise, previous studies have estimated the relative bioavailability of the oral liquids in children to be 0.47 and 0.62 [52,53]. Such low bioavailability may explain the high incidence of subtherapeutic efavirenz levels among children [19-21] and suggests the need to use oral liquid formulations at doses that are 150% of the capsule doses.

In our analysis, we were unable to demonstrate an association between the MDR1-C3435T polymorphism and any of the efavirenz pharmacokinetic parameters. MDR-1 gene is the gene that codes for the cellular drug efflux pump; P-glycoprotein and its expression enhances elimination and reduces drug exposure [54]. Previous studies have had contradicting results with regards to the influence of MDR1-C3435T polymorphism on efavirenz exposure [55,56]. Fellay et al [56] has reported an association between MDR1-C3435T polymorphism and efavirenz pharmacokinetics. Haas et al [55] on the other hand, has found this polymorphism not to be associated with altered efavirenz exposure but it

was a predictor of a decreased risk for virologic failure and a lower incidence of resistance emergence. Moreover, an in vitro study has failed to show that efavirenz is a substrate for P-glycoprotein [57].

No effect of gender or race was found in our analysis on efavirenz clearance. Some previous studies have also shown no correlation between efavirenz pharmacokinetics and race [58] or gender [5,11,13,58]. This could be attributed to the insignificant differences in CYP2B6 expression between males and females [18]. Other studies, however, have reported lower efavirenz levels in males than in females [10,17] and lower clearance in blacks and Hispanics than in whites [11-13].

After accounting for the covariates effect on clearance, the remaining inter-individual and inter-occasion variability in efavirenz oral clearance was still high (45.7 and 30.0%, respectively). Similarly high variability has been estimated in other studies as well [4,5,59,60] and could be attributed to polymorphisms in metabolizing enzymes and to the unique circumstances that hinder adherence in HIV-infected children [33]. About 20 to 250-fold inter-individual variability is believed to exist in CYP2B6 expression at the level of mRNA, protein and catalytic activity [50,60]. In addition, polymorphisms in CYP2A6 and CYP3A4 isoforms have been recently associated with efavirenz inter-individual variability in clearance [13]. Such high variability in efavirenz pharmacokinetics may suggest the need for therapeutic monitoring of the drug levels in order to optimize its antiviral effect and minimize its toxicity [59].

In conclusion, we have described the first population pharmacokinetic model that accounts for the influence of growth, maturation and CYP2B6 G516T polymorphism on efavirenz pharmacokinetics. The model shows good predictability performance and its

application to improve dosing and optimize exposure in pediatrics warrants further investigation.

**Table 2-1: The baseline characteristics of the subjects included in the analysis**

| Characteristic | Value |
|---|---|
| Age--(months) | |
| Mean ±SD | 68.4±48.6 |
| Median | 66 |
| Range | (2-202) |
| Weight --(kilogram) | |
| Mean ±SD | 20.5±13.6 |
| Median | 18.7 |
| Range | (4.8-96.4) |
| Body Surface Area* -- ($m^2$) | |
| Mean ±SD | 0.76±0.33 |
| Median | 0.75 |
| Range | (0.27-2.07) |
| Sex --no. (%) | |
| Female | 57 (59) |
| Male | 39 (41) |
| Race --no. (%) | |
| Non-Hispanic, White | 12 (13) |
| Non-Hispanic, Black | 54 (56) |
| Hispanic | 28 (29) |
| Native American | 1 (1) |
| Others | 1 (1) |
| CYP2B6-G516T Polymorphism --no. | |

| | |
|---|---|
| (%) | 34 (36) |
| G/G | 28 (30) |
| G/T | 12 (13) |
| T/T | 22 (23) |
| Missing | |
| MDR1-C3435T Polymorphism -- no. (%) | |
| C/C | 31 (33) |
| C/T | 33 (35) |
| T/T | 7 (7) |
| Missing | 25 (26) |

* Calculated using the Mosteller formula [61]:

$BSA\ (m^2) = (Height(cm) \times Weight(kg)]/\ 3600)^{0.5}$

**Table 2-2: Impact of sequential inclusion of covariates on objective function value (OFV)**

| Model | OFV | ΔOFV |
|---|---|---|
| Base Model | 4155.3 | 0 |
| Allometric Model | 4114.6 | -40.7 |
| Allometric Model + Formulation effect on BAV | 4085.2 | -70.1 |
| Allometric Model + Formulation effect on BAV+ CYP2B6 Polymorphism on CL/F | 4064.2 | -91.1 |
| Allometric Model + Formulation effect on BAV + CYP2B6 Polymorphism on CL/F +Maturation of CL/F | 4046.6 | -108.7 |
| Allometric Model + Formulation effect on BAV + CYP2B6 Polymorphism on CL/F +Maturation of CL/F + Maturation of Relative BAV | 4022.3 | -133 |

OFV is a measure of goodness of fit and is equal to -2*log likelihood; ΔOFV= OFV of the model-OFV of the base model; BAV is the bioavailability.

**Table 2-3: Final Model Parameter Estimates from fit to the original dataset and the 500 bootstrap samples:**

| Parameter | Original Dataset | | Bootstrap Datasets | |
|---|---|---|---|---|
| | Estimate (RSE%) | 90% C.I. | Median | $5^{th}$-$95^{th}$ Percentiles |
| $K_a(hr^{-1})$ | 0.84 (12.6) | 0.68-1.05 | 0.84 | 0.68-1.06 |
| $CL_{pop}(L.hr^{-1}.70kg^{-1})$ | 11.2 (6.8) | 9.9-12.5 | 11.4 | 10.0-12.6 |
| $TM_{50,CL}$ (months) | 4.6 (8.6) | 3.9-5.3 | 4.6 | 3.9-5.6 |
| $H_{CL}$ | 3.4 (8.1) | 2.9-3.9 | 3.4 | 2.8-6.9 |
| $\theta_{Cyp}$ | 0.49 (11.5) | 0.40-0.58 | 0.47 | 0.39-0.59 |
| $V_{pop}(L.70kg^{-1})$ | 468.0 (8.7) | 400.8-535.2 | 468.4 | 412.1-548.4 |
| $F_{pop}$ | 0.79 (12.5) | 0.63-0.95 | 0.80 | 0.65-1.00 |
| $TM_{50,F}$ (months) | 10.6 (38.7) | 3.8-17.4 | 10.3 | 4.9-21.8 |
| IIV of CL/F (%CV) | 45.7 (28.4) | 24.3-67.1 | 44.8 | 32.7-54.7 |
| IIV of V/F(%CV) | 43.6 (30.5) | 21.7-65.5 | 43.3 | 31.6-55.3 |
| IOV of CL/F(%CV) | 30.0 (13.7) | 23.2-36.8 | 30.0 | 26.4-33.4 |
| IIV of $F_{pop}$ (%CV) | 39.9 (32.8) | 18.3-61.5 | 37.8 | 27.6-49.3 |

C.I. is confidence interval; *K*a is the absorption rate constant; $CL_{pop}$ is the population estimate for the oral clearance standardized to a 70-kg person using allometric model; CL/F is oral clearance; $TM_{50,CL}$ is the age in months at which CL/F is 50% that of the mature CL/F; $H_{CL}$ is the Hill factor in the maturation sigmoid Emax model for CL/F; $\theta_{Cyp}$ has an exponent of 1 if the patient has a CYP2B6-516-T/T genotype or is equal to 0 if not; $V_{pop}$ is the population estimate for the apparent volume of distribution standardized to a 70-kg person; $F_{pop}$ is the relative bioavailability of oral liquid formulations relative to the capsule formulation at maturity; $TM_{50,F}$ is is the age in months at which $F_{Liq/Cap}$ is 50% that of the mature value, IIV is inter-individual variability, IOV is inter-occasion variability. The residual unexplained variability in efavirenz observed concentrations was described by a proportional error of 25% and an additive standard deviation of 0.25 mg/L.

**Figure 2-1: Maturation of Oral Clearance**

Circles demonstrate individual predicted efavirenz oral clearance standardized to a 70-kg subject. Solid lines represent the sigmoid Emax model used to describe the relationship between age and oral clearance.

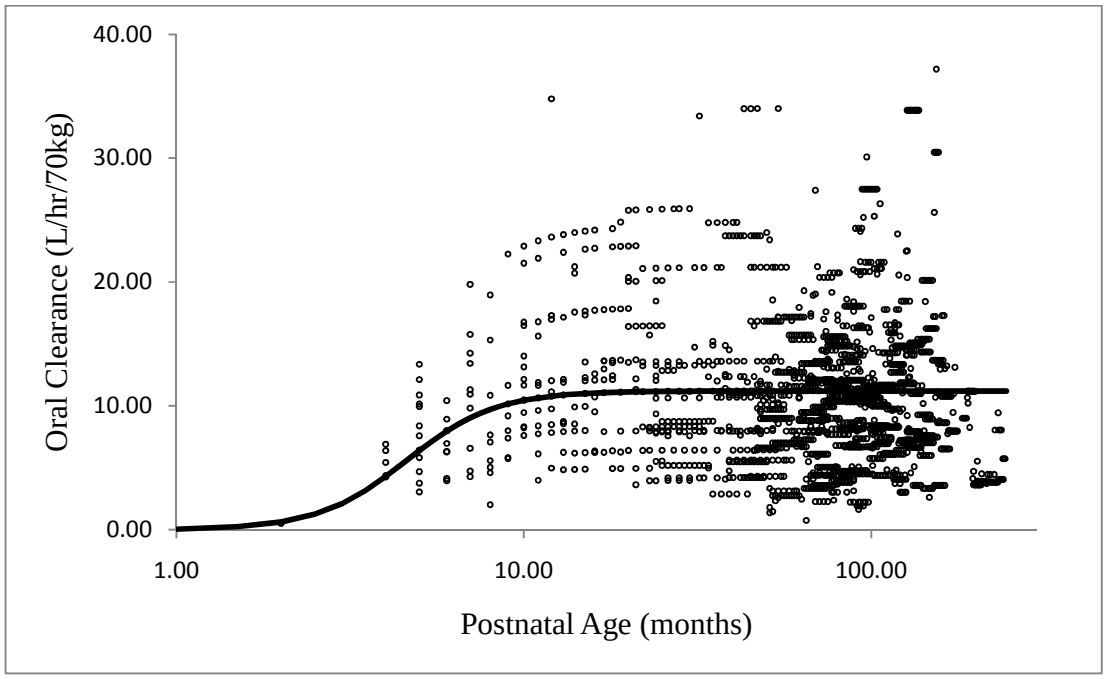

**Figure 2-2: Concordance plot of Observed Concentration versus Population Predicted Concentration (PRED)**

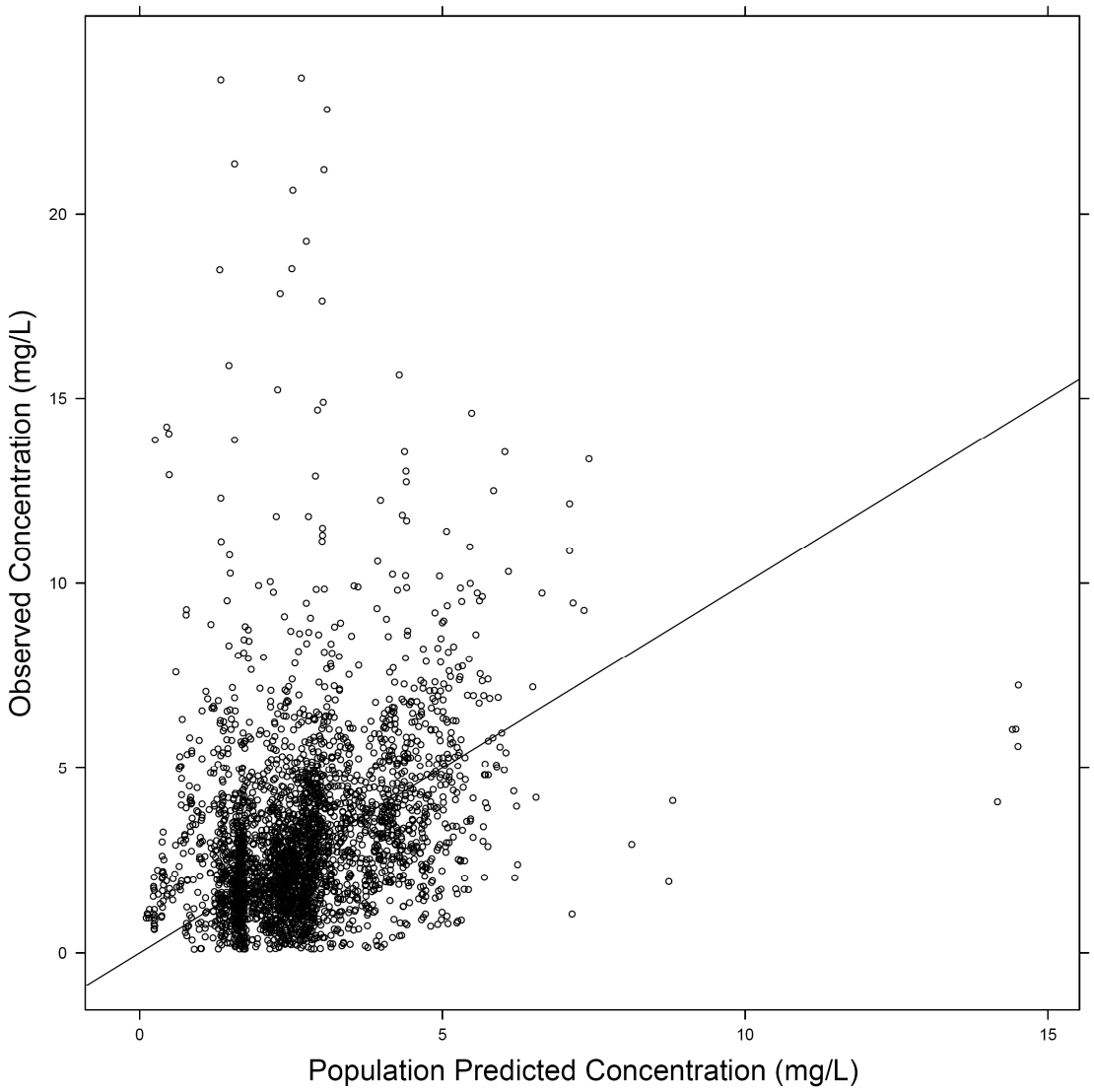

**Figure 2-3: Concordance plot of Observed Concentration versus Individual Predicted Concentration (IPRED)**

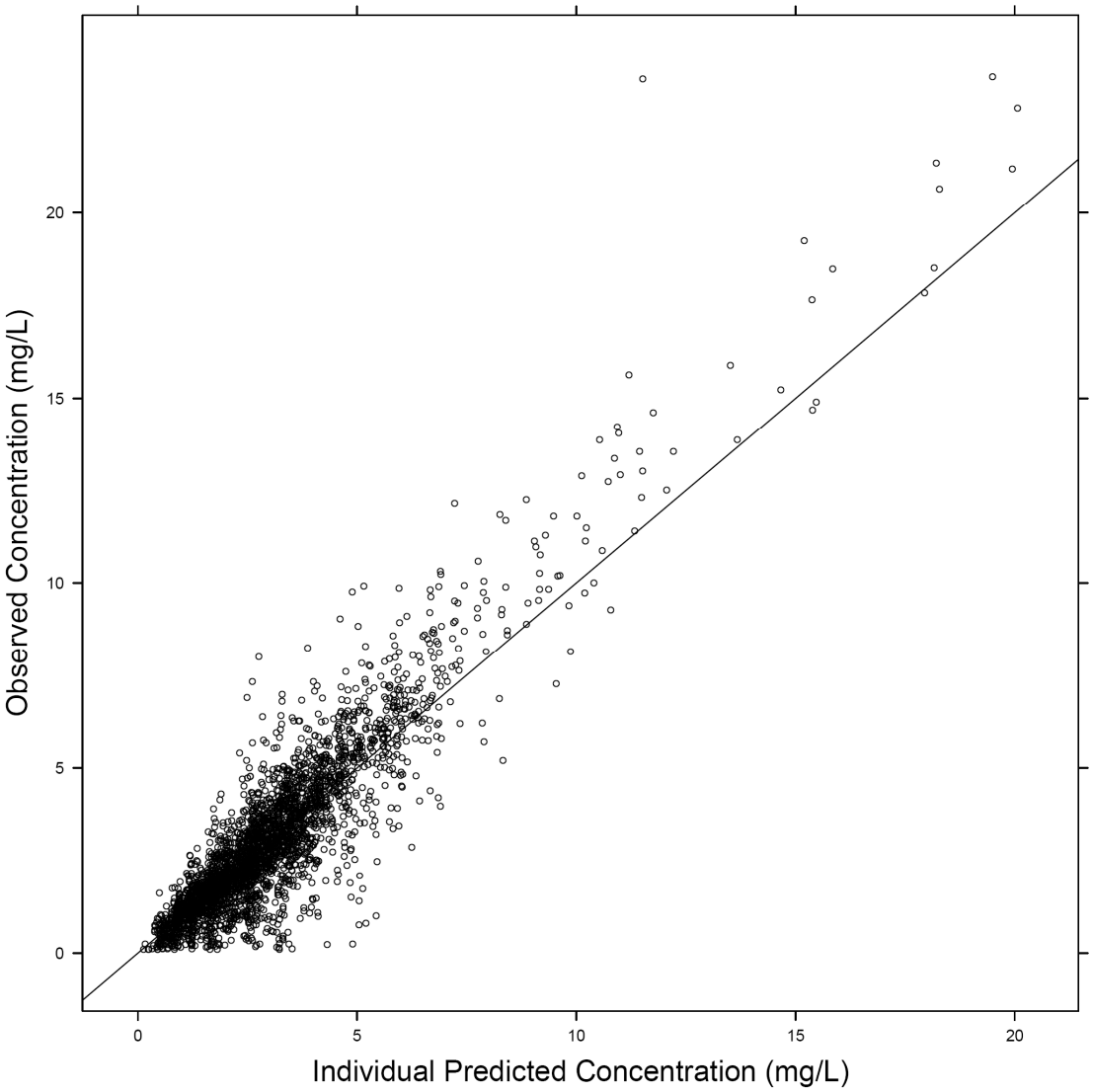

**Figure 2-4: Conditional Weighted Residuals versus Population Predicted Concentration**

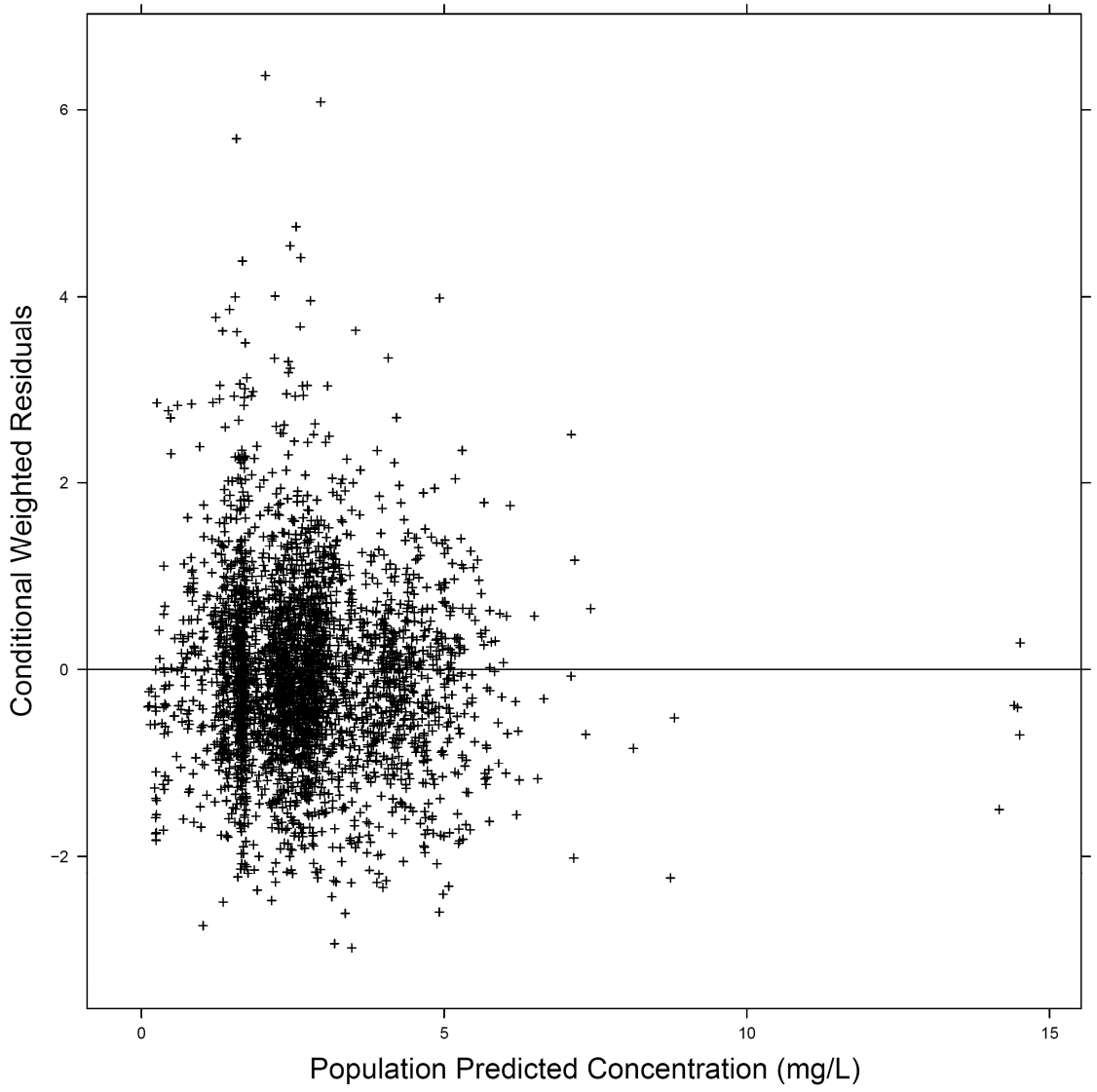

**Figure 2-5: Conditional Weighted Residuals versus Time after Dose**

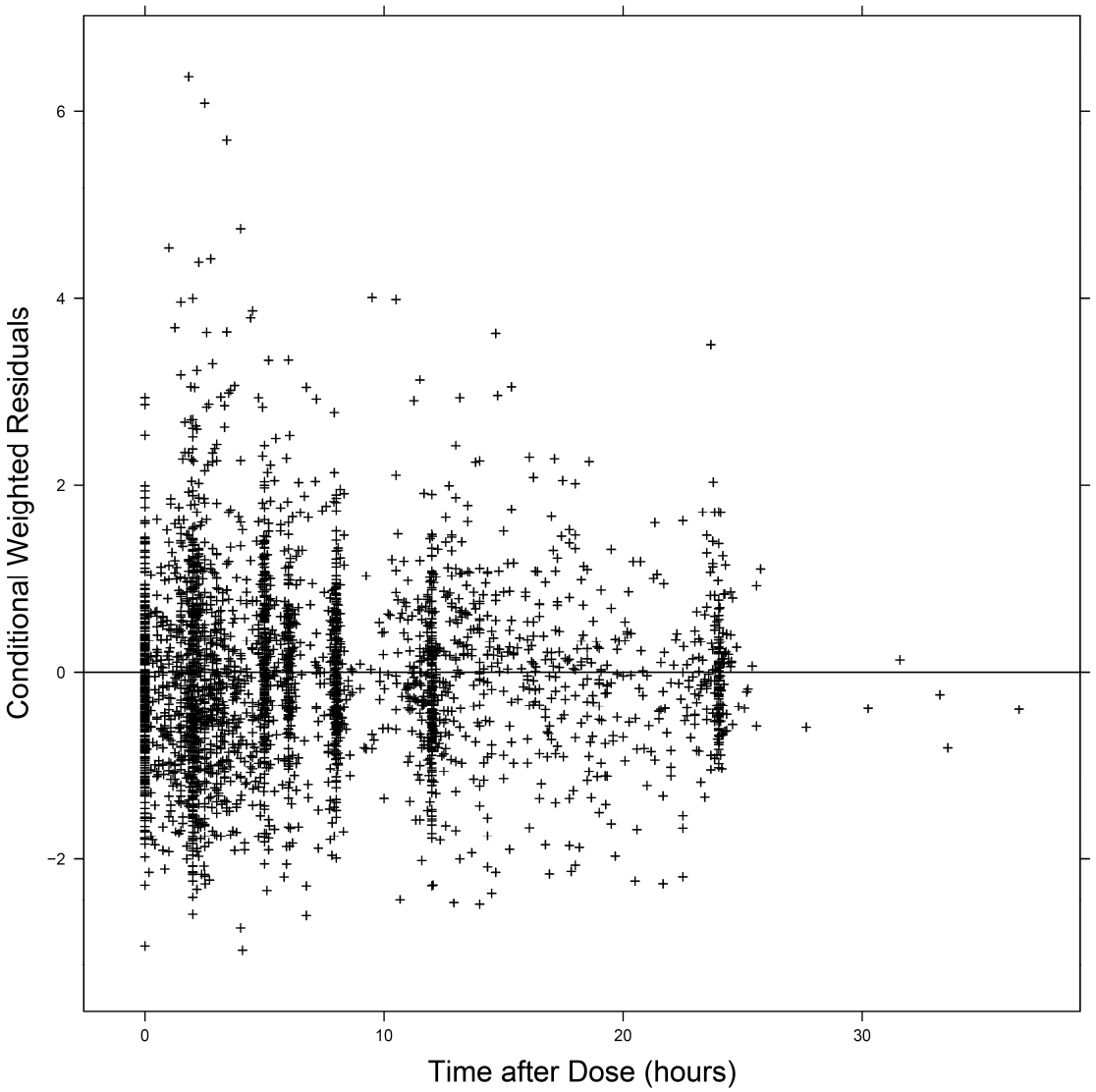

**Figure 2-6: Prediction Corrected Visual Predicted Check (PC-VPC) Plot of observed concentrations (open circles), median (solid line) and 5$^{th}$ and 95$^{th}$ percentiles (dashed lines) of 1000 simulated data sets**

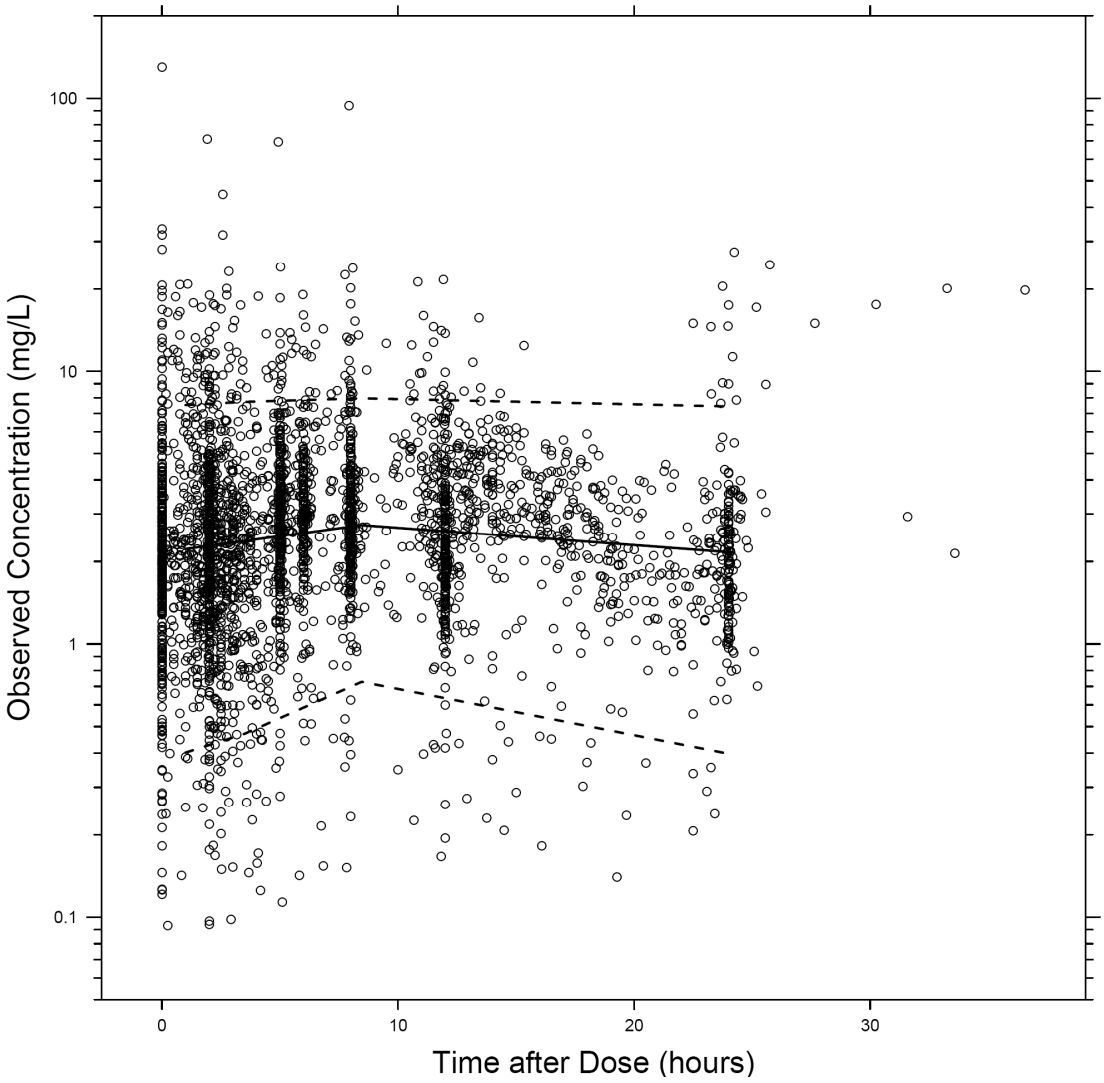

# Comparative Pharmacodynamics of Ceftobiprole, Dalbavancin, Daptomycin, Tigecycline, Linezolid and Vancomycin in the Treatment of MRSA-Infected ICU Patients

This chapter was presented in part in the Infectious Diseases Society of America meeting, October 2007

# 3.1 INTRODUCTION

Gram-positive organisms, such as *Staphylococcus aureus*, are among the most common pathogens infecting patients in the intensive care units (ICUs) [1]. Methicillin-resistant *S. aureus* (MRSA) has been reported to account for 55% of the ICU infections in the US [2]. MRSA is a multi-drug resistant pathogen that emerged concomitantly to the introduction of the penicillinase-resistant penicillins in the 1960s [3] and has continued to spread causing severe morbidity and mortality worldwide [4-6]. It has been shown that patients who suffered from MRSA bacteremia had longer ICU-stay and ventilator dependency, more acute renal failure and worse hemodynamic instability than those with methicillin-sensitive *S. aureus* (MSSA) bacteremia [7].

Historically, MRSA isolates were exclusively nosocomial in origin. However, in the past decade, there was a clonal spread of MRSA in the community [8] and community acquired infections due to MRSA (CA-MRSA) have been increasingly problematic reaching 30% in some areas [9-13]. Currently, CA-MRSA strains do not only imply origin in the community but also a different genetic strain of MRSA that exhibits distinct phenotypic differences from hospital acquired MRSA (HA-MRSA) strains with regards to antibiotic susceptibility, virulence and spectrum [14]. In addition, unlike HA-MRSA, CA-MRSA often arises in children and adults without any obvious risk factors. Although cross-resistance is less common among CA-MRSA strains than HA-MRSA strains, CA-MRSA strains are a significant threat because they carry a range of genes that may enhance its transmissibility and account for the faster growth and higher infection burden associated with CA-MRSA versus HA-MRSA [14,15].

The mainstay therapy for MRSA associated infections has been vancomycin for long time but its use lately has been associated with suboptimal outcomes [16-19]. The decreased susceptibility to vancomycin may be attributed to the loss of the function of the accessory gene regulator operon [20]. It has also been suggested that the underdosing of vancomycin in the past may have led to selective pressure for the evolution of heteroresistant MRSA strains that have low susceptibility to vancomycin [20]. Moreover, vancomycin has a poor tissue penetration which may limit its therapeutic value in nosocomial pneumonia and complicated skin and soft-tissue infections. [20,21].

In the last few years, new anti-MRSA agents, such as ceftobiprole, dalbavancin, daptomycin, linezolid and tigecycline, have been launched. Ceftobiprole is a novel beta-lactam that retains its activity against MRSA as well as a wide spectrum of gram positive and gram-negative pathogens [22]. Dalbavancin is a second generation glycopeptide that has a superior pharmacodynamic profile compared with vancomycin against MRSA [23-25]. Daptomycin is a cyclic lipopeptide antibiotic that has exhibited bactericidal activity against S. aureus (including MRSA) as well as other clinically relevant gram-positive bacteria [26-28]. Linezolid is the first oxazolidinone antibiotic and has activity against gram-positive pathogens including MRSA and vancomycin-intermediate Staphylococcus aureus (VISA) [29]. Finally, tigecycline is a glycycline that can eradicate tetracycline-resistant pathogens including MRSA [30].

Appropriate initial treatment choices are very critical in the ICU settings. However, it has been reported that less than 25% of patients with MRSA infections receive correct therapy within the first 48 hours of hospitalization and only 40% receive

the proper therapy afterwards [31]. This inappropriate treatment has been suggested to enhance the pathogenicity of MRSA and encourage its overgrowth [32]. With the aim of helping making rational choices for MRSA treatment in the ICU settings, we conducted this study to compare the ability of the new anti-MRSA agents (ceftobiprole, dalbavancin, daptomycin, linezolid, tigecycline) as well as vancomycin to achieve the pharmacodynamic target of eradication against MRSA isolates collected in ICU settings.

## 3.2 METHODS

### 3.2.1 Pharmacodynamics

The pharmacodynamic profile of the tested antibiotics (ceftobiprole, dalbavancin, daptomycin, linezolid, tigecycline, or vancomycin) against MRSA was obtained from the Canadian National Intensive Care Unit (CAN-ICU) study [33]. Isolates were collected in the ICU of 19 medical centers in Canada. In this study, MRSA accounted for 21.9% of S. aureus isolates and 4.7% of all isolates collected during the study. CA-MRSA and HA-MRSA represented 9.3% and 90.7%, respectively, of the MRSA isolates. The isolate collection, patients demographics, methods of susceptibility testing and techniques for the molecular characterization of resistance mechanisms have been described previously [33,34]. Table 3-1 shows the MIC distribution of the MRSA isolates against the tested antibiotics.

### 3.2.2 Pharmacokinetics

The population estimates for total body clearance and their associated inter-individual variability as well as the extent of protein binding were obtained from published pharmacokinetic studies (Table 3-1) [35-41]. The simulated doses were the standard therapeutic doses for the tested agents and are also shown in Table 3-1. To simulate the dosage of daptomycin, a Gaussian distribution for the body weight was assumed with a mean of 70kg and a standard deviation of 15kg.

### 3.2.3 Calculation of the PK/PD Indices

Table 3-1 shows the PK/PD indices that were calculated for each drug as well as their target levels as suggested by the literature to be associated with favorable clinical outcome in MRSA infections [42-50]. The following equation was used to calculate the

percentage of the dosing interval during which the free ceftobiprole level will remain above the MIC (*f* T> MIC%) [51]:

$$T > MIC\% = \frac{100}{tau} \times \{t' - [\ln(\frac{K_o / CL}{K_o / CL - MIC}) \times \frac{t_{1/2}}{0.693}] + [(\ln\frac{K_o}{CL} - \ln MIC) \times \frac{t_{1/2}}{0.693}]\}$$

Where tau is dosing interval, $t'$ is the duration of infusion, $K_o$ is the infusion rate calculated as (Dose × fraction unbound/$t'$), $t_{1/2}$ is the terminal elimination half life of Ceftobiprole which was assumed to have a mean of 3.3 h and a standard deviation of 0.3 h [35,36].

For daptomycin, linezolid, tigecycline and vancomycin, the $AUC_{24}$/MIC was calculated using the following equation:

$$AUC_{24}/MIC = Dose_{24}/(CL \times MIC)$$

Where $Dose_{24}$ is the total dose administrated over 24 h and CL is the total body clearance. For daptomycin, $AUC_{24}$/MIC was corrected for the unbound fraction to calculate the free drug $AUC_{24}$/MIC (*f*$AUC_{24}$/MIC). For dalbavancin, the following equation was used to calculate an average *f*$AUC_{24}$/MIC after the administration of the dosage regimen of 1000 mg on day 1 followed by 500 mg on day 8 and assuming a half life of 7 days:

$$fAUC_{24}/MIC = f_u * 1000/(14 \times CL \times MIC)$$

Where $f_u$ is the unbound fraction of dalbavancin.

### 3.2.4 Determination of the PK/PD Susceptibility Breakpoints

In this analysis, a 10,000-subject Monte Carlo simulation was conducted for each drug at each of the following MICs: 0.03, 0.06, 0.12, 0.25, 0.5, 1, 2, 4, 8, 16, 32 μg/ml.

Pharmacokinetic parameters were assumed to follow a log-Gaussian distribution and the PK/PD indices was calculated for each simulated subject as described before. The probability of target attainment (PTA) was estimated at each MIC as the probability that at least the target value of the PK/PD index is achieved [52]. The PK/PD susceptibility breakpoint was defined as the highest value in which the PTA was ≥ 90% [53].

### 3.2.5 Estimation of the Cumulative Fractions of Response (CFR)

The CFR was estimated from a 10,000-subject Monte Carlo simulation that was conducted for each antibiotic dosing regimen against the entire MRSA bacterial population with its varying MICs. The pharmacokinetic parameters were assumed to follow a log-Gaussian distribution while a discrete MIC distribution was built based on the MIC frequencies observed in the CAN-ICU study. The PK/PD index for each simulated subject was calculated using randomly selected values for the pharmacokinetic parameter(s) as well as the MICs derived from the probability distributions of each. The CFR was defined as "the expected population probability of target attainment for a specific drug dose and a specific population of microorganisms" and could be calculated as following [52] :

$$\text{CFR} = \sum_{i=1}^{n} PTA_i \; x \; F_i$$

Where the subscript i indicates the MIC value ranked from lowest to highest MIC of the tested population of microorganisms, $PTA_i$ represents the probability of target attainment at each MIC and $F_i$ is the proportion of the CAN-ICU MRSA isolates that had this MIC. All simulations were performed using Oracle Crystal Ball software (version 11.1, Oracle USA, Inc., Denver, Colorado) [54].

## 3.3 RESULTS

The PTA of the simulated regimens as a function of increasing MICs is displayed in Figure 3-1 and the determined PK/PD susceptibility breakpoints are shown in Table 3-2. Although Clinical Laboratory and Standards Institute (CLSI) typically advocates one breakpoint for each antibiotic-microrganism combination, regimen-specific breakpoints were investigated in case of drugs for which more than one dosage regimen was tested, i.e. daptomycin and vancomycin. For both drugs, however, the breakpoints suggested by the PTAs profile agreed across the studied doses (Figure 3-1). The susceptibility breakpoints of ceftobiprole were 16 and 8 μg/ml at the target levels of 30% and 50%, respectively.

The median, $10^{th}$ percentile, $90^{th}$ percentile and the standard deviation of the PK/PD indices in the simulated patients in the CFR analysis are presented in Table 3-3. Figure 3-2 compares the CFR for all the tested antibiotics. Ceftobiprole (at both target levels) and dalbavancin achieved the highest probability (100%) of bactericidal effect against the MRSA isolates, followed by vancomycin at the higher dose attaining a CFR of 98.3%. Daptomycin (6mg/kg/day), linezolid, and vancomycin (1gm BID) had a similar likelihood for favorable outcome with CFR of 87.6%, 88.7% and 89.4%, respectively. Finally, the CFR of tigecycline and daptomycin (4mg/kg/day) were the lowest and were estimated to be 82.4% and 70.8%, respectively.

## 3.4 DISCUSSION

Monte Carlo simulation is a stochastic simulation analysis that involves resampling from one or more parametric distribution models [55]. Monte Carlo simulation has been commonly applied in antimicrobial pharmacodynamic studies to compare the efficacy of different antimicrobial agents and/or different dosage regimens of the same antibiotic against the pathogen of interest [56]. The analysis typically involves calculating the relevant PK/PD index using random samples drawn from the sampling distributions of the pharmacokinetic parameter(s) and the MIC values [57]. By repeating this process thousands of times, the distribution of the levels of the PK/PD index in the simulated population could be identified which allows estimation of the probability of attaining the PK/PD target. PK/PD targets have been shown to correlate with therapeutic efficacy in the clinical settings and hence can serve as a surrogate marker for efficacy [58-60]. This analysis has the advantage of accounting for the variability of the susceptibility of a specific pathogen to an antibiotic as well as the inter-individual variability in the antimicrobial pharmacokinetics in the target population.

In this study, we investigated the ability of several anti-MRSA regimens to achieve the PK/PD target associated with their efficacy. Daptomycin at a dosage of 4mg/kg/day, indicated for complicated skin and skin structure infections, had the lowest CFR among all studied regimens. The use of a higher daptomycin dosage of 6mg/kg/day, which is indicated for S. aureus bacteremia, substantially increased the CFR from 70.8% to 87.6% which suggests its relative advantage compared to the lower dose in eradicating MRSA infections in the ICU settings. On the other hand, ceftobiprole and dalbavancin were superior to all investigated agents and had 100% likelihood of bacterial eradication.

This corroborates the results of other clinical and pharmacodynamic studies that showed the therapeutic value of these two agents [43,61-64].

Use of vancomycin at a dose of 1.5gm twice daily is also suggested by this study. CFR analysis showed that this dosage has 98.3% probability of attaining the pharmacodynamic target against the MRSA isolates in the ICU, compared to 89.4% when the lower dose of 1gm twice daily was used. This is consistent with reports that suggested that vancomycin has been underdosed in the past[20] and supports the recent guidelines for dosing vancomycin at 15-20 mg/kg dose every 8-12 h [50,65]. However, the CFR values listed above were higher than what was reported by other pharmacodynamic studies [49,64]. This could be attributed to the minimal proportion of MRSA isolates in the CAN-ICU study that had MIC higher than 1μg/ml (2% of the isolates, Figure 3-1.f). In addition, the vancomycin clearance estimate used in our analysis (3.6 L/h) was obtained from a study conducted on ICU-patients [41], while the other studies have used higher estimates of CL (4.7 and 4.94 L/h) that represent a more general patient population. This lower clearance is potentially responsible for the higher exposure and hence higher CFR observed in this study against ICU MRSA isolates.

Traditionally, susceptibility breakpoints have been determined on the basis of the MIC distribution of the organism. Recently, however, Monte Carlo simulation analysis has been used by regulatory agents, such as CLSI, FDA and EUCAST to assist in defining the susceptibility breakpoints [66]. This allows the use of the exposure effect relationship measures as the parameters to describe the susceptibility rather than the static MIC values [67]. In the current analysis, we employed this approach to suggest the PK/PD susceptibility breakpoints for the tested agents. These breakpoints were well higher than

the $MIC_{90}$ of the tested isolates in case of ceftobiprole and dalbavancin and lower than the $MIC_{90}$ for daptomycin, linezolid and tigecycline. This explains the higher CFR observed with ceftobiprole and dalbavancin than the other agents (Figure 3-2). For vancomycin, the suggested breakpoint was found to be 1µg/ml which matches its $MIC_{90}$ in the study. This breakpoint was also observed at the higher vancomycin dose of 1.5gm twice daily which showed a low PTA of 60% against MRSA isolates of 2µg/ml. This confirms the results of two clinical studies that showed an inferior likelihood for successful therapy when the S. aureus MIC was 1-2µg/ml [68,69]and suggests a further reduction in the current CLSI breakpoint of 2µg/ml [70].

It is important to note the limitations of the use of the Monte Carlo simulation approach for pharmacodynamic profiling of antimicrobials. First, there is not a complete consensus about all the target PK/PD indices and their cut off levels could often be debated. For instance, we used in this analysis a *f*AUC/MIC target level of 189 for daptomycin which has been suggested and applied in several PD studies [45,71,72]. However, Dandekar et al [73] suggested lower target levels for daptomycin which can potentially result in higher CFR and breakpoints than what is reported in our study. It is also worth mentioning that although an in vitro study has suggested an AUC/MIC target level of 1113 for pharmacodynamic efficacy of vancomycin against MRSA [74], we choose to use the target level of 400 advocated in the recent vancomycin therapy guidelines [50,75]. The higher target tends to result in a very conservative and potentially clinically irrelevant estimate of vancomycin CFR (<10%, data not shown). Second, the susceptibility breakpoints suggested in our analysis should be interpreted cautiously and integrated with genotypic profiles and microbiologic information about the prevalence of resistance

factors in a larger and more general population of isolates. Finally, the results of the analysis are conditional on the simulated pharmacokinetic parameter and dispersion estimates which were obtained from published pharmacokinetic studies. Consequently, extrapolation of the results to some subpopulations, such as cystic fibrosis patients who tend to have higher clearance to most drugs, may lead to biased likelihood estimates [52,76].

In summary, ceftobiprole and dalbavancin had the highest likelihood of attaining their requisite PK/PD targets against the MRSA isolates incorporated in the study. Higher doses of daptomycin and vancomycin improved their CFR appreciably and seem necessary to ensure high likelihood of successful outcome. Our analysis also suggested PK/PD susceptibility breakpoints for the tested agents which can be integrated with data from other studies to select the breakpoints to be implemented in the clinical microbiology laboratories.

**Table 3-1: Summary of dosage regimens, pharmacokinetic, pharmacodynamic and pharmacokinetic/pharmacodynamic parameters incorporated in the Monte Carlo simulation analysis**

| Drug | Dosage Regimen(s) | Pharmacokinetics | | Pharmacodynamics | | | PK/PD | |
|---|---|---|---|---|---|---|---|---|
| | | CL (IIV%) L/h | Unbound Fraction | $MIC_{50}$ µg/mL | $MIC_{90}$ µg/mL | $MIC_{range}$ µg/mL | Index | Target Level |
| Ceftobiprole | 500mg /2hrs TID | 4.98 (11.6)[35,36] | 0.84[35] | 1 | 2 | 1-4 | *f* T> MIC% | 30, 50%[42,43] |
| Dalbavancin | 1000mg, 500mg[a] | 0.0579 (23.7)[37] | 0.07[37] | 0.06 | 0.06 | 0.03-0.12 | *f*$AUC_{24}$/MIC | 292[44] |
| Daptomycin | 4mg/kg QD 6mg/kg QD | 0.688 (52.1)[38] | 0.1 [38] | 0.12 | 0.25 | 0.12-0.5 | *f*$AUC_{24}$/MIC | 189[45] |
| Linezolid | 600mg BID | 6.85 (50.3)[39] | NA[b] | 2 | 2 | 1-4 | $AUC_{24}$/MIC | 59.1[46,49] |
| Tigecycline | 50mg BID | 18.6 (36.2)[40] | NA[b] | 0.12 | 0.5 | 0.06-0.5 | $AUC_{24}$/MIC | 17.9[47-49] |
| Vancomycin | 1gm BID 1.5 gm BID | 3.6 (29.2)[41] | NA[b] | 1 | 1 | 0.25-8 | $AUC_{24}$/MIC | 400[50] |

IIV is inter-individual variability, QD, BID and TID indicates once, twice and three times daily, respectively. [a]Dalbavancin is administered as 1000mg on the first day then 500mg after 7 days. [b]NA indicates that unbound fraction was not needed in the analysis since a total AUC/MIC was calculated for these antimicrobial agents.

**Figure 3-1: Probability of target attainment (PTA) as a function of increasing minimum inhibitory concentrations (MICs) for a) Ceftobiprole, b) Dalbavancin, c) Daptomycin, d) Linezolid, e) Tigecycline, f) Vancomycin.**

MIC Distributions are integrated in the plots to demonstrate the range and frequency of the isolates susceptibility.

a)

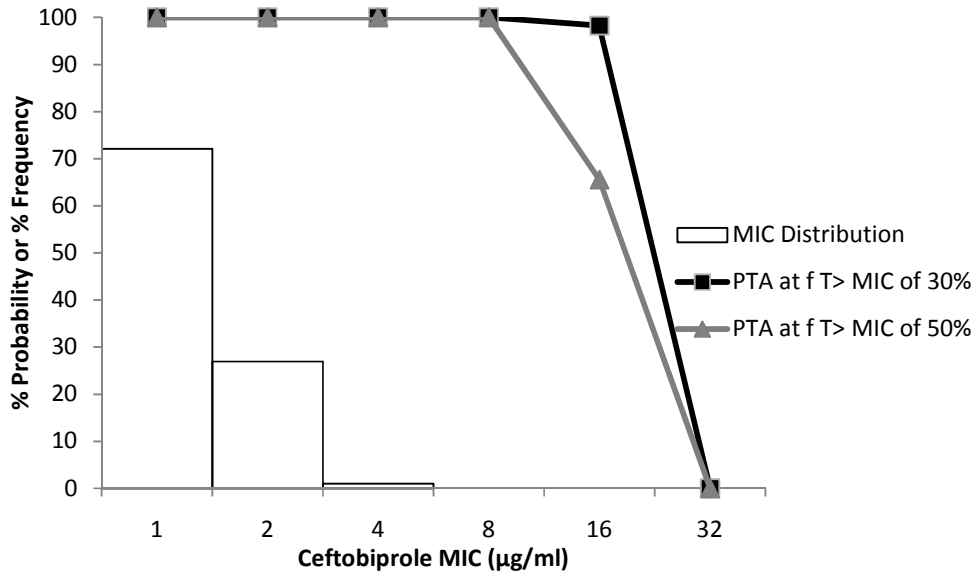


b)

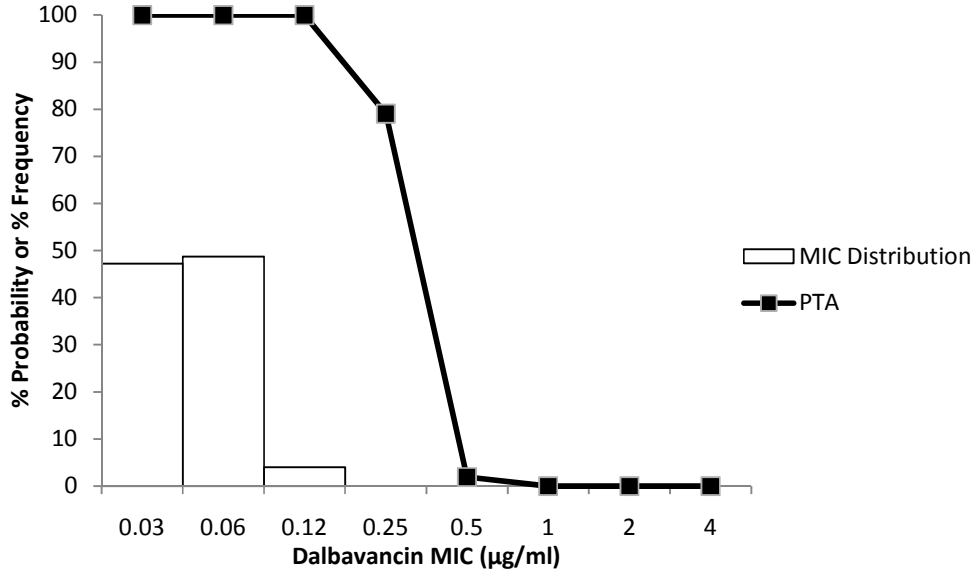

c)

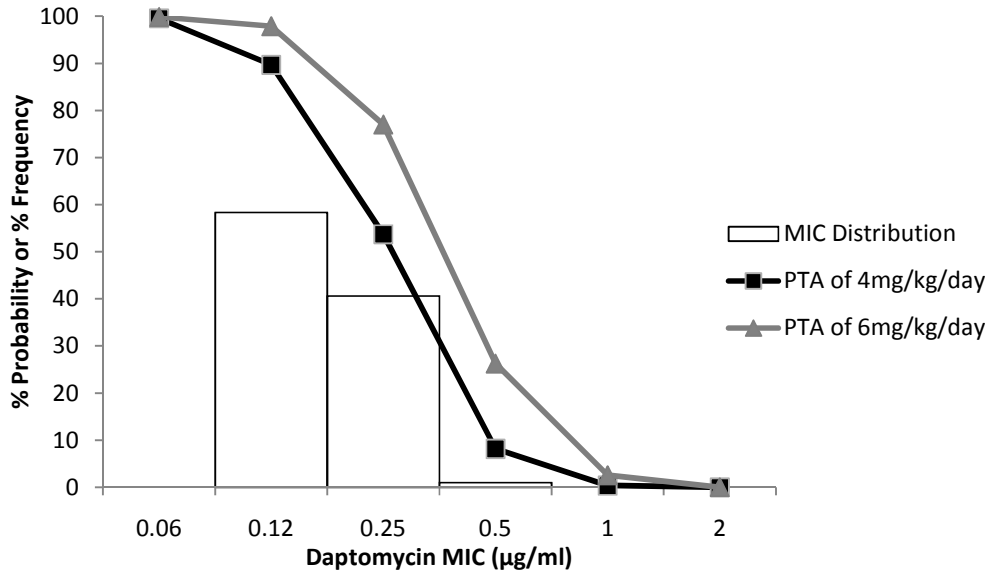
100
90
80
70
60
50
40
30
20
10
0
% Probability or % Frequency
0.06
0.12
0.25
0.5
1
2
Daptomycin MIC (µg/ml)
MIC Distribution
PTA of 4mg/kg/day
PTA of 6mg/kg/day

d)

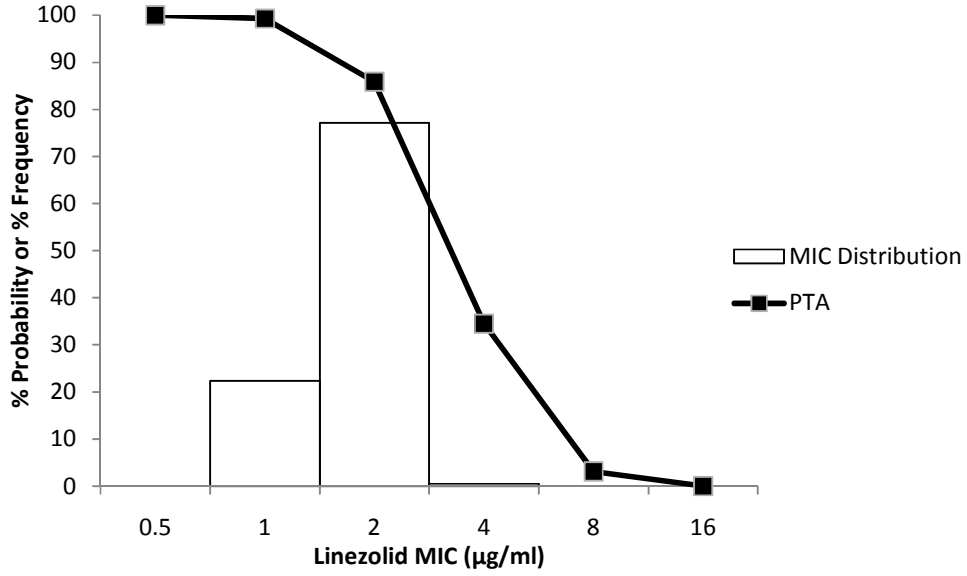
100
90
80
70
60
50
40
30
20
10
0
% Probability or % Frequency
0.5
1
2
4
8
16
Linezolid MIC (µg/ml)
MIC Distribution
PTA

e)

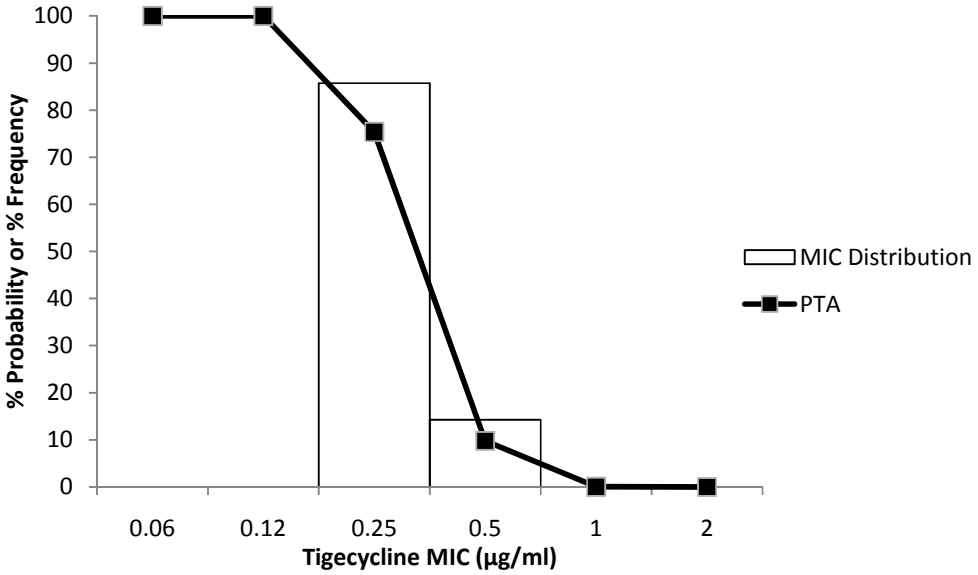
100
90
80
70
60
50
40
30
20
10
0
% Probability or % Frequency
0.06
0.12
0.25
0.5
1
2
Tigecycline MIC (µg/ml)
MIC Distribution
PTA

f)

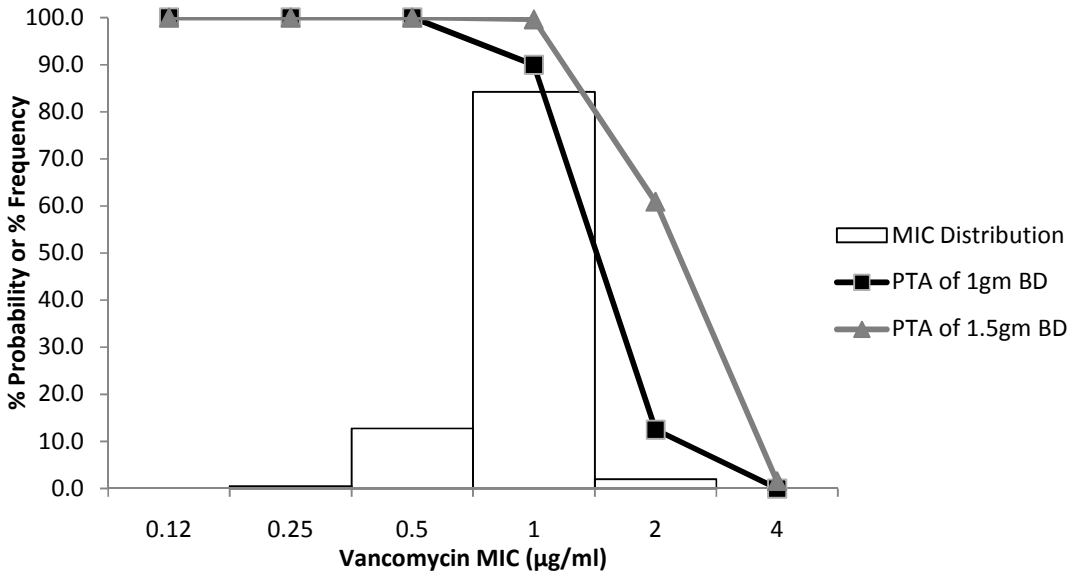
100.0
90.0
80.0
70.0
60.0
50.0
40.0
30.0
20.0
10.0
0.0
% Probability or % Frequency
0.12
0.25
0.5
1
2
4
Vancomycin MIC (µg/ml)
MIC Distribution
PTA of 1gm BD
PTA of 1.5gm BD

**Table 3-2: PK/PD Susceptibility breakpoints as suggested by the Monte Carlo Simulation analysis:**

| Drug | Suggested PK/PD Susceptibility Breakpoint (µg/ml) |
|---|---|
| Ceftobiprole | 8* |
| Dalbavancin | 0.12 |
| Daptomycin | 0.12 |
| Linezolid | 1 |
| Tigecycline | 0.12 |
| Vancomycin | 1 |

* Estimated at the *f* T> MIC% target level of 50%

**Table 3-3: Levels of the PK/PD indices achieved in the simulated patients in the CFR analysis**

| Drug | Dosage Regimen(s) | Simulated PK/PD Index* | | | |
|---|---|---|---|---|---|
| | | $10^{th}$ Percentile | Median | $90^{th}$ Percentile | Standard Deviation |
| Ceftobiprole | 500mg/2h TID | 138.9 | 177.7 | 197.8 | 22.62 |
| Dalbavancin | 1000mg,500mg | 1,130.9 | 1992.9 | 3,574.1 | 973.6 |
| Daptomycin | 4mg/kg QD | 115.0 | 275.3 | 631.4 | 233.8 |
| | 6mg/kg QD | 174.1 | 412.8 | 940.9 | 345.4 |
| Linezolid | 600mg BID | 57.3 | 110.4 | 235.3 | 82.7 |
| Tigecycline | 50mg BID | 12.8 | 39.1 | 71.5 | 24.4 |
| Vancomycin | 1gm BID | 275.3 | 603.1 | 1,061.3 | 328.4 |
| | 1.5gm BID | 591.4 | 902.3 | 1,572.8 | 476.3 |

* PK/PD indices were *f* T> MIC% for ceftobiprole, $fAUC_{24}$/MIC (µg.hr/ml) for dalbavancin and daptomycin, and $AUC_{24}$/MIC (µg.hr/ml) for linezolid, tigecycline and vancomycin

**Figure 3-2: Cumulative fraction of response (CFR %) for different antibiotic regimens against the MRSA isolates of the CAN-ICU surveillance study.**

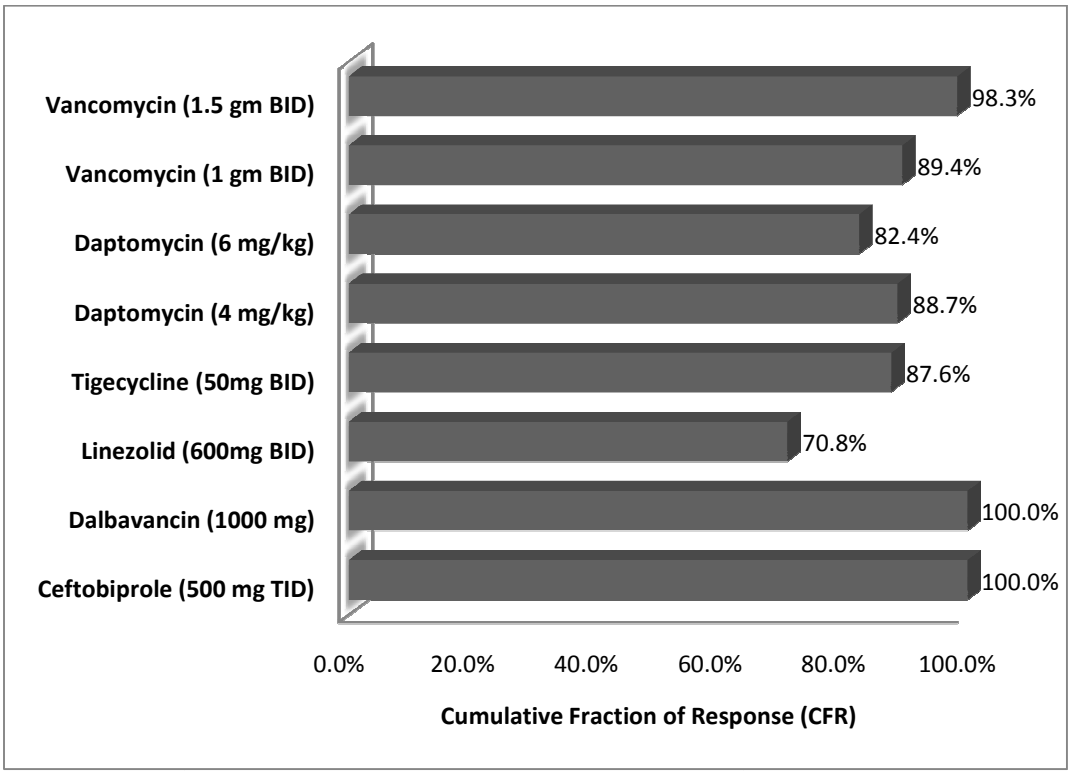

# Pharmacodynamic Assessment of Vancomycin-Rifampin Combination against Methicillin Resistant *Staphylococcus aureus* Biofilm: A Parametric Response Surface Analysis

This chapter was presented in part in the American Conference on Pharmacometrics, October 2009

# 4.1 INTRODUCTION

*Staphylococcus aureus* is one of the most common Gram positive pathogens encountered in both community and hospital settings [1]. Methicillin resistant *Staphylococcus aureus* (MRSA) accounts for 40% of all nosocomial *Staphylococcus aureus* infections [2] and 64% of *Staphylococcus aureus* infections in the intensive care units [3]. MRSA infections are associated with higher morbidity, mortality and health care cost than Methicillin sensitive *Staphylococcus aureus* (MSSA) infections [4,5] with some studies reporting the mortality rate from MRSA bacteremia to be higher than 50% [6,7].

Methicillin resistance is often associated with resistance to other antimicrobial agents such as macrolides, aminoglycosides and beta-lactams which limits the antimicrobial agents that could be prescribed for MRSA infections [8,9] . Although vancomycin has been the standard therapy of MRSA infections, staphylococcal isolates with decreased susceptibility to vancomycin, known as vancomycin intermediate *Staphylococcus aureus* (VISA) have been reported worldwide [10-12] . Moreover, the polymorphism, that is responsible for this decreased susceptibility, was also found to be associated with overproduction of biofilm [13]. Biofilm is a microbial derived sessile community characterized by cells that are reversibly attached to a substratum or interface or to each other, are embedded in a matrix of polymeric substances that they have produced, and exhibit an altered phenotype with respect to growth rate, antimicrobial resistance, and gene transcription [14]. *Staphylococcus aureus* is known to be able to colonize and form biofilm on indwelling medical devices such as intravascular catheters, prosthetic heart valves, pacemakers and orthopedic implants resulting in device-related and catheter-related blood stream infections [14,15]. Biofilm associated infections tend to be

persistent and very difficult to eradicate because of the inherent resistance of biofilm embedded bacteria. This biofilm resistance is due to the slow growth rate of sessile bacteria, the limited penetration of the antimicrobial agents through the biofilm matrix and/or gene expression or repression associated with the biofilm mode of growth [14].

Due to the current decline in development of novel antimicrobial agents [16], the use of combination therapy has gained more attention as an alternative strategy for combating biofilm resistance. Other potential advantages of the use of antibiotic combinations are decreased development of resistance and a broadened antibacterial spectrum through hitting multiple targets within the microbial cell [17,18]. Rifampin is a bactericidal agent against *Staphylococcus aureus* that is often used in combination to avoid the rapid emergence of resistance [19,20]. This agent has been reported to have a strong anti-biofilm activity that could be attributed to its ability to penetrate the biofilm [19] and/or its ability to inhibit the adherence of the bacteria to the surfaces [21]. Nevertheless, the efficacy of its combination with vancomycin against MRSA biofilm remains controversial [19-27], despite the common use of this combination for treatment of staphylococcal infections [28,29]. The objective of the current study is to use a newly developed quantitative methodology [30] to characterize the bactericidal effect of vancomycin and rifampin separately and in combination against MRSA biofilm.

## 4.2 METHODS

### 4.2.1 Bacterial Strain and Antimicrobial Agents

Methicillin resistant *Staphylococcus aureus* ATCC 43300 (American Type Culture Collection, Manassas, VA, USA) was used in the study. The bacterial culture was stored in skim milk at -80°C in cryotubes (Thermo Fisher Scientific, Inc., Waltham, MA, USA). Prior to each experiment, MRSA ATCC 43300 was sub-cultured twice on Tryptic Soy Broth (TSB, Sigma-Aldrich, St. Louis, MO, USA) and incubated for 16 h at 37°C. The inoculum was then prepared in cation–adjusted Mueller Hinton II broth (MHII) (Sigma-Aldrich, St. Louis, MO, USA) and diluted to match 0.5 McFarland standard which is equivalent to $1.5 \times 10^8$ CFU/ml.

Vancomycin and rifampin powders were purchased from Sigma-Aldrich (St. Louis, MO, US). Solutions of 20 mg/ml vancomycin and 6.4 mg/ml rifampin were prepared and stored as aliquots of stock solutions at -80°C according to the Clinical Laboratory and Standards Institute (CLSI) guidelines (31). Aliquots of the stock solutions were thawed at room temperature and diluted in MHII broth prior to experiments.

### 4.2.2 Planktonic Susceptibility Testing

The minimum inhibitory concentrations (MICs) of the antimicrobial agents were determined using the broth microdilution method as described by CLSI guidelines [31]. The experiments were performed in polystyrene, round bottom, 96-wells microplates (Greiner Bio-One North America, Monroe, NC, USA). Twofold serial dilutions of the antibiotics were used and the final bacterial count in each well was $5 \times 10^5$ CFU/ml. The MIC was

defined as the lowest concentration of the antibiotic that resulted in no visible growth after aerobic incubation at 37°C for 24 h.

### 4.2.3 Biofilm Susceptibility Testing

*Biofilm Formation*

75 µl inoculums of $1.5 \times 10^8$ CFU/ml TSB culture were incubated for 24 hours at 37 ˚C in polystyrene, round bottom, 96-wells microplates [32]. After incubation, the supernatant was aspirated and the wells were washed twice with sterile normal saline solution.

*Minimum Biofilm Inhibitory Concentration (MBIC)*

100 µl aliquots of two fold serial dilutions of the antibiotics in MHII were added to the wells with the established biofilms. After incubation for 18 hours at 37°C, the plates were examined visually for bacterial growth indicated by the presence of turbidity. The MBIC was defined as the lowest concentration of the antibiotic that resulted in no visible growth [33]. A positive control and a negative control were included in all experiments and all experiments were repeated at least in duplicates.

*Minimum Biofilm Bactericidal Concentration (MBBC)*

10µl aliquots from wells with no visible growth were transferred into a new 96 well plate and diluted with 90µl aliquots of TSB to minimize the carryover effect. After incubation for 24 hours at 37°C, the plates were examined visually for bacterial growth. The MBBC was defined as the lowest concentration of the antibiotic that prevented visible growth.

### 4.2.4 Biofilm Time-Kill Studies

*Biofilm Formation*

0.5ml aliquots of MHII broth containing $1.5 \times 10^6$ CFU/ml of the microorganism were used to inoculate 1.5ml polypropylene tubes (Greiner Bio-One North America, Monroe, NC, USA) [34]. The tubes were incubated for 24h at 37°C under aerobic condition without shaking. The supernatant was then carefully aspirated and the tubes were washed with normal saline solution. Establishment of MRSA biofilm in the tubes was confirmed using scanning electron microscopy. The photo was captured using variable pressure JEOL scanning electron microscope (Model JSM-6490LV, Peabody, Massachusetts) equipped with a tungsten filament with accelerating voltages of 20 kV and chamber pressure from 60 - 70 Pa according to the method described by van Heerden *et al.*[35].

*Anti-biofilm Assessment of Single Agents*

MRSA biofilm was exposed to vancomycin or rifampin at increasing concentrations of 0 (control), 0.25, 1, 4, 16, and 64 times MBIC. All experiments were run in duplicate. After 24 h of incubation at 37°C, the tubes were sonicated for 5 minutes in ultrasonic water bath (Fisher Scientific, Model FS-60, frequency of 40 kHz, ultrasonic power of 130 Watt) followed by vigorous vortexing for 60 seconds to dislodge and disperse the cells from the biofilm [36]. After sonication, samples of 100µl were withdrawn and were ten-fold serially diluted in sterile normal saline solution to minimize the antibiotic carryover effect by reducing the antibiotic concentration to sub-MIC levels. 50 µl samples were then plated onto Muller Hinton Agar (MHA, Sigma-Aldrich, St. Louis, MO, USA) plates to quantify the total biofilm-embedded bacterial burden. After

incubation of the MHA plates at 37°C for 24 h, the viable cell count was determined for different treatments and controls.

*Pharmacodynamic Modeling*

The total bacterial burdens after 24 hours of antibiotic exposure were logarithmically transformed and fitted to an inhibitory sigmoid Emax model in ADAPT II (Biomedical Simulation Resource, University of Southern California, Los Angelos, CA) using the maximum-likelihood estimation method [37]. The observations were weighted by the reciprocal of their variances. The baseline effect was fixed to the logarithm of the mean bacterial count observed after 24 hours in the control experiments.

*Determination of the Optimal Sampling Concentrations*

The parameters estimate obtained from the sigmoid Emax model were assumed to be the true parameter values and were used in ADAPT II to determine four optimal and clinically achievable sampling concentrations that would most precisely estimate the model parameters for each antibiotic. D-optimality criterion was employed to minimize the determinant of the variance-covariance matrix of the estimated parameters, or equivalently, to minimize the volume of the confidence region for the parameters estimates. The upper bounds of the concentrations constraint were the maximum clinically achievable concentrations of the two antibiotics (64 µg/ml for vancomycin and 32 µg/ml for rifampin). A conservative lower bound of 0.25 × MBIC was used in order to characterize the whole pharmacodynamic profile and identify any synergistic interactions at low concentrations.

*Anti-biofilm Assessment of the Combination*

MRSA biofilm was established in the same way described above with the single agent experiments. Twenty five combinations of the optimal sampling concentrations (including control) of the two agents were then assessed for their bactericidal activities against MRSA biofilm. After 24 hours of exposure, the total bacterial burden was retrieved, quantified and used to construct a three dimensional response surface. Using effect summation, another three dimensional response surface was simulated to describe the predicted combined antibacterial effect in case of null interaction as follows [30]:

$$\text{Effect}_{\text{combination}} = E_{\text{vancomycin}} + E_{\text{rifampin}} \qquad \text{Equation 1}$$

$$\text{LogCFU/ml} = E_o - \{[\frac{E_{\max r}.C_r^{Hr}}{C_r^{Hr} + C_{50r}^{Hr}}] + [\frac{E_{\max v}.C_v^{Hv}}{C_v^{Hv} + C_{50v}^{Hr}}]\} \quad \text{Equation 2}$$

Where $E_o$ represents the mean bacterial burden in the control experiments, $E_{\max r}$ and $E_{\max v}$ are the maximum effects of rifampin and vancomycin, $C_r$ and $C_v$ are the concentrations of rifampin and vancomycin, $C_{50r}$ and $C_{50v}$ are the concentrations of rifampin and vancomycin at 50% of the maximum effect, $H_r$ and $H_v$ are the Hill factors for rifampin and vancomycin, respectively.

*Computation of the Pharmacodynamic Interaction Index*

The volume under the simulated surface was estimated by double integration of equation 2 over the clinically achievable range. The volume under the observed data was estimated by linear interpolation between the observed data then estimating the volumes

of the cuboids formed. These volumes can be conceptualized as the integral bactericidal effect over the studied concentration ranges of the two antibiotics [30]. A 95% confidence interval (CI) of the volume under the observed surface was calculated using the confidence intervals of the mean observed data (mean ±1.96×standard deviation). The pharmacodynamic interaction index was computed as the ratio of the volumes under the observed and simulated surfaces. Synergy and antagonism were defined as interaction index values of < 1.0 and > 1.0, respectively. Matlab (version 7.1, The MathWorks, Natick, MA) was used for computation of the volumes and visualization of the results. The Matlab code as well as the Fortran code used in ADAPT II for pharmacodynamic modeling and generation of the D-optimal concentrations are available from the author.

## 4.3 RESULTS

The results of the susceptibility experiments are shown in Table 4-1. The MIC and MBIC values are consistent with those presented in other reports [23,38] . Although the MBIC of both agents were comparable, the MBIC was more than 800-fold the MIC in case of rifampin while it was only 8-fold higher for vancomycin.

The methodology adopted for biofilm formation and quantification in the time-kill studies was highly reproducible with less than 3.5% variability in the control experiments results across the study period. The mean bacterial density retrieved from the biofilm in the control experiments was $3.2 \times 10^9$ CFU/ml. The lower limit of bacterial quantification (LLQ) was 5 X $10^2$ CFU/ml. The coefficient of variation was 2.4% and 10% in the vancomycin and rifampin single agent experiments, respectively. Rifampin exhibited a superior antibacterial profile than vancomycin against MRSA biofilm (Figure 4-1). In the pharmacodynamic modeling, a proportional error model was used to describe the relationship between the assay variance and the mean observed bacterial burden. Observations lower than LLQ was substituted with LLQ/2 prior to modeling. The sigmoidal inhibitory Emax model fitted the data adequately, with $R^2$ of 0.97 and 0.99 for vancomycin and rifampin data, respectively (Figure 4-1). Table 4-2 shows the parameters estimates for both antibiotics as well as the precision associated with their estimation. The uncertainty in the parameters estimates was generally low, with the highest relative standard error% (RSE%) being 28.6. The sampling concentrations of the D-optimal design were estimated to be 2, 4.1, 12.8, and 64 µg/ml for vancomycin and 1.56, 4.2, 14.4, and 32 µg/ml for rifampin.

Figure 4-2 shows the parametric response surface that presents the additive anti-biofilm actvity of the combination simulated under null interaction assumption and calculated using equation 3.

$$\text{LogCFU/ml} = 9.5 - \{[\frac{7.27 x C_r^{0.86}}{C_r^{0.86} + 5.72^{0.86}}] + [\frac{3.21 x C_v^{1.34}}{C_v^{1.34} + 3.56^{1.34}}]\} \quad \text{Equation 3}$$

The bacterial densities observed at the different combination concentrations are demonstrated in Figure 4-3. Observations showed lower anti-biofilm activity than the simulated profile at all concentration combinations (Figure 4-4). The higher the concentrations of the agents, the higher the antagonism observed, with the highest antagonism observed with the combination of 64 µg/ml of vancomycin and 32 µg/ml of rifampin (Figure 4-5).

The volume under the simulated surface was 4113.3, while the volume under the observed points was found to be 13802.1 (95% CI, 13380.3 to 14223.9). The pharmacodynamic interaction index was estimated to be 3.36 (95% CI, 3.25 to 3.46).

## 4.4 DISCUSSION

The use of combinations of antimicrobial agents has emerged as a promising therapeutic approach to overcome the increased bacterial resistance and the poor pipeline of novel antimicrobial agents [39]. Since not all antimicrobial combinations act synergistically, use of combination therapy is not always advantageous and approaches that can predict the pharmacodynamic interaction between the combined antimicrobial agents would help to make a rational choice of the antimicrobial combinations. Although several *in vitro* methods have been used to evaluate antimicrobial combinations, their results may not correlate with each other [40-42] and they were often of little value in predicting the clinical outcome as assessed by *in vitro* pharmacokinetic models as well as animal and clinical studies [18,43-45] . In addition, the assumptions that some of them are built on have been questioned which invalidates the interpretation of their results [46].

The checkerboard titration is one of the most commonly used techniques to study the interaction of antimicrobial agents and its results are usually interpreted using the fractional inhibitory concentration index (FICi). Defining the lack of interaction between two agents, i.e. additivity, using the FICi is based on Loewe additivity model which assumes linear concentration effect relationship [46]. This assumption is clearly violated in many cases as seen in Figure 4-1. In addition, studies have reported the high dependence of the FICi estimates on the dilution series [47] and the poor reproducibility of results [48].

Time-kill studies have been commonly used to evaluate antimicrobial combinations. An advantage of this technique is that it allows quantitative assessment of the extent of the bacterial killing effect rather than the dichotomous visual evaluation of

bacterial inhibition used in the checkerboard technique. These studies, however, evaluate the antimicrobial interaction at one static concentration and hence its results cannot be extrapolated to the other concentrations. This limits the clinical relevance of the results given the fact that the drug concentration varies *in vivo* according to its pharmacokinetic parameters. Moreover, there is no widely accepted definition of synergy in time-kill experiments for bactericidal agents [18].

Tam *et al.* has recently proposed a response surface analysis approach for pharmacodynamic assessment of antimicrobial agents interactions [18,30]. This technique involves conducting time-kill studies at different concentrations combinations of the antimicrobial agents and using pharmacodynamic modeling and effect summation to define the parametric response surface representing additive effect of the combination. Data above or below this response surface indicates antagonism or synergism, respectively. In addition, a pharmacodynamic interaction index is computed to allow a quantitative measure of the interaction. A confidence interval for this index can be estimated as well by including the replicates variability in the analysis in order to provide a statistical basis for interpreting the results and comparing the different combinations [18].

In this study, we used the response surface analysis approach to evaluate the efficacy of the vancomycin and rifampin combination against MRSA biofilm. The effect of the biofilm on the susceptibility to vancomycin and rifampin was enormous as demonstrated in Table 4-1. This is consistent with previous reports about the association between biofilm formation and antimicrobial resistance [14,49]. Rifampin demonstrated higher efficacy than vancomycin against MRSA biofilm in the single agent time-kill studies. This could be attributed to rifampin's lower molecular weight and its lesser

structure complexity which enables higher penetration ability through the biofilm matrix compared to that of vancomycin. Combination experiments revealed antagonism at all concentrations and the interaction index was significantly higher than 1 suggesting strong antagonism between the two agents against MRSA biofilm.

Studies on the efficacy of vancomycin-rifampin combination against MRSA biofilm have had conflicting results [19-27]. Rose *et al.* showed that rifampin has a minimal effect against low and high biofilm-producing MRSA strains while its combination with vancomycin was bactericidal against all the strains [23]. Saginur *et al.* reported that vancomycin and rifampin combination was effective against MSSA biofilm but fusidic acid had to be added to this combination in order to produce a similar effect against MRSA biofilm [50]. LaPlante *et al.* showed that rifampin did not enhance the activity of vancomycin against MRSA biofilm while it antagonized and delayed the bactericidal effect of another glycopeptide, daptomycin [22]. This antagonism was attributed to the delaying effect of RNA synthesis inhibition on the activity of cell-wall active antibiotics [22]. In addition, antagonism between vancomycin and rifampin has been reported against MRSA in the planktonic state [51-53]. The heterogeneity in the testing methods used in the previous studies was suggested as the cause of this inconsistency in the results [19]. We believe, however, that the approach employed in our study provides a more robust quantitative assessment of the antimicrobial agents' interactions which in turn, potentiates the clinical relevance of the obtained results. In fact, despite the common use of this combination clinically, clinical studies have failed to show a therapeutic advantage of concomitant administration of rifampin and vancomycin in the treatment of MRSA endocarditis with a slight trend in favor of vancomycin monotherapy [19,25,27,54].

A limitation of our study is the use of one MRSA strain which limits the generalizability of the results. To the best of our knowledge, this is the first time that the response surface modeling approach was applied to assessing the anti-biofilm effect of an antimicrobial combination. As reported previously [30], this approach performs better when assessing the antimicrobial activity against inherently resistant bacteria, which makes its use in biofilm studies one of its best applications. However, this approach may not be convenient for routine clinical laboratory use due to its laborious nature and its use may be limited to research purposes.

In conclusion, using a new modeling based approach; we have demonstrated an *in vitro* antagonism between vancomycin and rifampin against MRSA biofilm at clinically achievable concentrations. The parametric approach employed to quantify the activity of the combination provides a scientific rationale for further *in vivo* investigations which will allow a better understanding of the therapeutic potential of this combination in biofilm-associated MRSA infections.

**Table 4-1: Susceptibilities of MRSA 43300 in the planktonic and biofilm states to vancomycin and rifampin.**

| Antimicrobial Agent | MIC (µg /ml) | MBIC(µg /ml) | MBBC(µg /ml) |
|---|---|---|---|
| Vancomycin | 1 | 8 | 32 |
| Rifampin | 0.0075 | 6.25 | 6.25 |

**Table 4-2: Parameter estimates of the pharmacodynamic models of vancomycin and rifampin.**

| Parameter | Estimate (%RSE) | |
|---|---|---|
| | Vancomycin | Rifampin |
| $E_{max}$ | 3.21 (3.39) | 7.27 (4.94) |
| $EC_{50}$ | 3.56 (16.9) | 5.72 (28.6) |
| H | 1.34 (21.74) | 0.86 (27.1) |

**Figure 4-1: Model fit of the total bacterial density after exposure of biofilm to varying concentrations of the Vancomycin (A) or Rifampin (B) for 24 hours in the single agent experiments.**

Data are shown as means ± SD. The bacterial density after exposure to rifampin at concentration of 400 µg/ml was below the LLQ and hence was not shown in the plot.

A

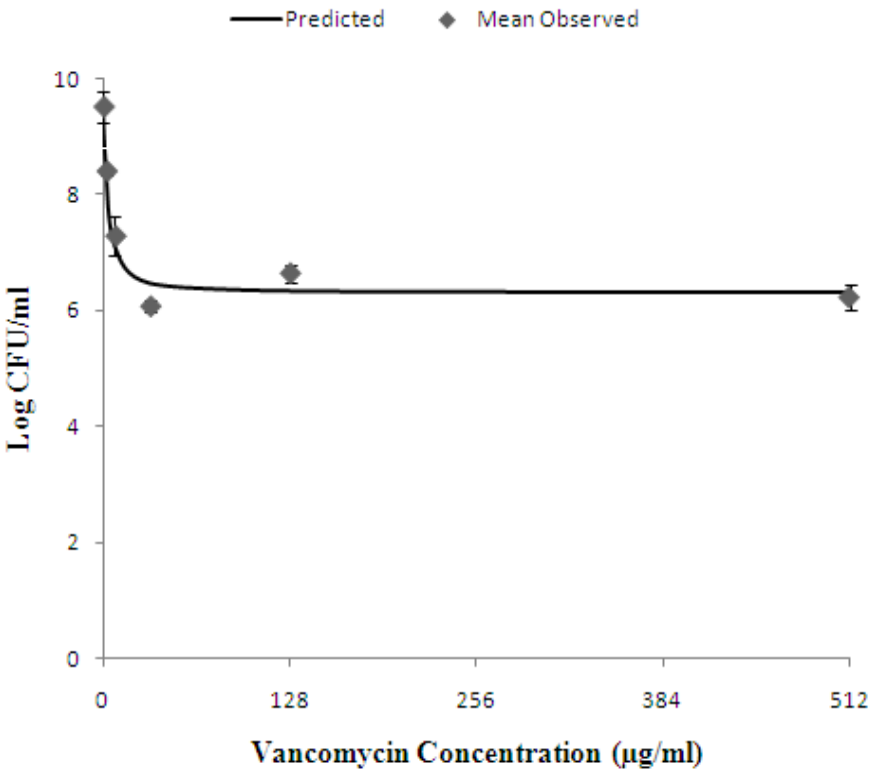

B

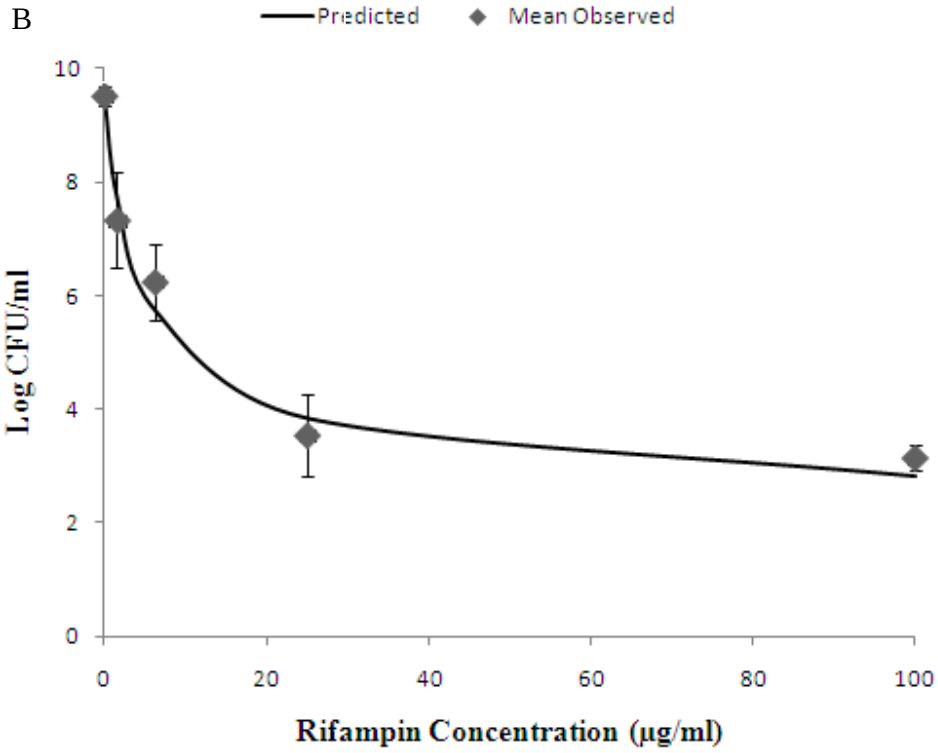
Predicted
Mean Observed
10
8
6
4
2
0
Log CFU/ml
0
20
40
60
80
100
Rifampin Concentration (µg/ml)

**Figure 4-2: Simulated response surface showing the expected anti-biofilm effect if the effect of Vancomycin- Rifampin combination was additive.**

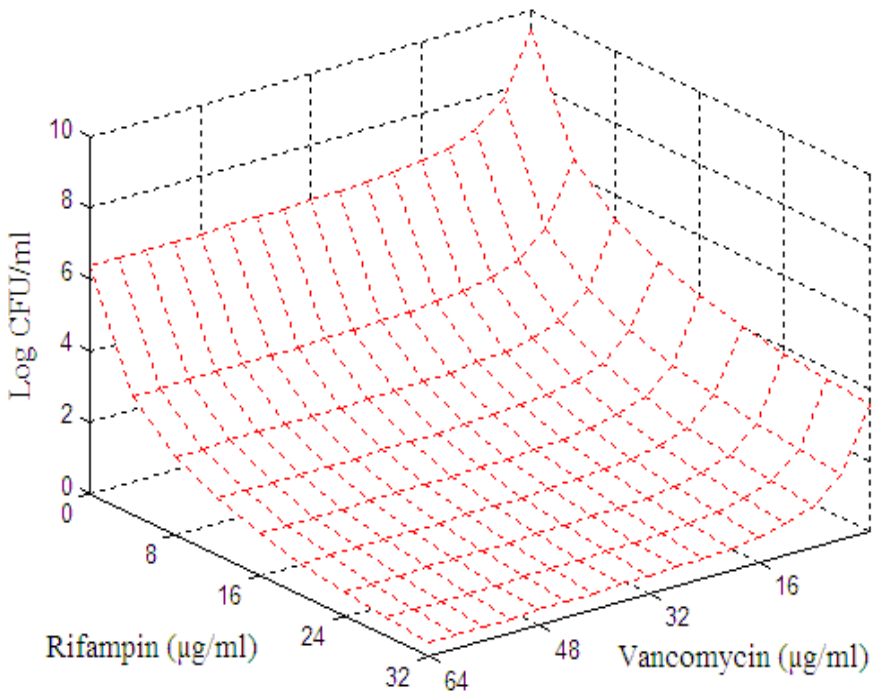

**Figure 4-3: The observed bacterial density after 24 hours of biofilm exposure to different concentrations of vancomycin– rifampin combinations.**

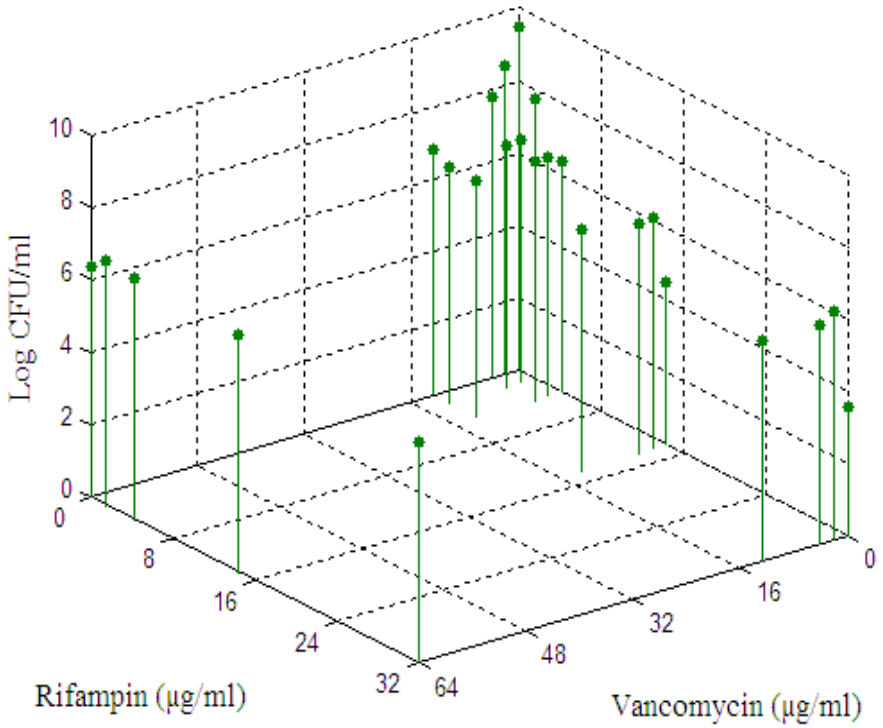

**Figure 4-4: Comparison of the observed (circles) and simulated (mesh) anti-biofilm activities of vancomycin–rifampin combinations.**

Observations show higher count (i.e. lower effect) than what is expected if the combination was additive.

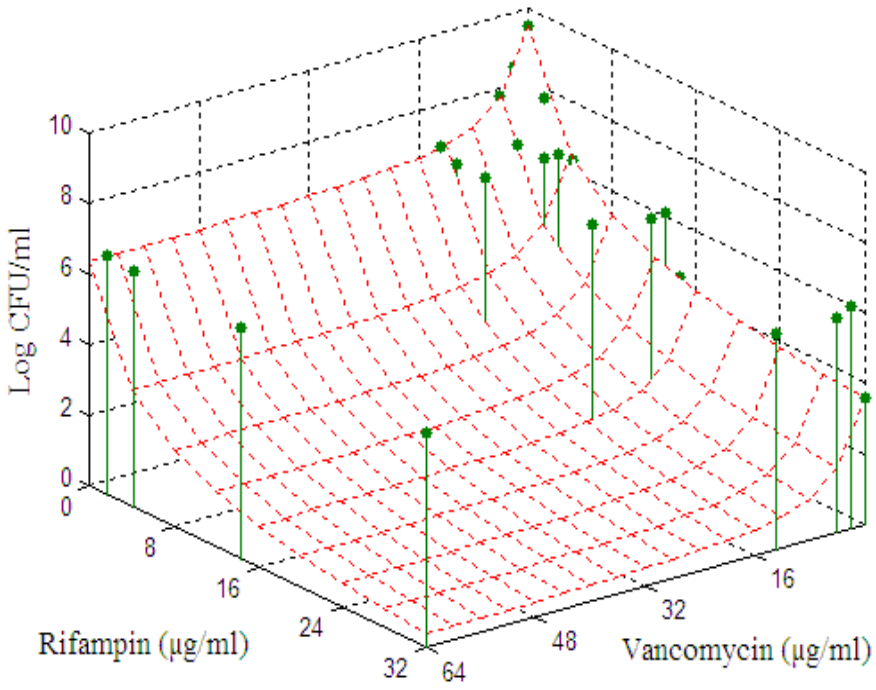

**Figure 4-5: The extent of antagonism at the different concentrations of vancomycin–rifampin combination**

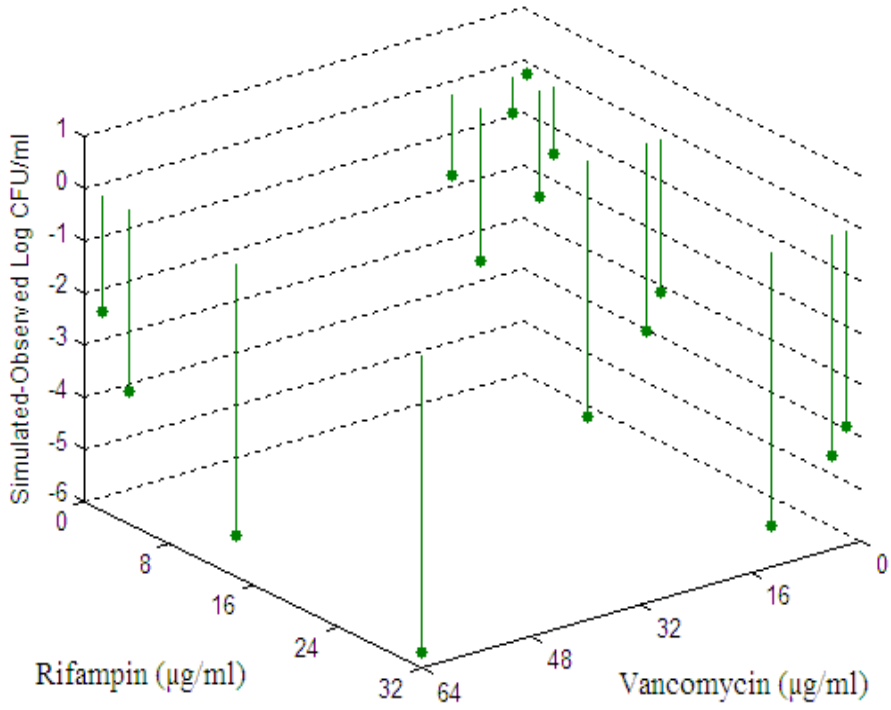

# Pharmacodynamics of Moxifloxacin versus Vancomycin against Biofilms of Methicillin Resistant *Staphylococcus aureus* and Methicillin Resistant *Staphylococcus epidermidis*

This chapter will be published in Journal of Chemotherapy 22(4), August 2010

# 5.1 INTRODUCTION

About 50% of nosocomial infections occurring every year in the United States are associated with indwelling medical devices such as intravascular catheters, urinary catheters, orthopedic devices and other implanted prosthetic devices [1]. *Staphylococcus aureus* as well as coagulase negative staphylococci (CoNS) such as *Staphylococcus epidermidis* are the most commonly associated pathogens with device-related and catheter-related infections [2-4]. This may be attributed to the commensal presence of these pathogens on the human skin and mucous membranes which allow them to invade and colonize foreign surfaces when the skin barrier is disrupted by inserted or implanted medical devices [4]. Staphylococci are known for their ability to adhere to the surface of the foreign implanted material forming a biofilm which plays a key role in the pathogenesis of the implant related infections [5]. The bacterial biofilm is a structured community of bacterial cells enclosed in a self-produced polymeric matrix and adherent to an inert or living surface [6]. The bacteria in biofilm communities are much less susceptible to killing by antimicrobial agents and hence, treatment of biofilm associated infections on the basis of standardized antimicrobial susceptibility testing results is frequently unsuccessful [6] and removal of the implanted device or catheter is required in many cases [7]. This leads to considerable cost, patient inconvenience, and increases the associated morbidity and mortality appreciably [8].

Most of biofilm forming staphylococci are resistant to methicillin (89% of biofilm forming CoNS isolates and 59% of biofilm forming *S. aureus* isolates) [4]. Glycopeptide antibiotics, particularly vancomycin, are regarded as the drugs of choice for treatment of methicillin resistant staphylococci [9]. However, resistance to these agents has emerged and

the polymorphism, that is responsible for this decreased susceptibility, was also found to be associated with overproduction of biofilm [10]. On the other hand, *in vitro* and *in vivo* studies have demonstrated the activity of fluoroquinolones against some bacterial biofilms and have suggested its potential in treatment of biofilm associated staphylococcal infections [11-18]. In the present study, we have utilized a novel *in vitro* pharmacodynamic biofilm model to compare the antimicrobial activities of clinically used doses of moxifloxacin and vancomycin against methicillin resistant *S. aureus* (MRSA) and methicillin resistant *S. epidermidis* (MRSE) biofilms.

## 5.2 METHODS

### 5.2.1 Microorganisms & Antimicrobial Agents

Methicillin-resistant *S. aureus* ATCC 43300 was purchased from the American Type Culture Collection (Manassas, VA, USA) and a Methicillin-resistant *S. epidermidis* clinical isolate SE 2905 was obtained from the Canadian Ward Surveillance Study (CANWARD) and was generously provided by Dr. George G. Zhanel (University of Manitoba, Winnipeg, Canada). Concentrated bacterial suspensions in 10% skim milk were prepared, divided into 1 ml aliquots and stored in cryotubes (Thermo Fisher Scientific, Inc., Waltham, MA, USA) at -80˚C until they were used in the experiments. Cultures were prepared according to ATCC guidelines. All cell culture media and supplements were purchased from Sigma-Aldrich (St. Louis, MO, USA). An inoculum of $1\text{-}2\times10^6$ colony-forming units (CFU)/ml was used in every experiment and was prepared using an overnight culture grown in Tryptic Soy broth (TSB), diluted based on 0.5 McFarland standard (Lenexa, KS, USA) which is equivalent to $1.5\times10^8$ CFU/ml.

Vancomycin and moxifloxacin powders were purchased from Sigma-Aldrich (St. Louis, MO, USA) and Thermo Fisher Scientific, Inc., (Waltham, MA, USA), respectively. Solutions of 86.3 mg/ml vancomycin and 16.0 mg/ml moxifloxacin were prepared and stored as stock solutions at -80°C. Prior to experiments, aliquots of the stock solutions were thawed and diluted in cation adjusted Mueller Hinton II (MHII) broth.

### 5.2.2 Antimicrobial Susceptibility Testing

The minimum inhibitory concentrations (MICs) of the antimicrobial agents were determined using the broth microdilution method as described by the Clinical and Laboratory Standards Institute (CLSI) guidelines [19]. The experiments were performed in polystyrene, round bottom, 96-wells microplates (Greiner Bio-One North America, Monroe, NC, USA). Twofold serial dilutions of the antibiotics in MHII were used and the final bacterial inoculums in each well was $5 \times 10^5$ CFU/ml. The MIC was defined as the lowest concentration of the antibiotic that resulted in no visible growth after aerobic incubation at 37°C for 24 h.

### 5.2.3 *In vitro* Pharmacodynamic Model

*Model Structure*

A previously described *in vitro* model [20] was used to compare the activities of therapeutic dosage regimens of vancomycin and moxifloxacin on MRSA and MRSE biofilms. The model consists of two conical glass vessels, known as the central compartment bioreactors (CCB). Each CCB provides 550 ml of operational fluid capacity and is covered with an autoclavable cap containing five ports (an inlet of fresh medium, an effluent connected to a waste vessel, coupons suspending port, antibiotic injection port, and sampling port). For each experiment, two bioreactors were used, one for testing the antimicrobial dosing regimen and the other for the control. Both bioreactors were contained in water bath and the temperature was maintained constant at 37˚C using a thermo-sensitive feedback probe (Thermo Fisher Scientific, Inc., Waltham, MA, USA) for simulation of human body temperature. A magnetic stir bar was used to ensure

thorough mixing of the drug and consistent shear to the biofilm coated coupons. In order to stimulate the biofilm embedded cells to produce stronger slime matrix, the agitation in the CCB was maintained at low rate (60 RPM) during the entire experiment using a digitally controlled magnetic stirring plate (Thermo Fisher Scientific, Inc., Waltham, MA, USA).

*Biofilm Formation*

In each experiment, bacterial biofilm was developed on two sets of silicone coupons (LabPure Saint-Gobain Corporation, Valley Forge, PA, USA) using overnight TSB culture (50 ml) of $1 - 2 \times 10^6$ CFU/ml of the respective microorganism. After incubation for 24 h under aerobic conditions at 37˚C, each set of coupons was aseptically inserted into one of the bioreactors using the coupons suspending port. Establishment of the biofilm on silicone coupons was confirmed using scanning electron microscopy. The photo was captured using variable pressure JEOL scanning electron microscope according to the method described by van Heerden *et al.* [21].

*Simulation of the Pharmacokinetic Profiles*

Sterile MHII broth was continuously supplied and removed from the bioreactors by peristaltic pumps (Masterflex, Cole-Parmer, Vernon Hills, IL, USA) adjusted at a fixed rate to simulate the half-lives of vancomycin (6 h) and moxifloxacin (12 h). The pumps flow rates were verified by measurement of the volume recovered in the waste vessel. Vancomycin was administered into the bioreactor via the injection port to simulate a dose of 1 gm every 12 h (peak concentration (Cmax) 40 mg/L, trough concentration 10 mg/L, area under the concentration-time curve from time zero to 24 h

($AUC_{0–24}$) = 519.4 µg•h/ml) [22]. Moxifloxacin was administered to simulate a dose of 400 mg every 24 h (Cmax 2 mg/L, trough concentration 0.5 mg/L, $AUC_{0–24}$ = 26 µg•h/ml) [23].

*Pharmacodynamic Analysis*

In each experiment, coupons representing the treated and the control biofilms were excised from the bioreactors after 0, 1.5, 3, 6, 12, and 24 h. Each coupon was placed in an Eppendorf tube containing 0.75 ml normal saline and the tubes were then sonicated for 5 min in ultrasonic water bath (Fisher Scientific, Model FS-60, frequency of 40 kHz, ultrasonic power of 130 W) followed by vigorous vortexing for 1 minute to dislodge and disperse the cells from the biofilm. 100 µl samples were then ten-fold serially diluted in sterile normal saline solution to minimize the antibiotic carryover effect by reducing its concentration to sub-MIC levels. Finally, 50 µl samples were plated onto Mueller Hinton agar plates to quantify the total biofilm-embedded bacterial burden. After incubation of the medium plates at 37 ˚C for 24 h, the viable cell count was determined at least in duplicate.

For each experiment, time-kill curves were plotted after log-transforming the mean viable cell count. The anti-biofilm activity was assessed based on the difference between log the bacterial count at the start and at the end of experiment (Δlog), the area under the bacterial kill curve (AUBC) as well as the area between the growth curve used as control and the killing curve of bacteria exposed to the antibiotic (ABBC) [24]. AUBCs were calculated by the trapezoidal rule using GraphPad Prism version 5.02 (GraphPad Software, San Diego, CA, USA). Analysis of Variance and Tukey's test for multiple comparisons was used to compare Δlog across the different treatments using SPSS

version 16.0 (SPSS, Inc., Chicago, IL, USA). The results were considered significant if the p-value $\leq 0.05$. In addition, the different pharmacokinetic/pharmacodynamic (PK/PD) indices, namely Cmax/MIC, %time above MIC and $AUC_{0-24}$ /MIC were computed for each drug-microorganism combination. The MICs used in calculating these parameters were obtained from the susceptibility testing by the broth microdilution method since this is the method used in studies conducted to estimate the cut off values of antimicrobial PK/PD indices [25].

## 5.3 RESULTS

### 5.3.1 Antimicrobial Susceptibility Testing

Resistance of the isolates to methicillin was confirmed and the oxacillin MICs were 16 and 256 µg/ml against MRSA ATCC 43300 and MRSE SE 62905, respectively. On the other hand, both isolates were susceptible in the planktonic form to vancomycin and moxifloxacin and the MICs of vancomycin and moxifloxacin were 1.0 and 0.0625 µg/ml against ATCC 43300 and 2.0 and 0.125 µg/ml against SE 62905, respectively.

### 5.3.2 *In vitro* Pharmacodynamic Model

The mean bacterial density retrieved from the biofilm in the control coupons was higher in the MRSE experiments ($6.6 \times 10^8$ CFU) than the MRSA experiments ($6.8 \times 10^6$ CFU). This could be explained by the higher ability of *S. epidermidis* to adhere to hydrophobic materials [26].

A comparison of the time kill kinetics of vancomycin and moxifloxacin as well as the growth curve of the control experiment for both organisms are shown in Figure 5-1. The killing rate was low in all experiments and vancomycin failed to produce 2 log reduction against either of the two organisms at any time point. Moxifloxacin treatment, however, resulted in 2.5 and 3.7 log reduction in the MRSA and MRSE microbial bioburdens, respectively, after 24 hours of the exposure.

The antibiofilm measures; Δlog, AUBC and ABBC and the PK/PD indices for each drug-microorganism combination are shown in Table 5-1. At the end of the treatment in the MRSA experiments, there was no significant difference between bacterial densities change in the vancomycin and the untreated control (*P* value > 0.05)

while the reduction in the microbial bioburden in the moxifloxacin treated biofilm was significantly higher than both vancomycin and control (*P* values< 0.001, Figure 5-2 a). In the MRSE experiments, both vancomycin and moxifloxacin showed a significant reduction in the bacterial density compared with the control experiment (*P* values <0.001, Figure 5-2 b). The reduction observed with moxifloxacin was found to be greater than vancomycin (*P* value< 0.001).

## 5.4 DISCUSSION

Bacteria in the biofilm mode of growth are phenotypically distinct from planktonic bacteria and are much more resistant to antimicrobial agents [6]. Standardized susceptibility testing techniques, such as broth microdilution and macrodilution methods, are performed on exponentially dividing planktonic bacteria and hence show poor correlation with the clinical outcome in device and catheter –related infections [27]. On the other hand, standardized assays developed for testing the antimicrobial susceptibility of bacterial biofilms such as MBEC™ and MAK assays [28,29] are static techniques that test the antibiotics at fixed concentrations and hence do not represent the clinical setting where the antibiotic concentration fluctuates over time according to its pharmacokinetic parameters. Therefore, alternative biofilm testing methodologies that show reproducibility and correlation with *in vivo* studies should be sought.

Our group has recently developed a novel *in vitro* pharmacodynamic model for studying the activity of antimicrobial agents against bacterial biofilms [20]. The medium flow rate through this model can be controlled to simulate the half lives of the antimicrobial agents in order to mimic their clinical pharmacokinetic profiles. In addition, this model allows monitoring of the bacterial growth and killing kinetics over time and at the different antibiotic concentrations. Silicone is used in this model as the substratum for development of the biofilm to represent the silicone catheters which are known to be more prone to the adherence of microorganisms than polyvinyl or polyethylene catheters [30]. The flow of the medium through the system allows studying of the bacterial attachment to substrata in the presence of shear force as usually is the case in the intravascular environment. Unlike other models that use shedding cells from the biofilm

as a surrogate marker of the biofilm bacterial density, this model allows direct measurement of the bacterial burden via removal of the biofilm by vortexing and sonication prior to examination and measurement by the viable plate count procedure. In a recent study, the model was validated and employed to study the effect of different dosage regimens of ofloxacin on *Pseudomonas aeruginosa* biofilm [20]. In the present study, we tested vancomycin and moxifloxacin against MRSA and MRSE biofilms. Moxifloxacin showed higher activity against both biofilms as shown by greater reduction in the bacterial count at the end of the experiment. Vancomycin lacked any activity against the biofilm formed by the tested strain of MRSA and neither of the two antibiotics was able to sterilize the biofilm formed by either of the two pathogens.

The results of the present study are in accordance with other studies that reported the activity of moxifloxacin against bacterial biofilms [11-18]. In an *in vitro* study, moxifloxacin was the most efficient antibiotic against the biofilms formed by periodontopathogenic bacteria [16]. Moxifloxacin also showed high activity against staphylococcal biofilm in a tissue-cage model of foreign-body infection [11] and in a rat model of osteomyelitis [13]. This activity might be related to the high ability of fluoroquinolones to penetrate bacterial biofilms [4].

It is worth emphasizing that the values of PK/PD indices such as AUC/MIC, Cmax/MIC and % T> MIC, achieved in this study were predictive of the moxifloxacin activity but have failed to predict the resistance of MRSA and MRSE biofilms to vancomycin. Moxifloxacin is a concentration dependent fluoroquinolone and its microbiologic and clinical efficacies have been shown to be correlated to AUC/MIC and Cmax/MIC in *in vitro* models, *in vivo* studies and human trials [31]. Andes *et al* has

demonstrated that for moxifloxacin AUC/MIC ≥ 100 or Cmax/MIC ≥ 8 was associated with significant reduction in number of CFU/ml of MRSE and MRSA in experimental endocarditis models [32]. In the current study, the PK/PD indices were much higher than these recommended cut off values for moxifloxacin and this may explain the activity it exhibited. However, vancomycin activity in the present study showed poor correlation with its AUC/MIC level. Vancomycin had no activity against MRSA biofilm despite achieving a higher AUC/MIC value than the recommended target level of 400 [33]. Moreover, vancomycin exhibited a better anti-biofilm activity against MRSE vs. control despite the lower AUC/MIC level achieved in the MRSE experiments. This suggests that the PK/PD indices determined using studies on planktonic bacteria do not always correlate to pharmacodynamics of antimicrobial agents against bacteria in the biofilm mode. This corroborates the findings of Blaser *et al* who reported that PK/PD indices were not predictive for therapeutic outcome in an *in vitro* pharmacodynamic biofilm studies and *in vivo* studies of device-related infections [34].

The results reported in the present research suggest the relative advantage of moxifloxacin use over vancomycin in the infections associated with MRSA and MRSE biofilms. However, certain limitations should be noted. First, the *in vitro* model does not take into consideration the immune factors and so the observed antibiofilm effect may be smaller than what would be observed *in vivo*. In addition, since the experiment was conducted for 24 hours, we cannot conclude that the results will hold true after this time period. On the other hand, the *in vitro* model we used does not suffer from the inoculum dilution that is often reported in *in vitro* pharmacodynamic studies [35]. Moreover, the

model can be easily adapted to accommodate different dosage regimens, antimicrobial pharmacokinetics as well as combination therapy.

In conclusion, using a novel *in vitro* pharmacodynamic model, we demonstrated the activity of moxifloxacin against MRSA and MRSE biofilms. The results of this study support the implementation of further *in vivo* and clinical studies aimed at demonstrating the efficacy of moxifloxacin in the treatment of biofilm-associated infections and identifying targets linked to anti-biofilm activities.

**Table 5-1: Pharmacodynamic parameters of vancomycin and moxifloxacin in the *in vitro* pharmacodynamic model experiments.**

| Drug/Dosage | MRSA | | | | | | MRSE | | | | | |
|---|---|---|---|---|---|---|---|---|---|---|---|---|
| | ΔLog | AUBC | ABBC | AUC/MIC | Cmax/MIC | %T>MIC | ΔLog | AUBC | ABBC | AUC/MIC | Cmax/MIC | %T>MIC |
| Vancomycin (1gm/12h) | 0.25 | 162.5 | 9.2 | 519.4 | 40 | 100% | -1.7 | 177 | 44.4 | 259.7 | 20 | 100% |
| Moxifloxacin (400mg/24h) | -2.5 | 122.3 | 49.4 | 415.5 | 32 | 100% | -3.7 | 146.8 | 74.6 | 207.8 | 16 | 100% |

AUC is the area under the concentration time curve from time zero to 24 hours ($AUC_{0-24}$) expressed as µg•h/ml.

ΔLog = log CFU/coupon at 24 hours – log CFU/coupon at 0 hours.

AUBC is the area under the bacterial kill curve from time zero to 24 hours and is compared to AUBC levels of 171.7 and 221.4 for the MRSA and MRSE control experiments, respectively.

ABBC is the area between the growth curve used as control and the killing curve of bacteria exposed to the antibiotic

**Figure 5-1: Time-Kill curves of vancomycin and moxifloxacin against MRSA (A) and MRSE (B)**

A

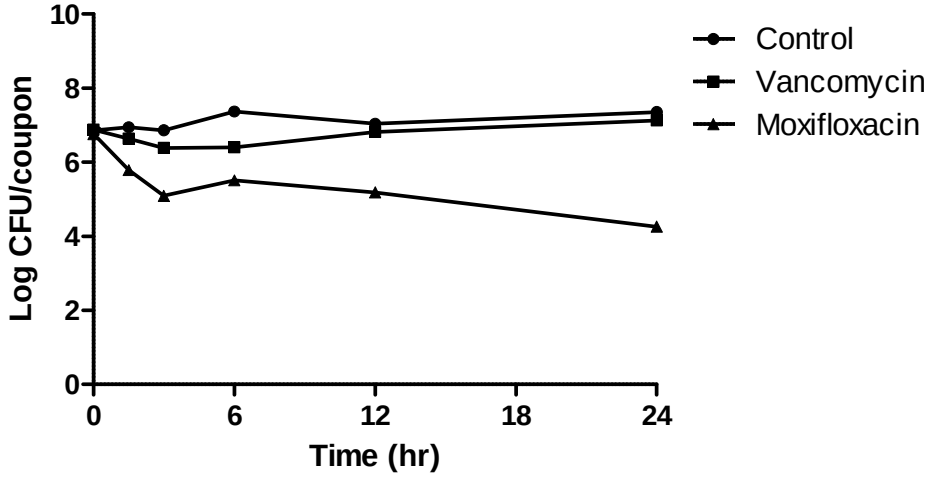


B

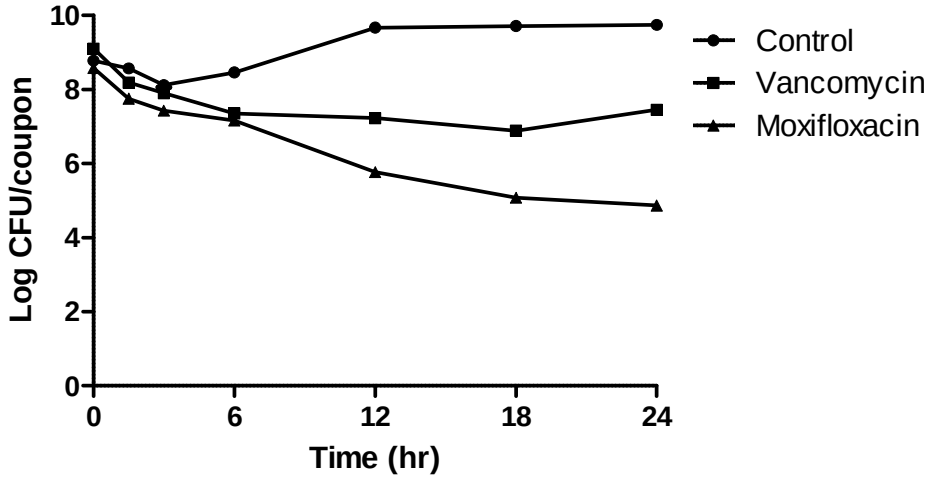

**Figure 5-2: Comparison of the decreases in Log CFU/coupon (means) in MRSA (A) and MRSE (B) between the treatments at the end of the experiment.**

Error bars indicate 95% confidence intervals.

A

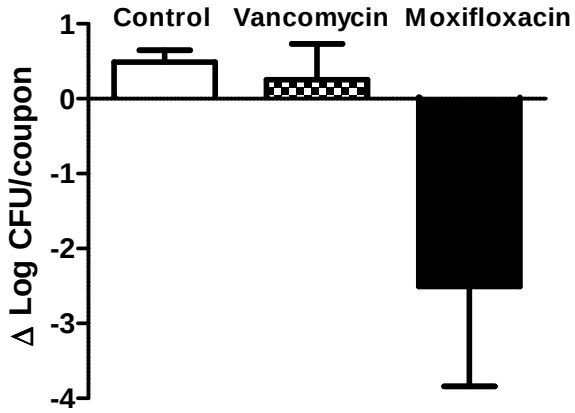


B

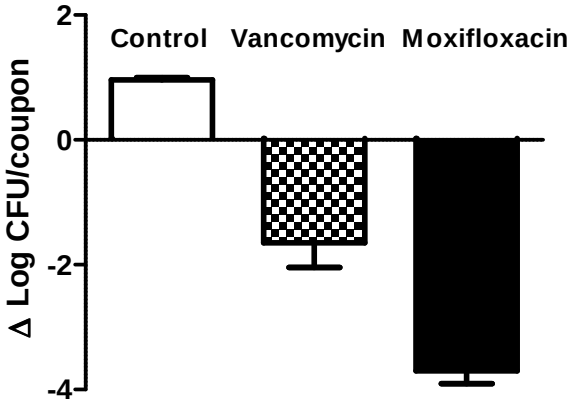

# References

# 6.1 REFERENCES FOR CHAPTER 1

1. Barrett JS, Fossler MJ, Cadieu KD, Gastonguay MR. Pharmacometrics: a multidisciplinary field to facilitate critical thinking in drug development and translational research settings. *The Journal of Clinical Pharmacology*. 2008;48(5):632.

2. Benet LZ, Rowland M. Pharmacometrics: A new journal section. *Journal of Pharmacokinetics and Pharmacodynamics*. 1982;10(4):349-350.

3. Grasela TH, Dement CW, Kolterman OG, et al. Pharmacometrics and the transition to model-based development. *Clinical Pharmacology & Therapeutics*. 2007;82(2):137-142.

4. Miller R, Ewy W, Corrigan BW, et al. How modeling and simulation have enhanced decision making in new drug development. *Journal of pharmacokinetics and pharmacodynamics*. 2005;32(2):185-197.

5. Department of Health and Human Services, US Food and Drug Administration. Guidance for Industry: Exposure–Response Relationships—Study Design, Data Analysis, and Regulatory Applications. . 2003.

6. Department of Health and Human Services, US Food and Drug Administration. Guidance for Industry: Population Pharmacokinetics. . 1999.

7. Department of Health and Human Services, US Food and Drug Administration. Challenge and opportunity on the Critical Path to New Products. . 2004.

8. Aarons L. Population pharmacokinetics: theory and practice. *Br J Clin Pharmacol*. 1991;32(6):669.

9. Steimer JL, Mallet A, Golmard JL, Boisvieux JF. Alternative approaches to estimation of population pharmacokinetic parameters: comparison with the nonlinear mixed-effect model. *Drug Metab Rev*. 1984;15(1-2):265-292.

10. Sheiner LB, Beal SL. Evaluation of methods for estimating population pharmacokinetic parameters. III. Monoexponential model: routine clinical pharmacokinetic data. *Journal of Pharmacokinetics and Pharmacodynamics*. 1983;11(3):303-319.

11. Sheiner LB, Beal SL. Evaluation of methods for estimating population pharmacokinetic parameters II. Biexponential model and experimental pharmacokinetic data. *Journal of Pharmacokinetics and Pharmacodynamics*. 1981;9(5):635-651.

12. Sheiner LB, Beal SL. Evaluation of methods for estimating population pharmacokinetic parameters. I. Michaelis-Menten model: routine clinical pharmacokinetic data. *Journal of Pharmacokinetics and Pharmacodynamics*. 1980;8(6):553-571.

13. Sheiner LB, Beal S, Rosenberg B, Marathe VV. Forecasting individual pharmacokinetics. *Clin Pharmacol Ther*. 1979;26(3):294-305.

14. Yukawa E, Mine H, Higuchi S, Aoyama T. Digoxin population pharmacokinetics from routine clinical data: role of patient characteristics for estimating dosing regimens. *J Pharm Pharmacol*. 1992;44(9):761-765.

15. Collart L, Blaschke TF, Boucher F, Prober CG. Potential of population pharmacokinetics to reduce the frequency of blood sampling required for estimating kinetic parameters in neonates. *Dev Pharmacol Ther*. 1992;18(1-2):71-80.

16. Pai SM, Shukla UA, Grasela TH, et al. Population pharmacokinetic analysis of didanosine (2', 3'-dideoxyinosine) plasma concentrations obtained in phase I clinical trials in patients with AIDS or AIDS-related complex. *The Journal of Clinical Pharmacology*. 1992;32(3):242.

17. Racine-Poon A, Wakefield J. Statistical methods for population pharmacokinetic modelling. *Stat Methods Med Res*. 1998;7(1):63.

18. Beal SB, Sheiner L. NONMEM User's guide version IV, part vii. Conditional estimation methods. *San Francisco, CA: University of California*. 1992.

19. Ette EI, Williams P, Fadiran E, Ajayi FO, Onyiah LC. The process of knowledge discovery from large pharmacokinetic data sets. *The Journal of Clinical Pharmacology*. 2001;41(1):25.

20. Ette EI, Ludden TM. Population pharmacokinetic modeling: the importance of informative graphics. *Pharm Res*. 1995;12(12):1845-1855.

21. Ette EI, Williams PJ, Lane JR. Population pharmacokinetics III: design, analysis, and application of population pharmacokinetic studies. *Ann Pharmacother*. 2004;38(12):2136.

22. Ette EI, Williams PJ. Population pharmacokinetics I: background, concepts, and models. *Ann Pharmacother*. 2004;38(10):1702.

23. Jonsson EN, Karlsson MO. Automated covariate model building within NONMEM. *Pharm Res*. 1998;15(9):1463-1468.

24. Akaike H. A new look at the statistical model identification. *IEEE transactions on automatic control*. 1974;19(6):716-723.

25. Hooker AC, Staatz CE, Karlsson MO. Conditional weighted residuals (CWRES): a model diagnostic for the FOCE method. *Pharm Res*. 2007;24(12):2187-2197.

26. Efron B. Estimating the error rate of a prediction rule: improvement on cross-validation. *Journal of the American statistical association*. 1983;78(382):316-331.

27. Ette EI, Williams PJ, Kim YH, Lane JR, Liu MJ, Capparelli EV. Model appropriateness and population pharmacokinetic modeling. *The Journal of Clinical Pharmacology*. 2003;43(6):610.

28. Ette EI. Stability and performance of a population pharmacokinetic model. *The Journal of Clinical Pharmacology*. 1997;37(6):486.

29. Holford N. The visual predictive check—superiority to standard diagnostic (Rorschach) plots [abstract 738]. . 2005;14.

30. Yano Y, Beal SL, Sheiner LB. Evaluating pharmacokinetic/pharmacodynamic models using the posterior predictive check. *Journal of Pharmacokinetics and Pharmacodynamics*. 2001;28(2):171-192.

31. Craig W. Pharmacodynamics of Antimicrobials: General Concepts and Applications. In: Nightingale CH, Ambrose PG, Drusano GL, Murakawa T, eds. *Antimicrobial pharmacodynamics in theory and clinical practice*. Second ed. Informa Healthcare; 2007:1.

32. Drusano GL. Human Pharmacodynamics of Anti-infectives: Determination from Clinical Trial Data. In: Nightingale CH, Ambrose PG, Drusano GL, Murakawa T,

eds. *Antimicrobial pharmacodynamics in theory and clinical practice.* Second ed. Informa Healthcare; 2007:411.

33. Ebert SC. Pharmacokinetic–pharmacodynamic modeling of irreversible drug effects. In: Derendorf H, Hochhaus G, eds. *Handbook of Pharmacokinetic-Pharmacodynamic Correlation.* CRC Press; 1995:35.

34. Andes D, Craig W. Understanding Pharmacokinetics and Pharmacodynamics: Application to the Antimicrobial Formulary Decision Process. In: Owens RC, Ambrose PG, Nightingale CH, eds. *Antibiotic Optimization: Concepts and Strategies In Clinical Practice.* Marcel Dekker; 2005:41.

35. Cars O, Odenholt-Tornqvist I. The post-antibiotic sub-MIC effect in vitro and in vivo. *J Antimicrob Chemother*. 1993;31(Supplement D):159.

36. McDonald PJ, Wetherall BL, Pruul H. Postantibiotic leukocyte enhancement: increased susceptibility of bacteria pretreated with antibiotics to activity of leukocytes. *Rev Infect Dis*. 1981;3(1):38-44.

37. McDonald PJ, Craig WA, Kunin CM. Persistent effect of antibiotics on Staphylococcus aureus after exposure for limited periods of time. *J Infect Dis*. 1977;135(2):217-223.

38. Craig WA, Gudmundsson S. Post-antibiotic effect. In: Lorian V, ed. *Antibiotics in Laboratory Medicine.* fourth ed. Baltimore, MD: Williams and Wilkins; 1996:296.

39. Sanchez-Recio MM, Colino CI, Sanchez-Navarro A. A retrospective analysis of pharmacokinetic/pharmacodynamic indices as indicators of the clinical efficacy of ciprofloxacin. *J Antimicrob Chemother*. 2000;45(3):321.

40. Schentag JJ. Antimicrobial action and pharmacokinetics/pharmacodynamics: the use of AUIC to improve efficacy and avoid resistance. *Journal of chemotherapy*. 1999;11(6):426-439.

41. Hyatt JM, McKinnon PS, Zimmer GS, Schentag JJ. The importance of pharmacokinetic/pharmacodynamic surrogate markers to outcome: focus on antibacterial agents. *Clin Pharmacokinet*. 1995;28(2):143-160.

42. Andes D, Craig WA. Animal model pharmacokinetics and pharmacodynamics: a critical review. *Int J Antimicrob Agents*. 2002;19(4):261-268.

43. Craig WA. Pharmacokinetic/pharmacodynamic parameters: rationale for antibacterial dosing of mice and men. *Clin Infect Dis*. 1998;26(1):1-10; quiz 11-2.

44. Preston SL, Drusano GL, Berman AL, et al. Pharmacodynamics of levofloxacin: a new paradigm for early clinical trials. *JAMA*. 1998;279(2):125.

45. Craig WA, Ebert SC. Killing and regrowth of bacteria in vitro: a review. *Scand J Infect Dis Suppl*. 1990;74:63-70.

46. Vogelman B, Gudmundsson S, Turnidge J, Leggett J, Craig WA. In vivo postantibiotic effect in a thigh infection in neutropenic mice. *J Infect Dis*. 1988;157(2):287-298.

47. Andes D. In vivo pharmacodynamics of antifungal drugs in treatment of candidiasis. *Antimicrob Agents Chemother*. 2003;47(4):1179.

48. Lacy MK, Lu W, Xu X, et al. Pharmacodynamic comparisons of levofloxacin, ciprofloxacin, and ampicillin against Streptococcus pneumoniae in an in vitro model of infection. *Antimicrob Agents Chemother*. 1999;43(3):672.

49. Craig WA. Interrelationship between pharmacokinetics and pharmacodynamics in determining dosage regimens for broad-spectrum cephalosporins. *Diagn Microbiol Infect Dis*. 1995;22(1-2):89-96.

50. Craig WA, Suh B. Protein Binding. In: Lorian V, ed. *Antibiotics in Laboratory Medicine*. third ed. Baltimore, MD: Williams and Wilkins; 1996:367.

51. Kunin CM, Craig WA, Kornguth M, Monson R. Influence of binding on the pharmacologic activity of antibiotics. *Ann N Y Acad Sci*. 1973;226:214-224.

52. Drusano GL, Johnson DE, Rosen M, Standiford HC. Pharmacodynamics of a fluoroquinolone antimicrobial agent in a neutropenic rat model of Pseudomonas sepsis. *Antimicrob Agents Chemother*. 1993;37(3):483.

53. Leggett JE, Ebert S, Fantin B, Craig WA. Comparative dose-effect relations at several dosing intervals for beta-lactam, aminoglycoside and quinolone antibiotics against gram-negative bacilli in murine thigh-infection and pneumonitis models. *Scand J Infect Dis Suppl*. 1990;74:179-184.

54. Leggett JE, Fantin B, Ebert S, et al. Comparative antibiotic dose-effect relations at several dosing intervals in murine pneumonitis and thigh-infection models. *J Infect Dis*. 1989;159(2):281-292.

55. Vogelman B, Gudmundsson S, Leggett J, Turnidge J, Ebert S, Craig WA. Correlation of antimicrobial pharmacokinetic parameters with therapeutic efficacy in an animal model. *J Infect Dis*. 1988;158(4):831-847.

56. Firsov AA, Vostrov SN, Shevchenko AA, Cornaglia G. Parameters of bacterial killing and regrowth kinetics and antimicrobial effect examined in terms of area under the concentration-time curve relationships: action of ciprofloxacin against Escherichia coli in an in vitro dynamic model. *Antimicrob Agents Chemother*. 1997;41(6):1281-1287.

57. Andes D, Diekema DJ, Pfaller MA, et al. In vivo pharmacodynamic characterization of anidulafungin in a neutropenic murine candidiasis model. *Antimicrob Agents Chemother*. 2008;52(2):539.

58. Andes D, Craig WA. In vivo pharmacodynamic activity of the glycopeptide dalbavancin. *Antimicrob Agents Chemother*. 2007;51(5):1633.

59. Andes D, Van Ogtrop ML, Peng J, Craig WA. In vivo pharmacodynamics of a new oxazolidinone (linezolid). *Antimicrob Agents Chemother*. 2002;46(11):3484.

60. Ambrose PG, Bhavnani SM, Rubino CM, et al. Pharmacokinetics-pharmacodynamics of antimicrobial therapy: it's not just for mice anymore. *Clin Infect Dis*. 2007;44(1):79-86.

61. Drusano GL, Preston SL, Hardalo C, et al. Use of preclinical data for selection of a phase II/III dose for evernimicin and identification of a preclinical MIC breakpoint. *Antimicrob Agents Chemother*. 2001;45(1):13.

62. Bonate PL. A brief introduction to Monte Carlo simulation. *Clin Pharmacokinet*. 2001;40(1):15-22.

63. DOWELL SF, BUTLER JAYC, GIEBINK GS, et al. Acute otitis media: management and surveillance in an era of pneumococcal resistance-a report from the Drug-resistant Streptococcus pneumoniae Therapeutic Working Group. *Pediatr Infect Dis J*. 1999;18(1):1.

64. Heffelfinger JD, Dowell SF, Jorgensen JH, et al. Management of community-acquired pneumonia in the era of pneumococcal resistance: a report from the Drug-Resistant Streptococcus pneumoniae Therapeutic Working Group. *Arch Intern Med*. 2000;160(10):1399.

65. Ambrose PG. Monte Carlo simulation in the evaluation of susceptibility breakpoints: predicting the future: insights from the society of infectious diseases pharmacists. *Pharmacotherapy*. 2006;26(1):129-134.

66. Bhavnani SM, Hammel JP, Cirincione BB, Wikler MA, Ambrose PG. Use of pharmacokinetic-pharmacodynamic target attainment analyses to support phase 2 and 3 dosing strategies for doripenem. *Antimicrob Agents Chemother*. 2005;49(9):3944.

67. Bhavnani SM. Application of Pharmacokinetics and Pharmacodynamics in Antimicrobial Global Drug Development. In: Nightingale CH, Ambrose PG, Drusano GL, Murakawa T, eds. *Antimicrobial pharmacodynamics in theory and clinical practice.* Second ed. Informa Healthcare; 2007:433.

# 6.2 REFERENCES FOR CHAPTER 2

1. Maggiolo F. Efavirenz: a decade of clinical experience in the treatment of HIV. *J Antimicrob Chemother*. 2009.

2. Smith PF, DiCenzo R, Morse GD. Clinical pharmacokinetics of non-nucleoside reverse transcriptase inhibitors. *Clin Pharmacokinet*. 2001;40(12):893-905.

3. Brundage RC, Yong FH, Fenton T, Spector SA, Starr SE, Fletcher CV. Intrapatient variability of efavirenz concentrations as a predictor of virologic response to antiretroviral therapy. *Antimicrob Agents Chemother*. 2004;48(3):979.

4. Stahle L, Moberg L, Svensson JO, Sönnerborg A. Efavirenz plasma concentrations in HIV-infected patients: inter-and intraindividual variability and clinical effects. *Ther Drug Monit*. 2004;26(3):267.

5. Csajka C, Marzolini C, Fattinger K, et al. Population pharmacokinetics and effects of efavirenz in patients with human immunodeficiency virus infection. *Clin Pharmacol Ther*. 2003;73(1):20-30.

6. Best BM, Goicoechea M, Witt MD, et al. A randomized controlled trial of therapeutic drug monitoring in treatment-naive and-experienced HIV-1-infected patients. *JAIDS J Acquired Immune Defic Syndromes*. 2007;46(4):433.

7. López-Cortés LF, Ruiz-Valderas R, Marín-Niebla A, Pascual-Carrasco R, Rodríguez-Díez M, Lucero-Muñoz MJ. Therapeutic drug monitoring of efavirenz: trough levels cannot be estimated on the basis of earlier plasma determinations. *JAIDS J Acquired Immune Defic Syndromes*. 2005;39(5):551.

8. Gutiérrez F, Navarro A, Padilla S, et al. Prediction of neuropsychiatric adverse events associated with long-term efavirenz therapy, using plasma drug level monitoring. *Clinical Infectious Diseases*. 2005;41:1648-1653.

9. Kappelhoff BS, van Leth F, Robinson PA, et al. Are adverse events of nevirapine and efavirenz related to plasma concentrations. *Antivir Ther (Lond )*. 2005;10(4):489-498.

10. Burger D, Van Der Heiden I, La Porte C, et al. Interpatient variability in the pharmacokinetics of the HIV non-nucleoside reverse transcriptase inhibitor efavirenz: the

effect of gender, race, and CYP2B6 polymorphism. *Br J Clin Pharmacol*. 2006;61(2):148.

11. Pfister M, Labbe L, Hammer SM, et al. Population pharmacokinetics and pharmacodynamics of efavirenz, nelfinavir, and indinavir: Adult AIDS Clinical Trial Group Study 398. *Antimicrob Agents Chemother*. 2003;47(1):130.

12. Barrett JS, Joshi AS, Chai M, Ludden TM, Fiske WD, Pieniaszek HJ,Jr. Population pharmacokinetic meta-analysis with efavirenz. *Int J Clin Pharmacol Ther*. 2002;40(11):507-519.

13. Arab-Alameddine M, Di Iulio J, Buclin T, et al. Pharmacogenetics-based population pharmacokinetic analysis of efavirenz in HIV-1-infected individuals. *Clinical Pharmacology & Therapeutics*. 2009.

14. Haas DW. Human genetic variability and HIV treatment response. *Current HIV/AIDS Reports*. 2006;3(2):53-58.

15. Ribaudo HJ, Haas DW, Tierney C, et al. Pharmacogenetics of plasma efavirenz exposure after treatment discontinuation: an Adult AIDS Clinical Trials Group Study. *Clinical Infectious Diseases*. 2006;42:401-407.

16. Haas DW, Ribaudo HJ, Kim RB, et al. Pharmacogenetics of efavirenz and central nervous system side effects: an Adult AIDS Clinical Trials Group study. *AIDS*. 2004;18(18):2391.

17. Lamba V, Lamba J, Yasuda K, et al. Hepatic CYP2B6 expression: gender and ethnic differences and relationship to CYP2B6 genotype and CAR expression. *J Pharmacol Exp Ther*. 2003:103054866.

18. Croom EL, Stevens JC, Hines RN, Wallace AD, Hodgson E. Human hepatic CYP2B6 developmental expression: The impact of age and genotype. *Biochem Pharmacol*. 2009;78(2):184-190.

19. Fletcher CV, Brundage RC, Fenton T, et al. Pharmacokinetics and pharmacodynamics of efavirenz and nelfinavir in HIV-infected children participating in an area-under-the-curve controlled trial. *Clinical Pharmacology & Therapeutics*. 2007;83(2):300-306.

20. Ren Y, Nuttall JJC, Egbers C, et al. High prevalence of subtherapeutic plasma concentrations of efavirenz in children. *JAIDS J Acquired Immune Defic Syndromes*. 2007;45(2):133.

21. Von Hentig N, Koenigs C, Elanjikal S, et al. Need for therapeutic drug monitoring in HIV-1 infected children receiving efavirenz doses according to international guidelines. *Eur J Med Res*. 2006;11(9):377-380.

22. Starr SE, Fletcher CV, Spector SA, et al. Combination therapy with efavirenz, nelfinavir, and nucleoside reverse-transcriptase inhibitors in children infected with human immunodeficiency virus type 1. *N Engl J Med*. 1999;341(25):1874.

23. Beal S, Sheiner LB, Boeckmann A, Bauer RJ. NONMEM User's Guide. . 1989-2009.

24. Holford NHG. A size standard for pharmacokinetics. *Clin Pharmacokinet*. 1996;30(5):329-332.

25. Anderson BJ, Holford NHG. Mechanistic basis of using body size and maturation to predict clearance in humans. *Drug Metabolism and Pharmacokinetics*. 2009;24(1):25-36.

26. Janmahasatian S, Duffull SB, Ash S, Ward LC, Byrne NM, Green B. Quantification of lean bodyweight. *Clin Pharmacokinet*. 2005;44(10):1051-1065.

27. Anderson BJ, Holford NHG. Mechanism-based concepts of size and maturity in pharmacokinetics. . 2008.

28. Anderson BJ, Allegaert K, Van den Anker JN, Cossey V, Holford NHG. Vancomycin pharmacokinetics in preterm neonates and the prediction of adult clearance. *Br J Clin Pharmacol*. 2006;63(1):75-84.

29. Anderson BJ, van Lingen RA, Hansen TG, Lin YC, Holford NHG. Acetaminophen developmental pharmacokinetics in premature neonates and infants: a pooled population analysis. *Anesthesiology*. 2002;96(6):1336.

30. Bouwmeester NJ, Anderson BJ, Tibboel D, Holford NHG. Developmental pharmacokinetics of morphine and its metabolites in neonates, infants and young children. *Br J Anaesth*. 2004;92(2):208.

31. Bergstrand M, Hooker AC, Wallin JE, Karlsson MO. Prediction Corrected Visual Predictive Checks [abstract]. *American Conference on Pharmacometrics*. 2009.

32. Lindbom L, Pihlgren P, Jonsson N. PsN-Toolkit--a collection of computer intensive statistical methods for non-linear mixed effect modeling using NONMEM. *Comput Methods Programs Biomed*. 2005;79(3):241-257.

33. King JR, Kimberlin DW, Aldrovandi GM, Acosta EP. Antiretroviral pharmacokinetics in the paediatric population: a review. *Clin Pharmacokinet*. 2002;41(14):1115-1133.

34. Johnson TN. The problems in scaling adult drug doses to children. *Arch Dis Child*. 2008;93(3):207.

35. Edginton AN, Schmitt W, Voith B, Willmann S. A mechanistic approach for the scaling of clearance in children. *Clin Pharmacokinet*. 2006;45(7):683-704.

36. Johnson TN. Modelling approaches to dose estimation in children. *Br J Clin Pharmacol*. 2005;59(6):663.

37. West GB, Brown JH, Enquist BJ. The fourth dimension of life: fractal geometry and allometric scaling of organisms. *Science*. 1999;284(5420):1677.

38. West GB, Brown JH, Enquist BJ. A general model for the origin of allometric scaling laws in biology. *Science*. 1997;276(5309):122.

39. Han PY, Duffull SB, Kirkpatrick CMJ, Green B. Dosing in obesity: a simple solution to a big problem. *Clinical Pharmacology & Therapeutics*. 2007;82(5):505-508.

40. Rhodin MM, Anderson BJ, Peters AM, et al. Human renal function maturation: a quantitative description using weight and postmenstrual age. *Pediatric Nephrology*. 2009;24(1):67-76.

41. Anderson BJ, Woollard GA, Holford NHG. A model for size and age changes in the pharmacokinetics of paracetamol in neonates, infants and children. *Br J Clin Pharmacol*. 2000;50(2):125.

42. Kimura T, Sunakawa K, Matsuura N, Kubo H, Shimada S, Yago K. Population pharmacokinetics of arbekacin, vancomycin, and panipenem in neonates. *Antimicrob Agents Chemother*. 2004;48(4):1159.

43. Anand K, Anderson B, Holford N, et al. Morphine pharmacokinetics and pharmacodynamics in preterm and term neonates: secondary results from the NEOPAIN trial. *Br J Anaesth*. 2008;101(5):680.

44. Hirt D, Urien S, Olivier M, et al. Is the Recommended Dose of Efavirenz Optimal in Young West African Human Immunodeficiency Virus-Infected Children? *Antimicrob Agents Chemother*. 2009;53(10):4407.

45. Holford N. Dosing in Children. *Clinical Pharmacology & Therapeutics*. 2010.

46. Saitoh A, Fletcher CV, Brundage R, et al. Efavirenz pharmacokinetics in HIV-1-infected children are associated with CYP2B6-G516T polymorphism. *JAIDS J Acquired Immune Defic Syndromes*. 2007;45(3):280.

47. Lang T, Klein K, Fischer J, et al. Extensive genetic polymorphism in the human CYP2B6 gene with impact on expression and function in human liver. *Pharmacogenetics and Genomics*. 2001;11(5):399.

48. Klein K, Lang T, Saussele T, et al. Genetic variability of CYP2B6 in populations of African and Asian origin: allele frequencies, novel functional variants, and possible implications for anti-HIV therapy with efavirenz. *Pharmacogenetics and genomics*. 2005;15(12):861.

49. Nyakutira C, Röshammar D, Chigutsa E, et al. High prevalence of the CYP2B6 516G→ T (* 6) variant and effect on the population pharmacokinetics of efavirenz in HIV/AIDS outpatients in Zimbabwe. *Eur J Clin Pharmacol*. 2008;64(4):357-365.

50. Wang H, Tompkins LM. CYP2B6: new insights into a historically overlooked cytochrome P450 isozyme. *Curr Drug Metab*. 2008;9(7):598.

51. Gatanaga H, Hayashida T, Tsuchiya K, et al. Successful efavirenz dose reduction in HIV type 1–infected individuals with cytochrome P450 2B6* 6 and* 26. *Clinical Infectious Diseases*. 2007;45:1230-1237.

52. ter Heine R, Scherpbier HJ, Crommentuyn KM, et al. A pharmacokinetic and pharmacogenetic study of efavirenz in children: dosing guidelines can result in subtherapeutic concentrations. *Antivir Ther*. 2008;13(6):779-787.

53. Brundage RC, Fletcher CV, Fiske W.D., et al. Pharmacokinetics of an efavirenz suspension in children [abstract 424]. *6th Conference on Retroviruses and Opportunistic Infections, Foundation for Retrovirology and Human Health*. 1999.

54. Kim RB, Fromm MF, Wandel C, et al. The drug transporter P-glycoprotein limits oral absorption and brain entry of HIV-1 protease inhibitors. *J Clin Invest*. 1998;101(2):289.

55. Haas DW, Smeaton LM, Shafer RW, et al. Pharmacogenetics of long-term responses to antiretroviral regimens containing efavirenz and/or nelfinavir: an Adult AIDS Clinical Trials Group Study. *J Infect Dis*. 2005;192:1931-1942.

56. Fellay J, Marzolini C, Meaden ER, et al. Response to antiretroviral treatment in HIV-1-infected individuals with allelic variants of the multidrug resistance transporter 1: a pharmacogenetics study. *The Lancet*. 2002;359(9300):30-36.

57. Störmer E, von Moltke LL, Perloff MD, Greenblatt DJ. Differential modulation of P-glycoprotein expression and activity by non-nucleoside HIV-1 reverse transcriptase inhibitors in cell culture. *Pharm Res*. 2002;19(7):1038-1045.

58. Fiske WD, Joshi AS, Labriola DF. An assessment of population pharmacokinetic parameters of efavirenz on nervous system symptoms and suppression of HIV RNA. . 2001:16–19.

59. Pereira SA, Branco T, Caixas U, et al. Intra-individual variability in efavirenz plasma concentrations supports therapeutic drug monitoring based on quarterly sampling in the first year of Therapy. *Ther Drug Monit*. 2008;30(1):60-66.

60. King J, Aberg JA. Clinical impact of patient population differences and genomic variation in efavirenz therapy. *AIDS*. 2008;22(14):1709.

61. Mosteller RD. Simplified calculation of body-surface area. *N Engl J Med*. 1987;317(17):1098.

## 6.3 REFERENCES FOR CHAPTER 3

1. Clark NM, Hershberger E, Zervosc MJ, Lynch JP,3rd. Antimicrobial resistance among gram-positive organisms in the intensive care unit. *Curr Opin Crit Care*. 2003;9(5):403-412.

2. Cosgrove SE, Qi Y, Kaye KS, Harbarth S, Karchmer AW, Carmeli Y. The impact of methicillin resistance in Staphylococcus aureus bacteremia on patient outcomes: mortality, length of stay, and hospital charges. *Infect Control Hosp Epidemiol*. 2005;26(2):166-174.

3. Jevons MP. Celbenin-resistant staphylococci. *Br Med J*. 1961;1(5219):124-125.

4. Rybak MJ, Akins RL. Emergence of methicillin-resistant Staphylococcus aureus with intermediate glycopeptide resistance: clinical significance and treatment options. *Drugs*. 2001;61(1):1-7.

5. Sista RR, Oda G, Barr J. Methicillin-resistant Staphylococcus aureus infections in ICU patients. *Anesthesiol Clin North America*. 2004;22(3):405-35, vi.

6. Fluit AC, Wielders CL, Verhoef J, Schmitz FJ. Epidemiology and susceptibility of 3,051 Staphylococcus aureus isolates from 25 university hospitals participating in the European SENTRY study. *J Clin Microbiol*. 2001;39(10):3727-3732.

7. Blot SI, Vandewoude KH, Hoste EA, Colardyn FA. Outcome and attributable mortality in critically Ill patients with bacteremia involving methicillin-susceptible and methicillin-resistant Staphylococcus aureus. *Arch Intern Med*. 2002;162(19):2229-2235.

8. Okuma K, Iwakawa K, Turnidge JD, et al. Dissemination of new methicillin-resistant Staphylococcus aureus clones in the community. *J Clin Microbiol*. 2002;40(11):4289-4294.

9. Eguia JM, Chambers HF. Community-acquired Methicillin-resistant Staphylococcus aureus: Epidemiology and Potential Virulence Factors. *Curr Infect Dis Rep*. 2003;5(6):459-466.

10. Fridkin SK, Hageman JC, Morrison M, et al. Methicillin-resistant Staphylococcus aureus disease in three communities. *N Engl J Med*. 2005;352(14):1436-1444.

11. King MD, Humphrey BJ, Wang YF, Kourbatova EV, Ray SM, Blumberg HM. Emergence of community-acquired methicillin-resistant Staphylococcus aureus USA 300 clone as the predominant cause of skin and soft-tissue infections. *Ann Intern Med*. 2006;144(5):309-317.

12. Moellering RC,Jr. The growing menace of community-acquired methicillin-resistant Staphylococcus aureus. *Ann Intern Med*. 2006;144(5):368-370.

13. Noskin GA, Rubin RJ, Schentag JJ, et al. The burden of Staphylococcus aureus infections on hospitals in the United States: an analysis of the 2000 and 2001 Nationwide Inpatient Sample Database. *Arch Intern Med*. 2005;165(15):1756-1761.

14. Cunha BA. Antimicrobial therapy of multidrug-resistant Streptococcus pneumoniae, vancomycin-resistant enterococci, and methicillin-resistant Staphylococcus aureus. *Med Clin North Am*. 2006;90(6):1165-1182.

15. Lodise TP,Jr, McKinnon PS. Burden of methicillin-resistant Staphylococcus aureus: focus on clinical and economic outcomes. *Pharmacotherapy*. 2007;27(7):1001-1012.

16. Fowler VG,Jr, Kong LK, Corey GR, et al. Recurrent Staphylococcus aureus bacteremia: pulsed-field gel electrophoresis findings in 29 patients. *J Infect Dis*. 1999;179(5):1157-1161.

17. Levine DP, Fromm BS, Reddy BR. Slow response to vancomycin or vancomycin plus rifampin in methicillin-resistant Staphylococcus aureus endocarditis. *Ann Intern Med*. 1991;115(9):674-680.

18. Chang FY, Peacock JE,Jr, Musher DM, et al. Staphylococcus aureus bacteremia: recurrence and the impact of antibiotic treatment in a prospective multicenter study. *Medicine (Baltimore)*. 2003;82(5):333-339.

19. Small PM, Chambers HF. Vancomycin for Staphylococcus aureus endocarditis in intravenous drug users. *Antimicrob Agents Chemother*. 1990;34(6):1227-1231.

20. Sakoulas G, Moellering RC,Jr, Eliopoulos GM. Adaptation of methicillin-resistant Staphylococcus aureus in the face of vancomycin therapy. *Clin Infect Dis*. 2006;42 Suppl 1:S40-50.

21. Stein GE, Wells EM. The importance of tissue penetration in achieving successful antimicrobial treatment of nosocomial pneumonia and complicated skin and soft-tissue infections caused by methicillin-resistant Staphylococcus aureus: vancomycin and linezolid. *Curr Med Res Opin*. 2010;26(3):571-588.

22. Lodise TP, Patel N, Renaud-Mutart A, Gorodecky E, Fritsche TR, Jones RN. Pharmacokinetic and pharmacodynamic profile of ceftobiprole. *Diagn Microbiol Infect Dis*. 2008;61(1):96-102.

23. Jones RN, Stilwell MG, Sader HS, Fritsche TR, Goldstein BP. Spectrum and potency of dalbavancin tested against 3322 Gram-positive cocci isolated in the United States Surveillance Program (2004). *Diagn Microbiol Infect Dis*. 2006;54(2):149-153.

24. Jones RN, Fritsche TR, Sader HS, Goldstein BP. Antimicrobial spectrum and potency of dalbavancin tested against clinical isolates from Europe and North America (2003): initial results from an international surveillance protocol. *J Chemother*. 2005;17(6):593-600.

25. Streit JM, Fritsche TR, Sader HS, Jones RN. Worldwide assessment of dalbavancin activity and spectrum against over 6,000 clinical isolates. *Diagn Microbiol Infect Dis*. 2004;48(2):137-143.

26. Snydman DR, Jacobus NV, McDermott LA, Lonks JR, Boyce JM. Comparative In vitro activities of daptomycin and vancomycin against resistant gram-positive pathogens. *Antimicrob Agents Chemother*. 2000;44(12):3447-3450.

27. Barry AL, Fuchs PC, Brown SD. In vitro activities of daptomycin against 2,789 clinical isolates from 11 North American medical centers. *Antimicrob Agents Chemother*. 2001;45(6):1919-1922.

28. Critchley IA, Blosser-Middleton RS, Jones ME, Thornsberry C, Sahm DF, Karlowsky JA. Baseline study to determine in vitro activities of daptomycin against gram-positive pathogens isolated in the United States in 2000-2001. *Antimicrob Agents Chemother*. 2003;47(5):1689-1693.

29. Moellering RC. Linezolid: the first oxazolidinone antimicrobial. *Ann Intern Med*. 2003;138(2):135-142.

30. Lentino JR, Narita M, Yu VL. New antimicrobial agents as therapy for resistant gram-positive cocci. *Eur J Clin Microbiol Infect Dis*. 2008;27(1):3-15.

31. Schramm GE, Johnson JA, Doherty JA, Micek ST, Kollef MH. Methicillin-resistant Staphylococcus aureus sterile-site infection: The importance of appropriate initial antimicrobial treatment. *Crit Care Med*. 2006;34(8):2069-2074.

32. Dancer SJ. The effect of antibiotics on methicillin-resistant Staphylococcus aureus. *J Antimicrob Chemother*. 2008;61(2):246-253.

33. Zhanel GG, DeCorby M, Laing N, et al. Antimicrobial-resistant pathogens in intensive care units in Canada: results of the Canadian National Intensive Care Unit (CAN-ICU) study, 2005-2006. *Antimicrob Agents Chemother*. 2008;52(4):1430-1437.

34. Zhanel GG, Decorby M, Nichol KA, et al. Characterization of methicillin-resistant Staphylococcus aureus, vancomycin-resistant enterococci and extended-spectrum beta-lactamase-producing Escherichia coli in intensive care units in Canada: Results of the Canadian National Intensive Care Unit (CAN-ICU) study (2005-2006). *Can J Infect Dis Med Microbiol*. 2008;19(3):243-249.

35. Murthy B, Schmitt-Hoffmann A. Pharmacokinetics and pharmacodynamics of ceftobiprole, an anti-MRSA cephalosporin with broad-spectrum activity. *Clin Pharmacokinet*. 2008;47(1):21-33.

36. Murthy B, Skee D, Wexler D. Pharmacokinetics of ceftobiprole following single and multiple intravenous infusions administered to healthy subjects (poster P779). . 2007.

37. Buckwalter M, Dowell JA. Population pharmacokinetic analysis of dalbavancin, a novel lipoglycopeptide. *J Clin Pharmacol*. 2005;45(11):1279-1287.

38. Dvorchik B, Arbeit RD, Chung J, Liu S, Knebel W, Kastrissios H. Population pharmacokinetics of daptomycin. *Antimicrob Agents Chemother*. 2004;48(8):2799-2807.

39. Meagher AK, Forrest A, Rayner CR, Birmingham MC, Schentag JJ. Population pharmacokinetics of linezolid in patients treated in a compassionate-use program. *Antimicrob Agents Chemother*. 2003;47(2):548-553.

40. Van Wart SA, Owen JS, Ludwig EA, Meagher AK, Korth-Bradley JM, Cirincione BB. Population pharmacokinetics of tigecycline in patients with complicated intra-abdominal or skin and skin structure infections. *Antimicrob Agents Chemother*. 2006;50(11):3701-3707.

41. Llopis-Salvia P, Jimenez-Torres NV. Population pharmacokinetic parameters of vancomycin in critically ill patients. *J Clin Pharm Ther*. 2006;31(5):447-454.

42. Lodise TP,Jr, Pypstra R, Kahn JB, et al. Probability of target attainment for ceftobiprole as derived from a population pharmacokinetic analysis of 150 subjects. *Antimicrob Agents Chemother*. 2007;51(7):2378-2387.

43. Kimko H, Xu X, Nandy P, et al. Pharmacodynamic profiling of ceftobiprole for treatment of complicated skin and skin structure infections. *Antimicrob Agents Chemother*. 2009;53(8):3371-3374.

44. Andes D, Craig WA. In vivo pharmacodynamic activity of the glycopeptide dalbavancin. *Antimicrob Agents Chemother*. 2007;51(5):1633.

45. Cha R, Grucz Jr RG, Rybak MJ. Daptomycin dose-effect relationship against resistant gram-positive organisms. *Antimicrob Agents Chemother*. 2003;47(5):1598.

46. Andes D, Van Ogtrop ML, Peng J, Craig WA. In vivo pharmacodynamics of a new oxazolidinone (linezolid). *Antimicrob Agents Chemother*. 2002;46(11):3484.

47. Meagher AK, Passarell JA, Cirincione BB, et al. Exposure-response analyses of tigecycline efficacy in patients with complicated skin and skin-structure infections. *Antimicrob Agents Chemother*. 2007;51(6):1939.

48. Ambrose PG, Meagher AK, Passarell JA, et al. Application of patient population-derived pharmacokinetic–pharmacodynamic relationships to tigecycline breakpoint determination for staphylococci and streptococci. *Diagnostic Microbiology & Infectious Disease*. 2009;63(2):155-159.

49. Kuti JL, Kiffer CR, Mendes CM, Nicolau DP. Pharmacodynamic comparison of linezolid, teicoplanin and vancomycin against clinical isolates of Staphylococcus aureus and coagulase-negative staphylococci collected from hospitals in Brazil. *Clinical Microbiology and Infection*. 2008;14(2):116.

50. Rybak M, Lomaestro B, Rotschafer JC, et al. Therapeutic monitoring of vancomycin in adult patients: a consensus review of the American Society of Health-System Pharmacists, the Infectious Diseases Society of America, and the Society of Infectious Diseases Pharmacists. *American Journal of Health-System Pharmacy*. 2009;66(1):82.

51. Kuti JL, Dandekar PK, Nightingale CH, Nicolau DP. Use of Monte Carlo simulation to design an optimized pharmacodynamic dosing strategy for meropenem. *The Journal of Clinical Pharmacology*. 2003;43(10):1116.

52. Mouton JW, Dudley MN, Cars O, Derendorf H, Drusano GL. Standardization of pharmacokinetic/pharmacodynamic(PK/PD) terminology for anti-infective drugs: an update. *J Antimicrob Chemother*. 2005;55(5):601-607.

53. Dudley MN, Ambrose PG. Pharmacodynamics in the study of drug resistance and establishing in vitro susceptibility breakpoints: ready for prime time. *Curr Opin Microbiol*. 2000;3(5):515-521.

54. Gentry B, Blankinship D, Wainwright E. Oracle crystal ball user manual. 11.1. Denver, USA: Orcale. . 2008.

55. Bonate PL. A brief introduction to Monte Carlo simulation. *Clin Pharmacokinet*. 2001;40(1):15-22.

56. Kuti JL, Nicolau DP. Making the most of surveillance studies: summary of the OPTAMA Program. *Diagnostic Microbiology & Infectious Disease*. 2005;53(4):281-287.

57. Ambrose PG, Grasela DM. The use of Monte Carlo simulation to examine pharmacodynamic variance of drugs: fluoroquinolone pharmacodynamics against Streptococcus pneumoniae. *Diagn Microbiol Infect Dis*. 2000;38(3):151-157.

58. Ambrose PG, Bhavnani SM, Rubino CM, et al. Pharmacokinetics-pharmacodynamics of antimicrobial therapy: it's not just for mice anymore. *Clin Infect Dis*. 2007;44(1):79-86.

59. Drusano GL, Preston SL, Fowler C, Corrado M, Weisinger B, Kahn J. Relationship between fluoroquinolone area under the curve: minimum inhibitory concentration ratio and the probability of eradication of the infecting pathogen, in patients with nosocomial pneumonia. *J Infect Dis*. 2004;189(9):1590-1597.

60. Preston SL, Drusano GL, Berman AL, et al. Pharmacodynamics of levofloxacin: a new paradigm for early clinical trials. *JAMA*. 1998;279(2):125.

61. Noel GJ, Bush K, Bagchi P, Ianus J, Strauss RS. A randomized, double-blind trial comparing ceftobiprole medocaril with vancomycin plus ceftazidime for the

treatment of patients with complicated skin and skin-structure infections. *Clinical Infectious Diseases*. 2008;46(5):647-655.

62. Jauregui LE, Babazadeh S, Seltzer E, et al. Randomized, double-blind comparison of once-weekly dalbavancin versus twice-daily linezolid therapy for the treatment of complicated skin and skin structure infections. *Clin Infect Dis*. 2005;41(10):1407-1415.

63. Seltzer E, Dorr MB, Goldstein BP, et al. Once-weekly dalbavancin versus standard-of-care antimicrobial regimens for treatment of skin and soft-tissue infections. *Clin Infect Dis*. 2003;37(10):1298-1303.

64. Dowell JA, Goldstein BP, Buckwalter M, Stogniew M, Damle B. Pharmacokinetic-pharmacodynamic modeling of dalbavancin, a novel glycopeptide antibiotic. *J Clin Pharmacol*. 2008;48(9):1063-1068.

65. Rybak MJ, Lomaestro BM, Rotschafer JC, et al. Vancomycin therapeutic guidelines: a summary of consensus recommendations from the Infectious Diseases Society of America, the American Society of Health-System Pharmacists, and the Society of Infectious Diseases Pharmacists. *Clinical Infectious Diseases*. 2009;49(3):325-327.

66. Ambrose PG. Monte Carlo simulation in the evaluation of susceptibility breakpoints: predicting the future: insights from the society of infectious diseases pharmacists. *Pharmacotherapy*. 2006;26(1):129-134.

67. Mueller M, de la Pena A, Derendorf H. Issues in pharmacokinetics and pharmacodynamics of anti-infective agents: kill curves versus MIC. *Antimicrob Agents Chemother*. 2004;48(2):369.

68. Hidayat LK, Hsu DI, Quist R, Shriner KA, Wong-Beringer A. High-dose vancomycin therapy for methicillin-resistant Staphylococcus aureus infections: efficacy and toxicity. *Arch Intern Med*. 2006;166(19):2138.

69. Sakoulas G, Moise-Broder PA, Schentag J, Forrest A, Moellering RC,Jr, Eliopoulos GM. Relationship of MIC and bactericidal activity to efficacy of vancomycin for treatment of methicillin-resistant Staphylococcus aureus bacteremia. *J Clin Microbiol*. 2004;42(6):2398-2402.

70. Tenover FC, Moellering RC,Jr. The rationale for revising the Clinical and Laboratory Standards Institute vancomycin minimal inhibitory concentration interpretive criteria for Staphylococcus aureus. *Clin Infect Dis*. 2007;44(9):1208-1215.

71. Rybak MJ, McKinnon P, Cha R, Dvorchik BH. Daptomycin pharmacodynamics (PD) versus MRSA at various doses as assessed by a Monte Carlo prediction model [abstr]. . 2001;16:19.

72. Tedesco KL, Rybak MJ. Daptomycin. *Pharmacotherapy*. 2004;24(1):41-57.

73. Dandekar PK, Tessier PR, Williams P, Nightingale CH, Nicolau DP. Pharmacodynamic profile of daptomycin against Enterococcus species and methicillin-resistant Staphylococcus aureus in a murine thigh infection model. *J Antimicrob Chemother*. 2003;52(3):405.

74. Aeschlimann JR, Allen GP, Hershberger E, Rybak MJ. Activities of LY333328 and vancomycin administered alone or in combination with gentamicin against three strains of vancomycin-intermediate Staphylococcus aureus in an in vitro pharmacodynamic infection model. *Antimicrob Agents Chemother*. 2000;44(11):2991.

75. Moise-Broder PA, Forrest A, Birmingham MC, Schentag JJ. Pharmacodynamics of vancomycin and other antimicrobials in patients with Staphylococcus aureus lower respiratory tract infections. *Clin Pharmacokinet*. 2004;43(13):925-942.

76. Mouton JW, Punt N, Vinks AA. A retrospective analysis using Monte Carlo simulation to evaluate recommended ceftazidime dosing regimens in healthy volunteers, patients with cystic fibrosis, and patients in the intensive care unit. *Clin Ther*. 2005;27(6):762-772.

# 6.4 REFERENCES FOR CHAPTER 4

1. Wisplinghoff H, Bischoff T, Tallent SM, Seifert H, Wenzel RP, Edmond MB. Nosocomial bloodstream infections in US hospitals: analysis of 24,179 cases from a prospective nationwide surveillance study. *Clin Infect Dis*. 2004;39(3):309-317.

2. Haddadin AS, Fappiano SA, Lipsett PA. Methicillin resistant Staphylococcus aureus (MRSA) in the intensive care unit. *Postgrad Med J*. 2002;78(921):385-392.

3. Klevens RM, Morrison MA, Nadle J, et al. Invasive methicillin-resistant Staphylococcus aureus infections in the United States. *JAMA*. 2007;298(15):1763-1771.

4. Abramson MA, Sexton DJ. Nosocomial methicillin-resistant and methicillin-susceptible Staphylococcus aureus primary bacteremia: at what costs? *Infect Control Hosp Epidemiol*. 1999;20(6):408-411.

5. Engemann JJ, Carmeli Y, Cosgrove SE, et al. Adverse clinical and economic outcomes attributable to methicillin resistance among patients with Staphylococcus aureus surgical site infection. *Clin Infect Dis*. 2003;36(5):592-598.

6. Cosgrove SE, Sakoulas G, Perencevich EN, Schwaber MJ, Karchmer AW, Carmeli Y. Comparison of mortality associated with methicillin-resistant and methicillin-susceptible Staphylococcus aureus bacteremia: a meta-analysis. *Clin Infect Dis*. 2003;36(1):53-59.

7. Inoue Y, Kohno S, Fujii T, et al. Clinical evaluation of catheter-related fungemia and bacteremia. *Intern Med*. 1995;34(6):485-490.

8. Baquero F. Gram-positive resistance: challenge for the development of new antibiotics. *J Antimicrob Chemother*. 1997;39 Suppl A:1-6.

9. Linden PK. Clinical implications of nosocomial gram-positive bacteremia and superimposed antimicrobial resistance. *Am J Med*. 1998;104(5A):24S-33S.

10. Hiramatsu K, Hanaki H, Ino T, Yabuta K, Oguri T, Tenover FC. Methicillin-resistant Staphylococcus aureus clinical strain with reduced vancomycin susceptibility. *J Antimicrob Chemother*. 1997;40(1):135-136.

11. Ploy MC, Grelaud C, Martin C, de Lumley L, Denis F. First clinical isolate of vancomycin-intermediate Staphylococcus aureus in a French hospital. *Lancet*. 1998;351(9110):1212.

12. Sieradzki K, Roberts RB, Haber SW, Tomasz A. The development of vancomycin resistance in a patient with methicillin-resistant Staphylococcus aureus infection. *N Engl J Med*. 1999;340(7):517-523.

13. Ikonomidis A, Vasdeki A, Kristo I, et al. Association of biofilm formation and methicillin-resistance with accessory gene regulator (agr) loci in Greek Staphylococcus aureus clones. *Microb Pathog*. 2009;47(6):341-344.

14. Donlan RM, Costerton JW. Biofilms: survival mechanisms of clinically relevant microorganisms. *Clin Microbiol Rev*. 2002;15(2):167-193.

15. Donlan RM. Biofilms and device-associated infections. *Emerg Infect Dis*. 2001;7(2):277-281.

16. Rice LB. Unmet medical needs in antibacterial therapy. *Biochem Pharmacol*. 2006;71(7):991-995.

17. Eliopoulos GM, Eliopoulos CT. Antibiotic combinations: should they be tested? *Clin Microbiol Rev*. 1988;1(2):139-156.

18. den Hollander JG, Mouton JW. The predictive value of laboratory tests for efifcacy of antibiotic combination therapy. In: Nightingale CH, Ambrose PG, Drusano GL, Murakawa T, eds. *Antimicrobial pharmacodynamics in theory and clinical practice.* Second ed. Informa Healthcare; 2007:103.

19. Perlroth J, Kuo M, Tan J, Bayer AS, Miller LG. Adjunctive use of rifampin for the treatment of Staphylococcus aureus infections: a systematic review of the literature. *Arch Intern Med*. 2008;168(8):805-819.

20. Raad I, Hanna H, Jiang Y, et al. Comparative activities of daptomycin, linezolid, and tigecycline against catheter-related methicillin-resistant Staphylococcus bacteremic isolates embedded in biofilm *Antimicrob Agents Chemother*. 2007;51(5):1656-1660.

21. Saginur R, Stdenis M, Ferris W, et al. Multiple combination bactericidal testing of staphylococcal biofilms from implant-associated infections. *Antimicrob Agents Chemother*. 2006;50(1):55-61.

22. LaPlante KL, Woodmansee S. Activities of daptomycin and vancomycin alone and in combination with rifampin and gentamicin against biofilm-forming methicillin-resistant Staphylococcus aureus isolates in an experimental model of endocarditis *Antimicrob Agents Chemother*. 2009;53(9):3880-3886.

23. Rose WE, Poppens PT. Impact of biofilm on the in vitro activity of vancomycin alone and in combination with tigecycline and rifampicin against Staphylococcus aureus *J Antimicrob Chemother*. 2009;63(3):485-488.

24. Rose WE, Leonard SN, Rybak MJ. Evaluation of daptomycin pharmacodynamics and resistance at various dosage regimens against Staphylococcus aureus isolates with reduced susceptibilities to daptomycin in an in vitro pharmacodynamic model with simulated endocardial vegetations. *Antimicrob Agents Chemother*. 2008;52(9):3061-3067.

25. Riedel DJ, Weekes E, Forrest GN. Addition of rifampin to standard therapy for treatment of native valve infective endocarditis caused by Staphylococcus aureus. *Antimicrob Agents Chemother*. 2008;52(7):2463-2467.

26. Rose WE, Rybak MJ, Tsuji BT, Kaatz GW, Sakoulas G. Correlation of vancomycin and daptomycin susceptibility in Staphylococcus aureus in reference to accessory gene regulator (agr) polymorphism and function. *J Antimicrob Chemother*. 2007;59(6):1190-1193.

27. Levine DP, Fromm BS, Reddy BR. Slow response to vancomycin or vancomycin plus rifampin in methicillin-resistant Staphylococcus aureus endocarditis. *Ann Intern Med*. 1991;115(9):674-680.

28. Miller LG, Quan C, Shay A, et al. A prospective investigation of outcomes after hospital discharge for endemic, community-acquired methicillin-resistant and -susceptible Staphylococcus aureus skin infection. *Clin Infect Dis*. 2007;44(4):483-492.

29. Iyer S, Jones DH. Community-acquired methicillin-resistant Staphylococcus aureus skin infection: a retrospective analysis of clinical presentation and treatment of a local outbreak. *J Am Acad Dermatol*. 2004;50(6):854-858.

30. Tam VH, Schilling AN, Lewis RE, Melnick DA, Boucher AN. Novel approach to characterization of combined pharmacodynamic effects of antimicrobial agents. *Antimicrob Agents Chemother*. 2004;48(11):4315-4321.

31. Clinical and Laboratory Standards Institute. Methods for dilution antimicrobial susceptibility tests for bacteria that grow aerobically. 6th ed. Approved standard. M7-A6. . 2003.

32. Cernohorska L, Votava M. Determination of minimal regrowth concentration (MRC) in clinical isolates of various biofilm-forming bacteria. *Folia Microbiol (Praha)*. 2004;49(1):75-78.

33. Cernohorska L, Votava M. Antibiotic synergy against biofilm-forming Pseudomonas aeruginosa. *Folia Microbiol (Praha)*. 2008;53(1):57-60.

34. Christensen GD, Simpson WA, Younger JJ, et al. Adherence of coagulase-negative staphylococci to plastic tissue culture plates: a quantitative model for the adherence of staphylococci to medical devices. *J Clin Microbiol*. 1985;22(6):996-1006.

35. van Heerden J, Turner M, Hoffmann D, Moolman J. Antimicrobial coating agents: can biofilm formation on a breast implant be prevented? *J Plast Reconstr Aesthet Surg*. 2009;62(5):610-617.

36. Noreddin AM, Elkhatib WF. Novel *in vitro* pharmacodynamic model simulating ofloxacin pharmacokinetics in the treatment of *Pseudomonas aeruginosa* biofilm-associated infections. *Journal of Infection and Public Health*. 2009;2(3):120-128.

37. D'Argenio DZ, Schumitzky A. ADAPT II User's Guide. . 1992.

38. Baltch AL, Ritz WJ, Bopp LH, Michelsen PB, Smith RP. Antimicrobial activities of daptomycin, vancomycin, and oxacillin in human monocytes and of daptomycin in combination with gentamicin and/or rifampin in human monocytes and in broth against Staphylococcus aureus. *Antimicrob Agents Chemother*. 2007;51(4):1559-1562.

39. Cottarel G, Wierzbowski J. Combination drugs, an emerging option for antibacterial therapy. *Trends Biotechnol*. 2007;25(12):547-555.

40. Mackay ML, Milne K, Gould IM. Comparison of methods for assessing synergic antibiotic interactions *Int J Antimicrob Agents*. 2000;15(2):125-129.

41. Cappelletty DM, Rybak MJ. Comparison of methodologies for synergism testing of drug combinations against resistant strains of Pseudomonas aeruginosa. *Antimicrob Agents Chemother*. 1996;40(3):677-683.

42. Bonapace CR, White RL, Friedrich LV, Bosso JA. Evaluation of antibiotic synergy against Acinetobacter baumannii: a comparison with Etest, time-kill, and checkerboard methods. *Diagn Microbiol Infect Dis*. 2000;38(1):43-50.

43. Hilf M, Yu VL, Sharp J, Zuravleff JJ, Korvick JA, Muder RR. Antibiotic therapy for Pseudomonas aeruginosa bacteremia: outcome correlations in a prospective study of 200 patients. *Am J Med*. 1989;87(5):540-546.

44. Norden CW, Wentzel H, Keleti E. Comparison of techniques for measurement of in vitro antibiotic synergism. *J Infect Dis*. 1979;140(4):629-633.

45. Saballs M, Pujol M, Tubau F, et al. Rifampicin/imipenem combination in the treatment of carbapenem-resistant Acinetobacter baumannii infections. *J Antimicrob Chemother*. 2006;58(3):697-700.

46. Boucher AN, Tam VH. Mathematical formulation of additivity for antimicrobial agents. *Diagn Microbiol Infect Dis*. 2006;55(4):319-325.

47. Horrevorts AM, de Ridder CM, Poot MC, et al. Chequerboard titrations: the influence of the composition of serial dilutions of antibiotics on the fractional inhibitory concentration index and fractional bactericidal concentration index. *J Antimicrob Chemother*. 1987;19(1):119-125.

48. Rand KH, Houck HJ, Brown P, Bennett D. Reproducibility of the microdilution checkerboard method for antibiotic synergy. *Antimicrob Agents Chemother*. 1993;37(3):613-615.

49. Costerton JW, Stewart PS, Greenberg EP. Bacterial biofilms: a common cause of persistent infections. *Science*. 1999;284(5418):1318-1322.

50. Saginur R, Stdenis M, Ferris W, et al. Multiple combination bactericidal testing of staphylococcal biofilms from implant-associated infections *Antimicrob Agents Chemother*. 2006;50(1):55-61.

51. Shelburne SA, Musher DM, Hulten K, et al. In vitro killing of community-associated methicillin-resistant Staphylococcus aureus with drug combinations. *Antimicrob Agents Chemother*. 2004;48(10):4016-4019.

52. Mercier RC, Kennedy C, Meadows C. Antimicrobial activity of tigecycline (GAR-936) against Enterococcus faecium and Staphylococcus aureus used alone and in combination. *Pharmacotherapy*. 2002;22(12):1517-1523.

53. Watanakunakorn C, Guerriero JC. Interaction between vancomycin and rifampin against Staphylococcus aureus. *Antimicrob Agents Chemother*. 1981;19(6):1089-1091.

54. Chi CY, Lauderdale TL, Wang SM, Wu JM, Yang YJ, Liu CC. Health care-associated endocarditis caused by Staphylococcus aureus with reduced susceptibility to vancomycin. *J Clin Microbiol*. 2008;46(2):810-813.

# 6.5 REFERENCES FOR CHAPTER 5

1. Darouiche RO. Treatment of infections associated with surgical implants. *N Engl J Med*. 2004;350(14):1422-1429.

2. Moreillon P, Que YA. Infective endocarditis. *Lancet*. 2004;363(9403):139-149.

3. Zimmerli W, Trampuz A, Ochsner PE. Prosthetic-joint infections. *N Engl J Med*. 2004;351(16):1645-1654.

4. Barriere SL. Protein Synthesis Inhibitors, Fluoroquinolones, and Rifampin for Biofilm Infections. In: Pace JL, Rupp ME, Finch RG, eds. *Biofilms, Infection, and Antimicrobial Therapy*. Boca Raton: Taylor & Francis Group; 2006.

5. Saginur R, Stdenis M, Ferris W, et al. Multiple combination bactericidal testing of staphylococcal biofilms from implant-associated infections *Antimicrob Agents Chemother*. 2006;50(1):55-61.

6. Costerton JW, Stewart PS, Greenberg EP. Bacterial biofilms: a common cause of persistent infections. *Science*. 1999;284(5418):1318-1322.

7. Duguid IG, Evans E, Brown MR, Gilbert P. Effect of biofilm culture upon the susceptibility of Staphylococcus epidermidis to tobramycin. *J Antimicrob Chemother*. 1992;30(6):803-810.

8. Rice LB. Unmet medical needs in antibacterial therapy. *Biochem Pharmacol*. 2006;71(7):991-995.

9. Dancer SJ. The effect of antibiotics on methicillin-resistant Staphylococcus aureus. *J Antimicrob Chemother*. 2008;61(2):246-253.

10. Ikonomidis A, Vasdeki A, Kristo I, et al. Association of biofilm formation and methicillin-resistance with accessory gene regulator (agr) loci in Greek Staphylococcus aureus clones. *Microb Pathog*. 2009;47(6):341-344.

11. Murillo O, Pachon ME, Euba G, et al. Antagonistic effect of rifampin on the efficacy of high-dose levofloxacin in staphylococcal experimental foreign-body infection. *Antimicrob Agents Chemother*. 2008;52(10):3681-3686.

12. Frank KL, Reichert EJ, Piper KE, Patel R. In vitro effects of antimicrobial agents on planktonic and biofilm forms of Staphylococcus lugdunensis clinical isolates. *Antimicrob Agents Chemother*. 2007;51(3):888-895.

13. Kalteis T, Beckmann J, Schroder HJ, et al. Treatment of implant-associated infections with moxifloxacin: an animal study. *Int J Antimicrob Agents*. 2006;27(5):444-448.

14. Gander S, Kinnaird A, Finch R. Telavancin: in vitro activity against staphylococci in a biofilm model. *J Antimicrob Chemother*. 2005;56(2):337-343.

15. Presterl E, Grisold AJ, Reichmann S, Hirschl AM, Georgopoulos A, Graninger W. Viridans streptococci in endocarditis and neutropenic sepsis: biofilm formation and effects of antibiotics. *J Antimicrob Chemother*. 2005;55(1):45-50.

16. Eick S, Seltmann T, Pfister W. Efficacy of antibiotics to strains of periodontopathogenic bacteria within a single species biofilm - an in vitro study. *J Clin Periodontol*. 2004;31(5):376-383.

17. Di Bonaventura G, Spedicato I, D'Antonio D, Robuffo I, Piccolomini R. Biofilm formation by Stenotrophomonas maltophilia: modulation by quinolones, trimethoprim-sulfamethoxazole, and ceftazidime. *Antimicrob Agents Chemother*. 2004;48(1):151-160.

18. Perez-Giraldo C, Gonzalez-Velasco C, Sanchez-Silos RM, Hurtado C, Blanco MT, Gomez-Garcia AC. Moxifloxacin and biofilm production by coagulase-negative staphylococci. *Chemotherapy*. 2004;50(2):101-104.

19. Clinical and Laboratory Standards Institute. Methods for dilution antimicrobial susceptibility tests for bacteria that grow aerobically. 6th ed. Approved standard. M7-A6. . 2003.

20. Noreddin AM, Elkhatib WF. Novel *in vitro* pharmacodynamic model simulating ofloxacin pharmacokinetics in the treatment of *Pseudomonas aeruginosa* biofilm-associated infections. *Journal of Infection and Public Health*. 2009;2(3):120-128.

21. van Heerden J, Turner M, Hoffmann D, Moolman J. Antimicrobial coating agents: can biofilm formation on a breast implant be prevented? *J Plast Reconstr Aesthet Surg*. 2009;62(5):610-617.

22. Leonard SN, Rybak MJ. Evaluation of vancomycin and daptomycin against methicillin-resistant Staphylococcus aureus and heterogeneously vancomycin-intermediate S. aureus in an in vitro pharmacokinetic/pharmacodynamic model with simulated endocardial vegetations. *J Antimicrob Chemother*. 2009;63(1):155-160.

23. Schafer J, Hovde LB, Simonson D, Rotschafer JC. In vitro pharmacodynamics of moxifloxacin versus levofloxacin against 4 strains of Streptococcus pneumoniae: 1 wild type, 2 first-step parC mutants, and 1 pump mutant. *Diagn Microbiol Infect Dis*. 2008;60(2):155-161.

24. Firsov AA, Vostrov SN, Shevchenko AA, Cornaglia G. Parameters of bacterial killing and regrowth kinetics and antimicrobial effect examined in terms of area under the concentration-time curve relationships: action of ciprofloxacin against Escherichia coli in an in vitro dynamic model. *Antimicrob Agents Chemother*. 1997;41(6):1281-1287.

25. LaPlante KL, Woodmansee S. Activities of daptomycin and vancomycin alone and in combination with rifampin and gentamicin against biofilm-forming methicillin-resistant Staphylococcus aureus isolates in an experimental model of endocarditis *Antimicrob Agents Chemother*. 2009;53(9):3880-3886.

26. Lerebour G, Cupferman S, Bellon-Fontaine MN. Adhesion of Staphylococcus aureus and Staphylococcus epidermidis to the Episkin reconstructed epidermis model and to an inert 304 stainless steel substrate. *J Appl Microbiol*. 2004;97(1):7-16.

27. Mack D, Horstkotte MA, Rohde H, Knobloch JK-. Coagulase-Negative Staphylococci. In: Pace JL, Rupp ME, Finch RG, eds. *Biofilms, Infection, and Antimicrobial Therapy.* Boca Raton: Taylor & Francis Group; 2006.

28. Knobloch JK, Von Osten H, Horstkotte MA, Rohde H, Mack D. Minimal attachment killing (MAK): a versatile method for susceptibility testing of attached biofilm-positive and -negative Staphylococcus epidermidis. *Med Microbiol Immunol*. 2002;191(2):107-114.

29. Ceri H, Olson M, Morck D, et al. The MBEC Assay System: multiple equivalent biofilms for antibiotic and biocide susceptibility testing. *Methods Enzymol*. 2001;337:377-385.

30. Schaberg DR, Culver DH, Gaynes RP. Major trends in the microbial etiology of nosocomial infection. *Am J Med*. 1991;91(3B):72S-75S.

31. Zhanel GG, Fontaine S, Adam H, et al. A Review of New Fluoroquinolones : Focus on their Use in Respiratory Tract Infections. *Treat Respir Med*. 2006;5(6):437-465.

32. Andes DR, Craig WA. Pharmacodynamics of fluoroquinolones in experimental models of endocarditis. *Clin Infect Dis*. 1998;27(1):47-50.

33. Rybak MJ, Lomaestro BM, Rotscahfer JC, et al. Vancomycin therapeutic guidelines: a summary of consensus recommendations from the infectious diseases Society of America, the American Society of Health-System Pharmacists, and the Society of Infectious Diseases Pharmacists. *Clin Infect Dis*. 2009;49(3):325-327.

34. Blaser J, Vergeres P, Widmer AF, Zimmerli W. In vivo verification of in vitro model of antibiotic treatment of device-related infection *Antimicrob Agents Chemother*. 1995;39(5):1134-1139.

35. Keil S, Wiedemann B. Mathematical corrections for bacterial loss in pharmacodynamic in vitro dilution models. *Antimicrob Agents Chemother*. 1995;39(5):1054-1058.

# Appendix

**NONMEM Code for the Population Pharmacokinetic Model of Efavirenz**

```
;Model Desc: Final Efavirenz Model

$PROB RUN# 109
$INPUT c ID TIME NTIM DV PID rxcode FORM Cohort Strat1 SITE OCC
Week Label Label3 TADChanged DOSE AMT EVID SS II WT HT BSA AGE GENDER
RACE GT516 C3435T BUN BUNGrade ALB BILI BILIULN ALT ALTULN ALTGrade AST
ASTULN ASTGrade
$DATA DATA1REDUCED.CSV IGNORE=c
$SUBROUTINES ADVAN2 TRANS2
$ABBREVIATED DERIV2=NOCOMMON
$PK

FMATCL=1/(1+(AGE/THETA(4))**(-THETA(5)))

FCYP=1
IF (GT516.EQ.3) THEN
   FCYP=THETA(6)
ENDIF

TVCL=THETA(1)*FCYP*(WT/70)**0.75*FMATCL

IF (OCC.EQ.1) THEN
   BOVCL=ETA(3)
ENDIF
IF (OCC.EQ.2) THEN
   BOVCL=ETA(4)
ENDIF
IF (OCC.EQ.3) THEN
   BOVCL=ETA(5)
```

```
ENDIF
IF (OCC.EQ.4) THEN
   BOVCL=ETA(6)
ENDIF
IF (OCC.EQ.5) THEN
   BOVCL=ETA(7)
ENDIF
IF (OCC.EQ.6) THEN
   BOVCL=ETA(8)
ENDIF
IF (OCC.EQ.7) THEN
   BOVCL=ETA(9)
ENDIF
IF (OCC.EQ.8) THEN
   BOVCL=ETA(10)
ENDIF
IF (OCC.EQ.9) THEN
   BOVCL=ETA(11)
ENDIF
IF (OCC.EQ.10) THEN
   BOVCL=ETA(12)
ENDIF
IF (OCC.EQ.11) THEN
   BOVCL=ETA(13)
ENDIF

   CL=TVCL*EXP(ETA(1)+BOVCL)

   TVV=THETA(2)*(WT/70)

   V=TVV*EXP(ETA(2))
```

```
   TVKA=THETA(3)
   KA=TVKA;*EXP(ETA(3))

S2=V

F1=1
TVF=THETA(7)/(1+(AGE/THETA(8))**(-THETA(9)))
Frel=TVF*EXP(ETA(14))
IF (FORM.GT.1) THEN
 F1=F1*Frel
ENDIF

DELCL=CL-TVCL
DELV=V-TVV

$ERROR
 DEL=0
 IF (F.LE.0.0001) DEL=1
 IPRE=F
 W1= 1
 W2= F
 IRES= DV-IPRE
 IWRE=IRES/(W1+W2)
 Y = F + W1*ERR(1)+W2*ERR(2)

$EST  METHOD=1  INTERACTION  PRINT=5  MAX=9999  SIG=3  MSFO=109.MSF
NOABORT

$THETA  (0,11.50000) ; [CL]
 (0,481.0000) ; [V]
 (0,0.854000) ; [KA]
```

```
 4.870000 ; [CL_TM50]
 3.870000 ; [CL_HILL]
 (0,0.429000) ; [FCYP]
(0,0.7410000) ; [Fmultiplier_form]
9 ; [F_TM50]
1, FIX ; [F_Hill]

$OMEGA
 0.282000; IIVCL
 0.280000;IIVV
$OMEGA  BLOCK(1)
 0.091800  ;     BOVCL1
$OMEGA  BLOCK(1) SAME
$OMEGA  BLOCK(1) SAME
$OMEGA  BLOCK(1) SAME
$OMEGA  BLOCK(1) SAME
$OMEGA  BLOCK(1) SAME
$OMEGA  BLOCK(1) SAME
$OMEGA  BLOCK(1) SAME
$OMEGA  BLOCK(1) SAME
$OMEGA  BLOCK(1) SAME
$OMEGA  BLOCK(1) SAME
$OMEGA  0.282000;IIVFrel

$SIGMA  0.099300  ; [A] sigma(1,1)
0.104000  ; [P] sigma(2,2)

$COV PRINT=E
```